

**INVESTIGATIONS ON SOME Y-ZEOLITE
ENCAPSULATED TRANSITION METAL COMPLEXES
OF SCHIFF BASES**

**THESIS SUBMITTED TO THE
COCHIN UNIVERSITY OF SCIENCE AND TECHNOLOGY
IN PARTIAL FULFILMENT OF THE
REQUIREMENTS FOR THE DEGREE OF**

**DOCTOR OF PHILOSOPHY
IN
CHEMISTRY
UNDER THE FACULTY OF SCIENCE**

BY

PREETHA G. PRASAD

**DEPARTMENT OF APPLIED CHEMISTRY
COCHIN UNIVERSITY OF SCIENCE AND TECHNOLOGY
KOCHI - 682 022, KERALA, INDIA**

JANUARY 2002

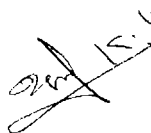
To my beloved parents and brother....

***whose immense support and sacrifices made this a
reality...***

3rd January, 2002

CERTIFICATE

This is to certify that this thesis is an authentic record of research work carried out by Miss. Preetha G. Prasad under my supervision, in partial fulfilment of the requirements for the degree of Doctor of Philosophy of Cochin University of Science and Technology, and further no part thereof has been presented before for any other degree.



Prof. K. K. Mohammed Yusuff

Department of Applied Chemistry

Cochin University of Science and Technology

Kochi-22.

DECLARATION

I hereby declare that the work presented in this thesis entitled "Investigations on some Y Zeolite encapsulated transition metal complexes of Schiff bases" is entirely original and was carried out by me independently under the supervision of Prof. Dr K. K. Mohammed Yusuff, Department of Applied Chemistry, Cochin University of Science and Technology, and has not been included in any other thesis submitted previously for the award of any degree.

Kochi-22
3rd January, 2002.



Preetha G. Prasad

ACKNOWLEDGEMENT

This is a statement of gratitude for a number of wonderful persons who had bestowed selfless help and consideration upon me, during my period of research.

The work presented here owes its existence from and foremost to my respected supervising guide Dr. K.K. Mohammed Yusuff, Professor, Dept. of Applied Chemistry, Cochin University of Science and Technology. He led me through the complications of the subject as a true guide. Without him this work would not have been materialized. I wish to express my deep gratitude to Prof. S. Sugunan, Head of the Dept. of Applied chemistry, Cochin University of Science and Technology, Kochi for his constant encouragement during the course of this study.

I would like to place on record my heartfelt thanks to Prof. P. Madhavan Pillai, retired professor and ex-head of the Dept. of Applied Chemistry, Cochin University of Science and Technology, Kochi for the kind and valuable help he rendered.

My sincere thanks are due to Dr. Prathapachandra Kurup, Dr. S. Prathapan, Dr. P.A. Unnikrishnan, Dr. K.Sreekumar, Dr. K. Girish Kumar, Dr. A.G.Ramachandran and Mrs. Sabura Begam for their cooperation.

I stand in debt to my beloved friends and colleagues, Dr. N.Sridevi, Dr. S. Mayadevi, Dr. Jose Mathew, Dr. Sudha George Valavi, Ms. Suja N.R., Mrs. C.P. Vineetha, Mr. K. Anas, Mrs Jyothi Mariam John, Mrs. Jelaja, Ms. Jean John, Ms.S. Pyroja, Ms. K. Bindu, Mr. S. Shaji and Mr. S. Santhosh for their timely help at all stages of this work and during the thesis preparation.

I am thankful to all research scholars, students and non-teaching staff of the Department of Applied Chemistry for their cooperation. I also thank all my friends for the cooperation they have extended to me throughout my work.

I thank RSIC Madras, RSIC Bombay, CSMCRI Bhavanagar, IISc Bangalore, CIFT, Kochi for providing me the necessary spectral facilities and library. I am grateful to CSIR, New Delhi for the award of a research fellowship.

Finally I thank my parents and my brother for being with me throughout my work.

Preetha G. Prasad

PREFACE

Zeolites are competing class of micro porous materials with tunable architecture and selectivity towards several catalytic reactions. The catalytic activity of these materials can be enhanced by encapsulation of certain chemically active materials with redox centers in the cavities. Metal Schiff base complexes are a fascinating class of molecular complexes, which can fine-tune the redox center. With this objective, we have investigated the interesting structural features of a series of transition metal Schiff base complexes encapsulated in Y zeolite. The catalytic properties of these complexes were studied with a view to know if there is any fine-tuning of the redox properties of the metal ion by the ligand environment within the supercage.

The use of chiral catalyst is a powerful strategy in modern synthetic organic chemistry. The homogeneous catalysts can be logically improved by heterogenisation. We have attempted the heterogenisation of chiral catalysts in the pores of Y zeolite. The interesting outcome of this study was that the encapsulated Ni(II) chiral complex was found to be the most efficient catalyst in bringing about good enantiomeric excess in the asymmetric epoxidation of styrene.

The thesis is divided into eight chapters with Chapter I giving an overview about the zeolite encapsulated complexes. The material and methods employed are presented in Chapter II. Chapters III to VI describe the synthesis and characterization of zeolite encapsulated Schiff base complexes. The screening studies of the catalytic activity of the complexes are presented in Chapter VII. Chapter VIII gives the details of the heterogenisation of the asymmetric catalyst and its catalysis in the asymmetric epoxidation of styrene. Summary and conclusion of our investigation are provided at the end of this thesis.

CONTENTS

Chapter I	Zeolite Encapsulated Metal Complexes - An Overview	1
1.1	Introduction	1
1.2	Structural consideration	5
1.3	Zeolite encapsulation methods	6
1.3.1	Metal Cluster Synthesis	7
1.3.2.	Flexible ligand method	8
1.3.3.	Template synthesis method	9
1.3.4.	Zeolite synthesis method	10
1.4.	Characterization of intrazeolite complexes	10
1.4.1.	Vibrational spectroscopy	11
1.4.2	Electronic spectroscopy	12
1.4.3	Electron paramagnetic resonance	13
1.4.4	Nuclear magnetic resonance	13
1.4.5	Electrochemistry	13
1.4.6	X-ray methods	14
1.4.7	Surface area	15
1.4.8	Thermal studies	15
1.4.9	Surface techniques	16
1.5	Scope of the present investigation	16
	References	19
Chapter II	Materials and Methods	23
2.1	Introduction	23
2.2	Reagents	23
2.3	Synthesis of Y Zeolite Encapsulated Metal-Schiff base complexes	24
2.3.1	Modification of Y Zeolite	24
2.3.2	Preparation of the Y Zeolite encapsulated Metal-Schiff base complexes	25
2.4	Analytical methods	25
2.4.1	Analysis of the zeolite samples for Si, Al, Na and transition metal ions by the complete dissolution method	25
2.4.2	CHN analysis	26
2.5	Physico-Chemical methods	26
2.5.1	Magnetic susceptibility measurements	26
2.5.2	Surface area analysis	26
2.5.3	Infrared spectra	27
2.5.4	Diffuse reflectance spectra	27
2.5.5	EPR spectroscopy	27
2.5.6	X-ray diffraction studies	28
2.5.7	Scanning electron microscopy	28
2.5.8	T.G. analysis	28
2.6	Catalytic studies	28
2.6.1	Gas chromatography	29
2.6.2	Polarimeter	29
	References	30

Chapter III	Studies on Y Zeolite Encapsulated Transition Metal Complexes of the Schiff Base <i>N,N'</i>-bis(Salicylidene)-1,2-Phnylenediamine	31
3.1	Introduction	31
3.2	Experimental	33
3.2.1	Materials	33
3.2.2	Synthesis of zeolite encapsulated complexes of <i>N,N'</i> -bis(salicylidene)-1,2-phenylenediamine	33
3.2.3	Analytical methods	34
3.3	Results and discussion	34
3.3.1	Metal exchanged zeolite supports	34
3.3.1.1	Chemical analysis	34
3.3.1.2	X-ray diffraction pattern	35
3.3.1.3	Surface area analysis	35
3.3.1.4	FTIR spectra	36
3.3.2	Y Zeolite encapsulated SALOPH complexes	37
3.3.2.1	Chemical analysis	37
3.3.2.2	T.G. Studies	38
3.3.2.3	SEM analysis	39
3.3.2.4	X-ray diffraction analysis	39
3.3.2.5	Surface area analysis	40
3.3.2.6	Magnetic moment	41
3.3.2.7	Electronic spectra	42
3.3.2.8	Infrared spectra	48
3.3.2.9	EPR spectroscopy	48
	References	51
Chapter IV	Studies on Y Zeolite Encapsulated Transition Metal Complexes of <i>N,N'</i>-bis(2-Hydroxymethylbenzylidene)-1,2-Phenylenediamine	53
4.1	Introduction	53
4.2	Experimental	54
4.2.1	Materials	54
4.2.2	Synthesis of zeolite encapsulated metal complexes	54
4.2.3	Analytical methods	55
4.3	Results and discussion	55
4.3.1	Chemical analysis	55
4.3.2	T.G. studies	56
4.3.3	SEM analysis	57
4.3.4	X-ray diffraction studies	58
4.3.5	Surface area analysis	58
4.3.6	Magnetic susceptibility measurements	59
4.3.7	Electronic spectra	60
4.3.8	Infrared spectra	66
4.3.9	EPR spectroscopy	68
	References	69
Chapter V	Studies on Y Zeolite Encapsulated Transition Metal Complexes of <i>N,N'</i>-bis(2-Pyridinemethylene)-1,2-Diaminoethane	70
5.1	Introduction	70

5.2	Experimental	71
5.2.1	Materials	71
5.2.2	Synthesis of zeolite Y encapsulated <i>N,N'</i> -bis(2-pyridinemethylene)-1,2-diaminoethane complexes	71
5.2.3	Analytical methods	72
5.3	Results and discussion	72
5.3.1	Chemical analysis	72
5.3.2	TG studies	73
5.3.3	X-ray diffraction studies	73
5.3.4	Scanning electron microscopy	74
5.3.5	Surface area analysis	74
5.3.6	Magnetic moment	75
5.3.7	Electronic spectra	76
5.3.8	Infrared spectra	80
5.3.9	EPR spectra	80
	References	82
Chapter VI	Studies on the Zeolite Y Encapsulated Transition Metal Complexes of <i>N,N'</i>-bis(3-Pyridinemethylene)-1,2-Diaminoethane	83
6.1	Introduction	83
6.2	Experimental	83
6.2.1	Materials	83
6.2.2	Synthesis of zeolite encapsulated 3 PyEn complexes	84
6.2.3	Analytical methods	84
6.3	Results and discussion	84
6.3.1	Chemical analysis	84
6.3.2	TG studies	85
6.3.3	X-ray diffraction studies	85
6.3.4	SEM analysis	86
6.3.5	Surface area analysis	86
6.3.6	Magnetic moment	87
6.3.7	Electronic spectra	88
6.3.8	FTIR spectra	91
6.3.9	EPR spectra	91
	References	93
Chapter VII	Catalytic Activity Studies of the Y Zeolite Encapsulated Schiff Base Complexes	94
7.1	Catalytic activity studies of the encapsulated Schiff base complexes in the oxidation of ascorbic acid	95
7.1.1	Experimental	96
7.1.1.1	Materials	96
7.1.1.2	Preparation of stock solutions	96
7.1.1.3	Reaction mixtures	97
7.1.1.4	Apparatus	97
7.1.1.5	Catalytic Experiments	97
7.1.2	Results and discussion	98
7.2	Catalytic activity studies of the encapsulated Schiff base complexes in the oxidation of 3,5-ditert-butylcatechol	101
7.2.1	Experimental	102

7.2.1.1	Materials	102
7.2.1.2	Reaction mixtures	102
7.2.1.3	Catalytic experiments	102
7.2.2	Results and discussion	103
	References	105
Chapter VIII	Studies on Y Zeolite Encapsulated Chiral Transition Metal Complexes	107
8.1	Introduction	107
8.2.A	Experimental	109
8.2.A.1	Materials	109
8.2.A.2	Synthesis of zeolite encapsulated asymmetric catalysts (MSALHENY)	109
8.2.A.3	Analytical methods	109
8.3.A	Results and discussion	110
8.3.A.1	Chemical analysis	110
8.3.A.2	X-ray diffraction patterns	110
8.3.A.3	SEM analysis	110
8.3.A.4	Surface area analysis	111
8.3.A.5	Magnetic moment	112
8.3.A.6	Electronic spectroscopy	112
8.3.A.7	EPR spectroscopy	115
8.B.1	Asymmetric catalytic activity studies	116
8.B.2	Experimental	116
8.B.2.1	Materials	116
8.B.3	Asymmetric epoxidation of styrene	116
8.B.3.1	Sodiumhypochlorite	117
8.B.3.2	<i>tert</i> -butylhydroperoxide	117
8.B.3.3	3-Chloroperoxybenzoic acid	118
8.B.4	Recyclability and stability of the catalyst	118
8.B.5	Results and discussion	119
	References	121
	Summary and Conclusions	122

CHAPTER I

ZEOLITE ENCAPSULATED METAL COMPLEXES – AN OVERVIEW

1.1. INTRODUCTION

A thermodynamically favourable reaction may be slow at modest temperature and so not at all valuable for synthesis. The rate can be accelerated by increasing the temperature. But providing energy to do so may be expensive and induce side reactions that will affect the product yield. A more attractive approach to increase the rate of a reaction is the use of catalysts. A catalyst can accelerate a thermodynamically allowed reaction by lowering the energy barrier.

Catalysts are classified as homogeneous if they are soluble in the reaction medium and heterogeneous if they are insoluble. Each type has its own advantages and disadvantages. Heterogeneous catalysts are easily separable from the reaction products, but require high temperature and pressure and may lead to mixture of products. So they are said to have low selectivity. But homogeneous catalysts can not be readily separated from the products. They operate at low temperatures and pressures and give good selectivity.

Finding a commercially viable pathway for the stereoselective organic synthesis of biologically important chemicals may be considered as one of the major thrust area of chemistry today. Among the many routes attempted those involving the use of chiral reagents and chiral catalysts are very important in the synthesis of effective drugs. An Inorganic Chemist's perspective in this matter is to develop commercially exploitable chiral catalysts involving metal ions. The earlier attempts to develop such size and shape selective catalysts using specially designed

ligands such as picket fence and basket type porphyrin complexes were encouraging.

The potential for coupling the shape selectivity associated with the well-defined channels and cages of zeolites with the reactivity of metal complexes makes these molecular sieves particularly attractive as solid supports. Zeolites have a distinct advantage over conventional support materials in that a metal complex can be physically trapped in the pores and not necessarily bound to the oxide surface. A metal complex of the appropriate dimensions might be encapsulated in a zeolite yet be free to move within the confines of a cage or channel. This could be viewed as a bridge between a homogeneous and heterogeneous system.

One of the goals of catalysis researchers in recent times has been the synthesis of inorganic mimics of enzymes such as cytochrome P-450. One approach has been the encapsulation of transition metal complexes inside the cages and void spaces of zeolite and zeolitic materials. The porous inorganic mantle zeolite provide the right steric requirement for the metal complexes and impose certain restrictions based on size and shape to the access of the active site by the substrate molecules. Though many porous materials have been used, the most popular supports have been zeolites X and Y possessing large cages 12 Å diameter [1-3].

Recent studies on copper phthalocyanine CuPc encapsulated in zeolite Y provide unequivocally the evidence for the encapsulation of the complex inside the cages with a distortion of the CuPc. The catalytic study of encapsulated materials in the epoxidation of styrene with *tert*-butylhydroperoxide is also reported [4].

The synthesis of the transition metal complexes inside the zeolite super cage has an added advantage that they create a favourable condition for reversible addition of molecular oxygen and decreases considerably the oxidation of the central metal ion. With this view, zeolite encapsulated cobalt tetramethylporphyrin complex was prepared and studied its dioxygen binding property [5]. Several studies have been carried out on the usage of the zeolite Y encapsulated cobalt

complexes as successful reversible oxygen binders, a property that is very important in mimicking biological systems [6-9].

Some copper(II) and manganese(II) Salen complexes confined to X and Y zeolites showed good performance as catalysts in the decomposition of H₂O₂ and *tert*-butylhydroperoxide [10]. So these encapsulated catalysts were used in the oxidation of phenol and styrene. They are found to be well catalysing in the oxidation reaction of *p*-xylene and are found to be thermally stable.

The *cis*-manganese(II) bis-2,2'-bipyridyl complex encapsulated in zeolite X or Y are reported to be very good catalysts for the selective alkene oxidation [11]. They showed moderate to high conversion and selectivity towards the oxidation of a variety of olefinic substrates even at room temperature. The above-mentioned catalysts were active in the oxidation of cyclohexene for up to 1000 cycles with H₂O₂. Repeated catalyst regeneration is possible in these cases.

Zeolite Y Mn(III)Salen complexes catalyse oxidation reactions using iodosylbenzene as the oxidant [12]. An increase of turnover numbers by 200 fold on using a zeolite encapsulated iron phthalocyanine complex has been observed for the oxidation of *n*-octane [13]. Tatsumi and *et al.* used H₂O₂ as an efficient oxidant for alkenes in the presence of the zeolite Y encapsulated manganese tetramethylporphyrin [14]. Bein and *et al.* have reported the encapsulation of methyltrioxorhenium in zeolite Y host and the activity of the resulting hybrid catalysts for olefin metathesis [15]. Intrazeolite complex of manganese trimethyltriazacyclononane is found to be a highly selective epoxidation catalyst for a number of olefins with H₂O₂ [16].

The use of chiral catalysts is now a powerful methodology in modern synthetic organic chemistry. In this regard, the Sharpless epoxidation of allylic alcohols constituted an authentic breakthrough. A further logical improvement of the catalytic method would consist of the incorporation of the catalyst in zeolite supports to perform the reaction heterogeneously. Corma *et al.* have accomplished the first time preparation of the Jacobsen catalyst into the super cage of Y zeolite

[17]. The encapsulated complexes show catalytic activity very similar to that of the complex in the homogeneous phase.

Zeolite encapsulated metal complexes have applications as ecofriendly catalysts. They are recyclable and are less poisonous. Zeolite encapsulated transition metal complexes of Cu(II) and Mn(II) with Salen or substituted Salens or the tetraminooctaazamacrocyclic ligand have been utilised in the oxidation of the green house gas methane to methanol [18]. The Osmium carbonyl clusters entrapped in Y zeolite are known to be very stable and selective catalysts for the carbon monoxide hydrogenation reaction [19]. The product distribution was markedly different from all the conventional catalysts.

Syntheses and design of the metal complexes with desired properties is still a developing field. So it is worthwhile to look at the various structural aspects of the zeolite supports. In general, zeolites are the crystalline, hydrated aluminosilicates of group I and II elements. The framework of aluminosilicate is formed by a three dimensional net work of alumina and silica tetrahedra joined together through the oxygen atoms. The framework is open with channels and cavities in which the cations and water molecules are located. The cations being highly mobile facilitates ion exchange. The water molecules are readily lost and regained, which accounts for the well-known desiccant properties of zeolite.

The structural formula of the unit cell of a zeolite can be expressed as: $M_{x/n} \{(Al_2O_3)_x (SiO_2)_y\} \cdot nH_2O$, where M = cation of valence n and n = No. of water molecules. The ratio y/x usually has a value of 1-5 depending upon the structure. The portion in $\{(Al_2O_3)_x (SiO_2)_y\}$ represents framework composition.

For practical purposes there is considerable interest in designing and engineering ordered porous materials possessing pore diameters in the range 5-20 Å [20].

1.2. Structural consideration

There are a large variety of zeolite structure types due to the flexibility of the Al-O-Si linkage. This flexibility is dependent on the condition of their hydrothermal synthesis. The tetrahedral coordination around Si and Al permits a wide variety of ring structures containing 4,5,6,10 or 12 Si or Al atoms. These rings are joined to form prisms and more complex cages. These structures contain pores and channels of uniform size in the range of 4 to 13 Å and so the zeolites are able to recognise, discriminate and organise molecules with high precision [21].

The tetrahedra are arranged in such a way that two AlO_4 tetrahedra are always separated by at least one silicon tetrahedron. The secondary building unit of A, X and Y zeolite is a sodalite unit, which is a cubo-octahedron formed from 24 tetrahedra of SiO_4 and AlO_4 and consists of six 4-membered cube faces and eight 6-membered octahedron faces. When the sodalite units are connected to each other at their square faces, zeolite A is formed, and if they are joined at the hexagonal faces X and Y structures are formed. The large cavity enclosed by the sodalite units is called an α -cage or supercage. The sodalite cages enclose a small cavity within itself known as β -cage. The structure of Y zeolite is shown in fig.1.1. The unit cell formulae and other characteristics of A, X and Y zeolites [22] are given in Table I.1.

The silicon tetrahedra remain electrically neutral. But the trivalent Al atom is bound to four oxygen atoms and so the alumina tetrahedra have a net negative charge. Sodium ions are usually present as non-framework in zeolite structure to balance the negative charge of the framework generated by the formal -1 charge on alumina tetrahedra. The exchangeable extra framework cations provide the framework with extra properties such as fine-tuning of channel and pore dimensions and the inclusion of chemically interesting molecules.

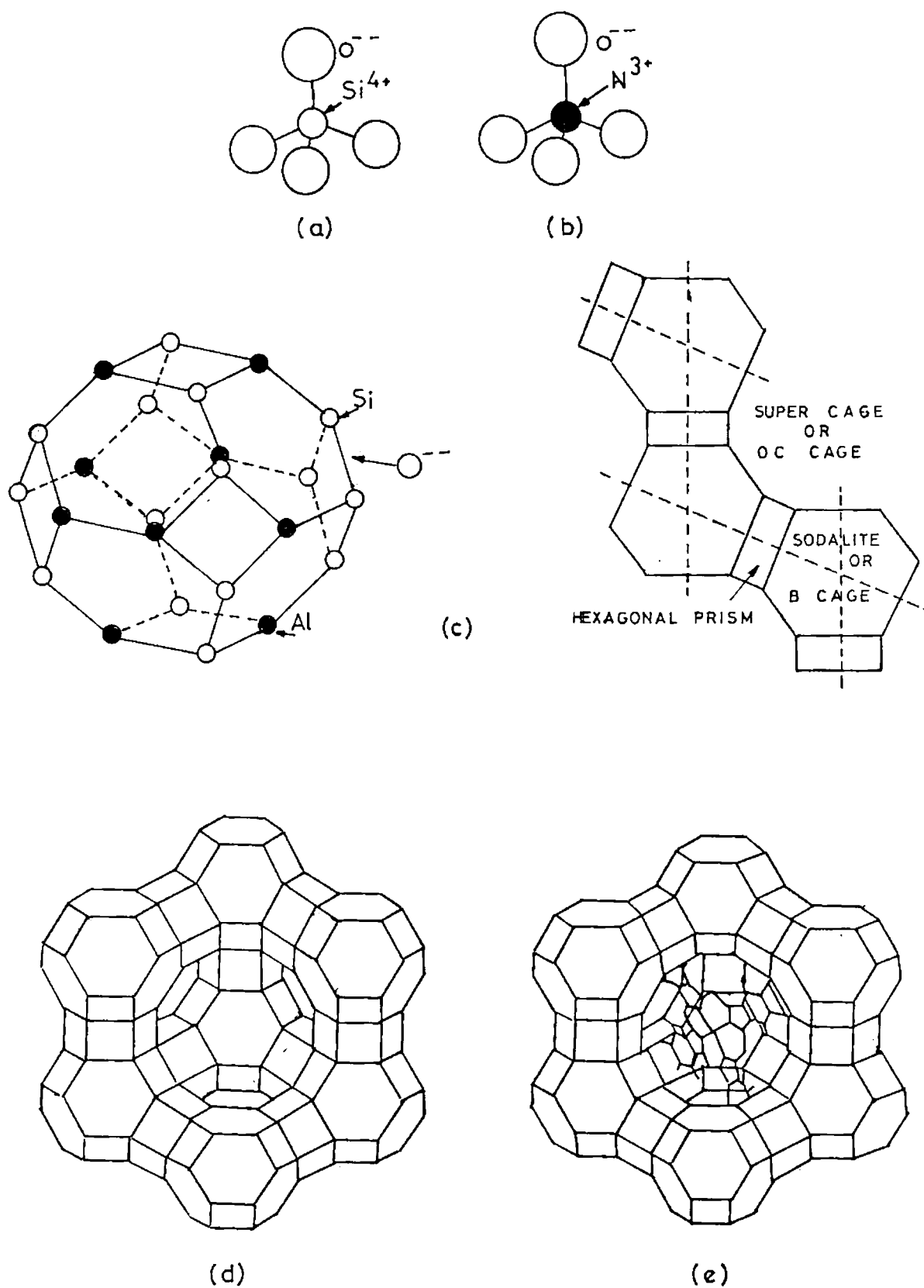


Fig. I.1 (a) SiO_4 tetrahedra (b) AlO_4 tetrahedral (c) Sodalite unit
 (d) Y Zeolite and (e) Y Zeolite encapsulated iron phthalocyanine

Table I.1 Properties of zeolite A, X and Y

Zeolite	Unit cell formula	Mol. ratio SiO ₂ /Al ₂ O ₃	α -cage diameter	α -cage aperture
A	Na ₁₂ (AlO ₂) ₁₂ (SiO ₂) ₁₂ nH ₂ O	2:1	11Å	4Å
X	Na ₈₆ (AlO ₂) ₈₆ (SiO ₂) ₁₀₆ nH ₂ O	2.5:1	13Å	8Å
Y	Na ₅₆ (AlO ₂) ₅₆ (SiO ₂) ₁₃₆ nH ₂ O	5:1	13Å	8Å

1.3. Zeolite encapsulation methods

The channels and chambers of molecular dimension provide a rigid aluminosilicate framework within which reaction chemistry may be performed. As a result, the intrazeolitic chemistry is very attractive.

The zeolite framework may function as a ligand, an anion and a solvent in forming a complex inside. Usually the zeolite plays two or three of these roles simultaneously. The neutral molecules are better ligands and so replace the oxide ions of the lattice to form stable complexes. At moderate temperatures, the metal ions may move to the large cavities to provide adequate volume for complex formation. Furthermore, the metal ions in the zeolite are offering a way to have complex with unusual symmetries and coordination numbers.

There are four general strategies for the encapsulation of metal complexes in molecular sieves. These are:

- i) The *in situ* preparation of intrazeolite metal carbonyl cluster
- ii) The flexible ligand method
- iii) The template synthesis method
- iv) The zeolite synthesis method

The first three methods find application in the case of large pore zeolites and molecular sieves. An intrazeolite metal complex should be smaller than the super cage and be effectively larger than the cavity openings. The diffusion of the

reagents through the channels limit the encapsulation of the complex inside zeolite. Zeolite A, which has a large cavity of 11.9 Å and small openings of 4.1 Å, cannot find very good application as encapsulating materials. However, if the zeolite is synthesized around the metal complex, window size is not important. In this case, the metal complex must meet the requirement of stability during crystallisation. But this is not a major restriction as zeolites can be synthesized under many conditions. The zeolite synthesis approach has been employed to encapsulate metal complexes in a variety of molecular sieves.

1.3.1. Metal cluster Synthesis

Metal carbonyls grafted on supports such as zeolites offer a preparative method for the tailored metal catalysts [23,24]. As there is no cluster aggregation within the framework, zeolites find a promising role to ensure the unique activity of these materials.

Metal carbonyl adducts form the most widely studied group of intrazeolite coordination complexes [25]. In the light of the catalytic potential of these systems the encapsulation of carbonyl and subcarbonyl species is of interest.

Metal carbonyl clusters with a nuclearity greater than three could be encapsulated in Faujasite type zeolite and form a special subclass of ship-in-a-bottle complexes. The reaction of CO/H₂ or CO/H₂O with a metal ion exchanged Y type zeolite has led to the encapsulation of Rh₆(CO)₁₆ [26-30], Rh₄(CO)₁₂ [30] and Ir₄(CO)₁₂ [30]. This method has also been used for the encapsulation of bimetallic derivatives Rh_{6-x}Ir_x(CO)₁₆ (x= 0 to 6) inside zeolite Y [31,32]. Clusters as large as Pd₁₃(CO)_x have been characterized in NaY zeolites [33,34]. The necessity for the presence of H₂ or H₂O suggests that the formation of the metal cluster occur through the reductive carbonylation of intrazeolite metal ions. This method is an easy way to generate anionic complexes in the supercages of X and Y type zeolites.

The 12-ring windows to the super cage are defined by oxygen that bears partial negative charge. Passage of anions through this aperture is unfavourable so that entry of the smaller anionic clusters may be electrostatically restricted.

Activation of carbon monoxide, which arises from the interaction of a metal bound carbonyl with a charge balancing cation, may stabilize the intrazeolite cluster. The numerous possibilities of carbonyl cluster as molecular precursors dramatically expands the potential for new and interesting intrazeolite species.

1.3.2. Flexible ligand method

In this method, a multidentate ligand is diffused into the zeolite pores where it could coordinate to a previously exchanged metal ion. Once the complex is formed, it may reside there due to its large and rigid structure and may not escape the cages. This presumes that the ligand should be sufficiently flexible to twist its way through a very restrictive passage. This method is well adopted for encapsulating metal Salen complexes since the Salen ligand offers the desired flexibility. Thus, a large variety of cobalt [35], iron [36], rhodium [37] and palladium Salen [38] complexes within Y zeolite super cage were prepared through this method. In zeolite Y, the 8 Å pore dimension is sufficiently large to allow the Salen ligand access to all metal sites within the super cage pore system. The size encapsulation for the cobalt Salen complexes arises from the rigid square planar or square pyramidal coordination geometry adopted by the complex. The flexible Salen ligand has a minimum kinetic diameter of $<6.5 \text{ \AA}$. It is getting locked into a complex with a minimum kinetic diameter of 9 \AA that is too large to exit from the $\sim 8 \text{ \AA}$ zeolite pores.

So the flexible ligand method requires a ligand of such dimensions so that intrazeolite complex precludes diffusion out of the zeolite. This places severe limitations on the number and type of ligands that might be employed. The intrazeolite complexation must occur from the outer surface to the cages. So the pore blocking would result in a heterogeneous distribution of complexes. Nevertheless, this approach is probably the easiest in practice.

1.3.3. Template Synthesis Method

The template synthesis method involves the diffusion of ligand precursors into the zeolite pores where they assemble around an intrazeolite metal ion that acts as a template. This method is exemplified by the preparation of intrazeolite metallophthalocyanines [39-54].

The large pore zeolites X, Y and the aluminophosphate VPI-5 modified with metal ions, metallocenes or metal carbonyl complexes can be reacted with dicyanobenzene (DCB) to form intrazeolite MPc complexes. The synthesis generally involves heating an intimate mixture of partially dehydrated zeolite with an excess of DCB in a bomb reactor between 150 and 350°C. The synthesis can be done at lower temperatures in the presence of solvents. It has been recently reported that solvent mediated reaction at 180°C appears to lower the reaction temperature [55].

The condensation of four DCB molecules around a metal ion to form the encapsulated phthalocyanine requires two electrons, the source of which is the subject of much debate. These electrons may originate from water or the metal ions in the case of the organometallic precursors. This is consistent with the fact that intrazeolite metal phthalocyanine complexes are formed easily with zero valent metal carbonyls, followed by metallocenes and metal ions. The formation of encapsulated complexes will be easier if the metal exchanged zeolites are partially dehydrated.

Several metal phthalocyanine derivatives have been encapsulated in X and Y type zeolites including perhalogenated phthalocyanine complexes [56], *t*-butylphthalocyanines [14] and nitrophthalocyanines [56] using substituted dicyanobenzenes. But it was shown for tetranitrophthalocyanines that they are mostly located on the external surface [44]. There have been claims of Co porphyrin [54] Fe and Mn tetramethylporphyrin complexes [55] as well as tetraphenylporphyrin complexes [52] encapsulated in NaY. The porphyrin template

synthesis usually requires two reagents, pyrrole and either formaldehyde, acetaldehyde or benzaldehyde. However, the possible presence of uncomplexed metal ion and free ligand inside zeolite by this strategy might be expected to complicate characterization and reactivity studies.

1.3.4. Zeolite Synthesis Method

This is the most recent method for encapsulating metal complexes inside zeolites. This involves the addition of the metal complex (especially metallophthalocyanine), possibly in a template role, during the crystallisation of the zeolite host [53,54,57]. This would afford the advantage of encapsulating a well-defined intrazeolite complex without contamination from free ligand as well as uncomplexed and partially complexed metal ions at milder preparation conditions.

By carefully designing the zeolite synthesis procedure, the aggregation of the complex in the aqueous medium can be avoided. There were some earlier reports on encapsulating simple chelate complexes such as bis(ethylenediamine)cobalt(II) using zeolite synthesis method [58]. Recently, crown ethers have been employed as templates for zeolites. In particular, 18-crown-6 has been shown to be a template for zeolites having the EMT topology [59].

1.4. Characterization of Intrazeolite Complexes

The characterization of the encapsulated metal complexes is quite difficult and generally requires a battery of techniques to locate the complex within the cage. The first step in this procedure is, of course, the removal of the surface species by soxhlet extraction with a series of suitable solvents and or vacuum sublimation. Special attention is needed for the metal complexes such as metallophthalocyanines as they adsorb to the zeolite surface. In the case of some zeolites encapsulated with metal phthalocyanines, the surface adsorbed species cannot be removed by solvent extraction and sublimation. In such cases electrochemical techniques are used.

When a negative potential is applied to a freshly prepared zeolite encapsulated complex/graphite composite electrodes, a small amount of reduced metal complex is released from the surface, as evidenced by the faint blue colour in the electrolyte solution. In the case of zeolite encapsulated M Salen complexes, solvent extraction is sufficient to remove surface species. Even though the outer crystal surface area of most zeolites may be several orders of magnitude less than the internal surface area, it is clear that there is some possibility to adsorb on the outer surface or partially occluded in mesopores. Therefore, zeolites with very low loadings of metal complex should be used. In addition to traditional elemental analyses, encapsulated metal complexes such as phthalocyanines may be quantified by UV-VIS spectroscopy after digesting the framework. This is preferred for the phthalocyanine complexes prepared by the template method because the complexation may not be quantitative and elemental analysis does not necessarily reflect the amount of metal complex. But generally chemical analysis was used to obtain information on the bulk composition of the chemically modified zeolites and to quantify their degree of exchange. Complete characterization of the encapsulated complexes is required in order to ensure the feasibility of the intrazeolite synthesis. Several techniques must be used in conjunction to have a clear vision.

1.4.1. Vibrational Spectroscopy

Infrared spectroscopy is probably the most widely applied analytical tool for the characterisation of zeolite ship-in-a bottle complexes. Either diffuse reflectance or transmission IR spectra can provide idea about the zeolite lattice as well as the nature of guest molecule. In the mid-IR spectra of the metal carbonyl clusters encapsulated in zeolites, there is a shift for both bridging and terminal carbonyl stretching frequencies according to the type of interaction as compared to the free clusters [60-63].

The mid-IR spectral studies of intrazeolite MPc [43, 47, 49, 51, 56, 63] substituted MPc [56, 64] and M Salen [24, 26, 28] complexes have been reported.

The various T-O vibrational modes associated with the zeolite dominate most of the region between 1150-450 cm^{-1} and may mask the bands due to the complex in this region. But with reasonable loading inside the cage, the complex can be detected. The bands associated with C=N and C=C stretching modes for the phthalocyanine ligand are easily observed and may show a slight shift to lower wave numbers inside the super cage. The complexation of the Salen ligand should result in a blue shift of the strong C=N stretch at 1504 cm^{-1}

FTIR has exhibited high sensitivity and resolution for detecting the carbonyl ligands of the metal carbonyl clusters and has provided essential information about the cluster structure. Characteristic C-O stretching modes are seen in the IR spectrum at 2098 and 1760 cm^{-1} representing 12 linear and 4 face bridging CO in $\text{Rh}_6(\text{CO})_{16}/\text{NaY}$, respectively [36].

1.4.2. Electronic spectroscopy

This tool is useful in evaluating the intrazeolite complexation with regard to any structural perturbation that might occur during encapsulation. The encapsulation of the MPc in FAU type zeolite cages can be confirmed by the red shift exhibited for the Q band of Pc relative to the free or surface physisorbed complexes. Herron [7] later suggested it to be due to the steric interactions within the super cage. The suppression of the Q band in the electronic spectra of zeolite encapsulated tetramethylporphyrin complexes has been interpreted as a result of ligand distortion in the supercage [14]. The UV-VIS spectra of intrazeolite Salen complexes are not quite very sensitive to the perturbations in structure. The light yellow Salen ligand exhibits bands at 323 and 409 nm, which is found to shift upon coordination. The encapsulated Mn(II) and Mn(III) Salen complexes are well characterized by UV-VIS spectroscopy [12].

1.4.3. Electron paramagnetic resonance

EPR spectroscopy can provide information regarding the oxidation states of iron based zeolite ship in a bottle complexes [65]. A dioxygen adduct of NaY

encapsulated Salen have been studied by this technique [23]. A cobalt(II)Salen complex prepared by the flexible ligand method was shown to be EPR silent and hence Co(II) might be in the high spin state. On exposing this to pyridine also makes no signal. But subsequent absorption of oxygen produces EPR spectrum of Co-O₂ adduct. As the complex is not rotating in the cage the signal is an axial one. Close examination of the EPR parameters showed similarity to the values obtained for the solution spectra suggesting absence of distortion for the complexes inside the cage.

1.4.4. Nuclear magnetic resonance

Many nuclei besides ²⁹Si, ²⁷Al and ¹H have been used as probes of zeolitic structure (e.g. ¹³C, ¹⁴N and ¹⁵N, ³¹P, ²³Na, ¹⁷O). Most of our knowledge derived from solid state NMR of zeolites comes from experiments, which have used these nuclei either alone or in concert [66]. Cross-polarisation MAS ¹³C NMR has been used to study the features of Li₂Pc, FePc, Fe(nitro)₄ Pc and Ti (Pc). Of the eight different carbons of Pc, only four were resolved for the intrazeolite species. One might expect the carbon resonance to shift as the hybridization or aromaticity is altered by distortion of the Pc macrocycle in the cage.

1.4.5. Electro chemistry

Electrochemical techniques such as cyclic voltammetry are used to provide information on the oxidation state and redox chemistry of the active metal atom and the ligand. There is an extensive effort to include zeolites in modifying the electrodes for the electrocatalytic reactions. Some recent reviews on this aspect appeared in the literature [67, 68].

The encapsulated Mn(III)Salen and Ru(III)Salen complexes exhibit the same electrochemical behaviour in solution and upon encapsulation. The encapsulated perhalogenated phthalocyanines of metals showed a reversible redox process that is difficult to observe in solution [69, 70].

The well defined redox behaviour of the inclusion compounds is a proof for the site isolation within the zeolite matrix, and excludes the possibility of any aggregate formation while the simple adsorption of the molecules on the electrode surface or on any other mineral support does not prevent aggregation formation [21]. For the zeolite ship in a bottle complexes, the electron transfer must occur inside the zeolite depending on the complex loading. When the occupied cages may prevent the solvent and electrolyte from reaching the redox sites the vacant sites may prevent electron transfer. The net result is that only a few percent of the encapsulated metal complexes are electro active. The electrochemical response can be improved by the addition of a very large metal complex as surface mediator. The intra zeolite redox site could be used for developing new types of electrocatalysts as can be seen in the case of Co and Mn Salen complexes [37].

1.4.6. X-ray methods

The powder XRD technique is an indispensable one for the zeolite synthesis method where phase identification and purity are critical. It also provides valuable information relating to crystallinity as well as any change in unit cell parameters that might arise from the *in situ* generation of intrazeolite ship in a bottle complex. When a cationic complex is included in zeolite due to the redistribution of charge balancing cations the peak intensities showed variation. Most of such complexes are neutral. It is interesting to note that the intrazeolite MPc complexes, including a perfluorinated analogue, even though they have a tight fit inside the cage, never show an expansion of X or Y zeolite unit cell [71]. Zeolite crystallinity is largely preserved here after template method of synthesis. The complexes prepared from ion-exchanged zeolites are more susceptible to dealumination as the formation of protons is likely. The preparation of RhPc complexes in Y or X zeolites results in a loss of crystallinity [72]. The zeolite crystallinity was reported to be intact after encapsulation of Mn Salen by the flexible ligand method.

1.4.7. Surface area

Zeolite surface area is largely internal. The inclusion of guest molecules should dramatically reduce the absorption capacity of such molecular sieves. The BET surface area of X and Y zeolites containing metal phthalocyanine complexes (M= Mn, Co, Cu) [73] and cobalt porphyrin are typically less than 100 m²/g which is reduced by at least 600 m²/g. Balkus and Gabrielov [74] also suggested such a reduction in surface area as a proof of encapsulation.

1.4.8. Thermal Studies

Differential scanning calorimetry has been used to study the energetics of intrazeolite formation of a large number of metallophthalocyanine in zeolite [75]. Another potential advantage of using DSC is the possibility of differentiating between the formation of the encapsulated and surface complex since there are no steric constraints associated with the formation of the latter. For the cobalt(II) and copper(II) phthalocyanine encapsulated in Y zeolite, the exotherms for the entrapped as well as the surface adsorbed species can easily be resolved. The exotherm for the formation of the intrazeolite complexes are at higher temperatures [74].

Thermal analysis and thermogravimetric analysis have also find application in monitoring the intrazeolite complex formation [75]. The amount of the entrapped metallophthalocyanine complexes can be estimated from the weight loss and more accurate result has been obtained when compared to the spectrophotometric determination after complete digestion of the zeolite framework. The presence of free ligand and organic residues can be obtained from the number of exotherms as reported for the decomposition of iron (II) phthalocyanine and tetranitrophthalocyanine complexes in NaY. From the TG plots, it is evident that encapsulation bring about stability to the neat complexes. But there are a few reports about the lesser stability of the encapsulated metal complexes while comparing to their unencapsulated counterparts just as for some

cobalt(II), copper(II) and nickel(II) phthalocyanines. This might be due to the distortion undergone by the phthalocyanine ligand in the supercage.

1.4.9. Surface Techniques

X-ray photoelectron spectroscopy provides information about the oxidation states and relative concentrations of elements in the first 50 Å of the zeolite. The agreement between the surface concentration estimated from metal/Si or metal/Al ratio and bulk elemental analyses is an evidence for the homogeneous distribution of intrazeolite complexes. Sometimes the XPS revealed a high concentration of the metal at the surface, which may necessarily not be the presence of extrazeolite metal complexes. The ions and molecules may migrate close to the surface as a consequence of the thermal treatment associated with the flexible ligand or template synthesis. XPS has been well used for the characterisation of intrazeolite metal phthalocyanines and M Salen. The shift in the binding energies for both the intrazeolite metals and nitrogen in Salen or phthalocyanine indicates complexation. Shpiro *et al.* reported the presence of two types of nitrogens for the Y zeolite encapsulated nickel, cobalt, copper and ruthenium phthalocyanines using XPS studies. Either the distortion of the ligand or strong interaction with the framework may be responsible for the presence of two types of nitrogen [43].

Scanning and transmission electron microscopy help to detect the decomposition of metal complexes or metal oxide on the outer surface of the zeolite. The SEM images of the metal phthalocyanine complexes within zeolites have been taken before and after soxhlet extraction [18]. TEM has provided evidence of uniform dispersions of osmium carbonyl clusters in Y-type zeolites.

1.5. Scope of the present investigation

Asymmetric epoxidation of unfunctionalised olefins catalysed by chiral metal complexes has proved to be one of the most useful strategies discovered in the last decade. Three scientists, William S. Knowles, Ryoji Noyori and K. Barry Sharpless, shared last year's Nobel Prize in Chemistry for their contributions in

developing catalytic asymmetric synthesis. The achievements are of great importance for academic research, for the development of new drugs and materials, and are being used in many industrial syntheses of pharmaceutical products. Heterogenising such potential catalysts while maintaining its structural and chemical features unaltered could be aimed with caution so that the derivative should be efficient in catalyzing the oxidations also. In that respect, zeolite has an added advantage over polymer supports because the zeolite encapsulated complexes could be viewed as a homogeneously heterogenised catalyst. Zeolite encapsulated metal complexes have already captured much attention in catalysis and biomimetic chemistry [1-3]. These new catalytic systems are of interest partially due to the shape selectivity that the zeolite framework may impose on the incoming reactant molecules and also due to the potential advantages in practical use. The high adsorption potential inside the channels of the zeolites raises the effective concentration of a catalyst at the active site and enhances their efficiency as catalytic centres. The zeolite structure can impose sieving and orienting effects upon the substrates approaching the otherwise non-selective metal active sites. The zeolite pore structure can provide 'reaction vessels' of molecular dimensions wherein the selective catalytic reactions can better take place.

The present study has been undertaken with the following objectives:

- To synthesise some stable zeolite encapsulated transition metal complex catalysts.
- To find out the chemical nature of such catalysts within the super cage of the framework.
- To under take a qualitative study using the above complexes as catalysts in the oxidation of ascorbic acid and 3,5-di-*tert*-butylcatechol.
- To study epoxidation of styrene using zeolite encapsulated chiral catalysts.

To achieve the above mentioned objectives, we have synthesized and characterized Y zeolite encapsulated transition metal [M= Mn(II), Co(II), Ni(II) and Cu(II)] complexes of certain Schiff base ligands such as: (a) *N,N'*-bis(salicylidene)-

1,2-phenylenediamine. (b) *N,N'*-bis(2-hydroxymethylbenzylidene)-1,2-phenylenediamine. (c) *N,N'*-bis(2-pyridinemethylene)-1,2-diaminoethane, and (d) *N,N'*-bis(3-pyridinemethylene)-1,2-diaminoethane. Catalytic activity of all the synthesized complexes are screened in the following reactions:

(a) Oxidation of ascorbic acid.

(b) Oxidation of 3,5-di-*tert*-butylcatechol.

Asymmetric epoxidation of styrene, using the Mn(II), Co(II), Ni(II) and Cu(II) complexes with the chiral Schiff base, *N,N'*-bis(salicylidene)-*trans*-1,2-diaminocyclohexane has also been carried out.

REFERENCES

- [1] K.J. Balkus Jr., A.G. Gabrielov, *J. Incl. Phenom. Mol. Reco. Chem.* **21** (1995) 159.
- [2] R. Parton, D. De Vos, P.A. Jacobs, in: E.G. Derouane, F. Lemos, C. Naccache, F.R. Riberio Eds., Proceedings of NATO Advanced Study Institute on Zeolite, Microporous Solids: Synthesis, Structure and Reactivity 555 Kluwer, Do-drecht, 1992, 578.
- [3] D. De Vos, F. Thibault-Starzyk, P.P. Knops-Gerrits, R.F. Parton, P.A. Jacobs, *Macromol. Symp.* **80** (1994) 157.
- [4] S. Sindhu, A.K. Sinha, D. Srinivas, S. Shivshankar, *J. Mol. Catal. A* **157** (2000) 163.
- [5] G.Q. Li, R. Govind, *Inorg. Chim. Acta* **217** (1994) 135.
- [6] K. Mizuno, S. Imamura, J.H. Lunsford, *Inorg. Chem.* **23** (1984) 3510.
- [7] N. Herron, *Inorg. Chem* **25** (1986) 4714.
- [8] R.J. Taylor, R.S. Drago, J. P. Hage, *Inorg. Chem.* **31** (1992) 253.
- [9] R.J. Taylor, R.S. Drago, J.E. George, *J. Am. Chem. Soc.* **111** (1989) 6610.
- [10] C.R. Jacob, S.P. Varkey, P. Ratnasamy, *Micro. Meso. Mater.* **22** (1998) 465.
- [11] P.P. Knops-Gerrits, D. De Vos, F. Thibault-Starzyk, P.A. Jacobs, *Nature* **369** (1994) 543.
- [12] C. Bowers, P.K. Dutta, *J. Catal.* **122** (1990) 271.
- [13] P.A. Jacobs, *Stud. Surf. Sci. Catal.* **59** (1991) 395.
- [14] M. Nakamura, T. Tatsumi, H. Tominaga, *Bull. Chem. Soc. Jpn.* **63** (1990) 3334.
- [15] T. Bein, C. Huber, K. Moller, Chun-Guey Wu, L. Xu, *Chem. Mater.* **9** (1997) 2252.
- [16] D. De Vos, J.L. Meinershagen, T. Bein, *Angew. Chem. Int. (Ed) Engl.* **35** (1996) 2211.
- [17] M.J. Sabater, A. Corma, A. Domenech, V. Fornes, H. Garcia, *Chem. Comm.* (1997) 1285.
- [18] S.P. Varkey, C.R. Jacob, *Ind. J. Chem.* **38A** (1999) 320.
- [19] Pei-Ling Zhou, B.C. Gates, *J. Chem. Soc. Chem. Comm.* (1989) 347.

- [20] J.M. Thomas, M. Audier, J. Klinowski, *J. Chem. Soc. Chem. Comm.* (1981) 1221.
- [21] F. Bedioui, *Coord. Chem. Rev.* **144** (1995) 39.
- [22] P.G. Menon, in S. Ramaseshan (Ed.) *Letters on Catalysis*, 41st Ann. Meeting, Ind. Acad. Sci. 1975.
- [23] M. Ichikawa, *Adv. Catal.* **38** (1992) 283.
- [24] H.G. Schuster-Woldan, F. Basolo, *J. Am.Chem. Soc.* **88** (1966) 1657.
- [25] R. Cramer, *J. Am.Chem. Soc.* **86** (1966) 217.
- [26] L.F. Rao, A. Fukuoka, M. Ichikawa, *J. Chem. Soc. Chem. Comm.* (1988) 458.
- [27] L.F. Rao, A. Fukuoka, N. Kosugi, H. Kuroda, M. Ichikawa, *J. Phys. Chem.* **94** (1990) 5317.
- [28] N. Takahashi, A. Mijin, H. Suematsu, S. Shinohara, H. Matsuoka, *J. Catal.* **177** (1989) 348.
- [29] B.E Hanson, M.E. Davis, D. Taylor, E. Rode, *Inorg. Chem.* **23** (1984) 52.
- [30] M. Ichikawa, L.F Rao, A. Fukuoka, *Catal. Sci. Tech.* **1** (1991) 111.
- [31] A. Fukuoka, L.F. Rao, N. Kosugi, H. Kuroda, M. Ichikawa, *Appl. Catal.*, **50** (1989) 295.
- [32] R.C. Schneider, R.F. Howe, K.C. Watters, *Inorg. Chem.* **23** (1984) 4600.
- [33] L.L Sheu, H. Knozinger, W.M.H Sachtler, *Catal. Lett.* **2** (1989) 129.
- [34] L.L Sheu, H. Knozinger, W.M.H. Sachtler, *J. Am.Chem. Soc.* **111** (1989) 8125.
- [35] R.S. Drago, I. Bresinska, J.E George, K.J. Balkus Jr., R.J. Taylor, *J. Am. Chem. Soc.* **110** (1988) 304.
- [36] L. Gallion, N. Sajot, F. Bedioui, J. Devynch, K.J. Balkus Jr., *J. Electroanal. Chem. Interface. Electrochem.* **345** (1993) 157.
- [37] K.J. Balkus Jr., A.A. Welch, B.E. Gnade, *Zeolites*, **10** (1990) 722.
- [38] S. Kowalak, R.C.Weiss, K.J. Balkus Jr., *J. Chem. Soc., Chem. Comm.* (1991) 57.
- [39] N. Herron, *J. Coord. Chem.* **19** (1988) 25.
- [40] B.V. Romanovsky, Proc. 8th Int. Congr. Catal., Verlag Chemie, Weinheim (1984) 657.
- [41] G. Meyer, D. Wohrle, M. Mohl, G. Schulz-Ekloff, *Zeolites* **4** (1984) 30.
- [42] H. Diegruber, P.J. Plath, G. Schulz-Ekloff, *J. Mol. Catal.* **24** (1984) 115.

- [43] E.S. Shpiro, G.V. Antoshin, O.P. Tkachenko, S.V. Gudkov, B.V. Romanovsky, Kh. M. Minachev, *Stud. Surf. Sci. Catal.* **18** (1984) 31.
- [44] A.N. Zakharov, B.V. Romanovsky, *J. Incl. Phenom.* **3** (1985) 389.
- [45] N. Herron, G.D. Stucky, C.A. Tolman, *J. Chem. Soc., Chem. Comm.* (1986) 1521.
- [46] C.A. Tolman, N. Herron, *Catal. Today* **3** (1988) 235.
- [47] N. Herron, *Chemtech.* (1989) 542.
- [48] A.D. Gabrielov, A.N. Zakharov, B.V. Ramanovsky, O. P. Tkachenko, E. S. Shpiro, Kh. M. Minachev, *Koord. Khim.* **14** (1988) 821.
- [49] A.N. Zakharov, B.V. Ramanovsky, D. Luca, V. I. Sokolov, *Metalloorg. Khim.* **1** (1988) 119.
- [50] G. Schulz-Ekloff, D. Wohrle, V. Iliev, E. Ignatzek, A. Andreev, *Stud. Surf. Sci. Catal.* **46** (1989) 315.
- [51] M. Tanaka, Y. Sakai, T. Tominaga, A. Fukuoka, T. Kimura, M. Ichikawa, *J. Radioanal. Nucl. Chem. Lett.* **137** (1989) 287.
- [52] T. Kimura, A. Fukuoka, M. Ichikawa, *Catal. Lett.* **4** (1990) 279.
- [53] K.J. Balkus Jr., J.P. Ferraris, *J. Phys. Chem.* **94** (1990) 8019.
- [54] R.F. Parton, L. Uytterhoeven, P.A. Jacobs, *Stud. Surf. Sci. Catal.* **59** (1991) 395.
- [55] K.J. Balkus Jr., S. Kowalak, K.T. Ly, C.D. Hargis, *Stud. Surf. Sci. Catal.* **69** (1991) 93.
- [56] X. Wang, Y. Liang, Y. Lui, L. Yu, Y. Li, X. Cao, *Gaodeng Xuexiao Hixue xuebao* **14** (1993) 19. [CA 119: 107854j (1990)].
- [57] K. J. Balkus Jr., C.D. Hargis, S. Kowalak, *ACS Symp. Ser.* **499** (1992) 347.
- [58] US Patent 4, 388 285 (1983).
- [59] F. Delprato, L. Demotte, J.L. Guth, L. Huve, *Zeolites* **10** (1990) 564.
- [60] S. Kawi, B.C. Gates, *J. Chem. Soc. Chem. Comm.* (1992) 702.
- [61] S. Kawi, J.R. Chang, B. C. Gates, *J. Catal.* **142** (1993) 585.
- [62] S. Kawi, B.C. Gates, *J. Chem. Soc. Chem. Comm.* (1991) 994.
- [63] A. De Mallmann, D. Barthomeuf, *Catal. Lett.* **5** (1990) 293.
- [64] M. Ichikawa, T. Kimura, A. Fukuoka, *Stud. Surf. Sci. Catal.* **60** (1991) 335.
- [65] S.K. Sur, R.G. Bryant, *J. Phys. Chem.* **97** (1993) 2686.
- [66] L.F. Rao, S.J. Hwang, T. S. King, M. Pruski, *J. Phys. Chem.* **100** (1996) 5668.

- [67] G.A. Ozin, A. Kuperman, A. Stein, *Angew. Chem. Int. (Ed.) Engl.* **28** (1989) 359.
- [68] D.R. Robinson, *Chem. Rev.* **90** (1990) 6867.
- [69] K.J. Balkus Jr., A.G. Gabrielov, S. L. Bell, F. Bedioui, L. Roue, J. Devynck, *Inorg. Chem.* **33** (1994) 67.
- [70] F. Bedioui, L. Roue, E. Briot, J. Devynck, S.L. Bell, K.J. Balkus Jr., *J. Electroanal. Chem.* **337** (1994) 19.
- [71] A.G. Gabrielov, K.J. Balkus Jr., F. Bedioui, J. Devynck, *Micropor. Mater.* **2** (1994) 119.
- [72] K.J. Balkus Jr., C.D. Hargis, S. Kowalak, *ACS. Sym. Ser.* **499** (1992) 347.
- [73] Z. Jiang, Z. Xi, *Fenzi Cuihua* **6** (1992) 467. [CA 118: 212554 (1992)]
- [74] J.P. Ferraris, K.J. Balkus Jr., A. Schade, *J. Incl. Phenom. Mol. Rec. Chem.* **14** (1992) 163.
- [75] K.J. Balkus Jr., A.A. Welch, B.E. Gnade, *J. Incl. Phenom. Molec. Recog. Chem.* **10** (1991) 141.

CHAPTER II

MATERIALS AND METHODS

2.1. INTRODUCTION

The details regarding the general reagents and other materials used in the present study, a brief account of the methods used for the synthesis of the zeolite encapsulated metal complexes, and the various analytical and physico-chemical methods employed for characterisation given in this chapter. Procedural details about the synthesis and catalytic activity studies of the complexes are given in appropriate chapters.

2.2. REAGENTS

The following metal salts were used: $\text{MnCl}_2 \cdot 4\text{H}_2\text{O}$ (E. Merck, GR); $\text{CoCl}_2 \cdot 6\text{H}_2\text{O}$ (E. Merck, GR); $\text{NiCl}_2 \cdot 6\text{H}_2\text{O}$ (E. Merck, GR); $\text{CuCl}_2 \cdot 2\text{H}_2\text{O}$ (E. Merck, GR).

Synthetic Y-type zeolite was obtained from Sud-Chemie India Ltd., Binanipuram, Cochin. Salicylaldehyde, 2-hydroxyacetophenone, 1,2-phenylenediamine and 1,2-ethanediamine obtained from E-Merck and pyridine-2-carboxaldehyde and pyridine-3-carboxaldehyde obtained from Aldrich were used as such for preparation of the encapsulated metal complexes. The chiral amine trans-1,2-cyclohexanediamine (Aldrich) was used for the preparation of the chiral Schiff base complexes encapsulated in zeolite-Y. Commercially available styrene used for the epoxidation reactions was purified by known procedures [1]. The 1,2-epoxyethylbenzene procured from Aldrich was used as the

standard for calculating the yield. For catalytic studies, 3,5-di-tert-butyl catechol (Aldrich) and L- ascorbic acid (SRL, LR) were used. Unless otherwise specified, all the other reagents were of analytical reagent grade. Solvents employed were either of 99% purity or purified by known laboratory procedures [1].

2.3. SYNTHESIS OF Y ZEOLITE ENCAPSULATED METAL -SCHIFF BASE COMPLEXES

2.3.1. Modification of Y zeolite

Metal exchanged Y zeolite support was prepared according to the following general procedure:

One negative charge present per aluminium on the framework is compensated by loosely attached, ion-exchangeable cations. These cation exchange sites within the internal void space of the crystallite allow the straightforward introduction of active metal ions for catalysis. So at first it is exchanged with sodium ions and it can be replaced afterwards with various ions easily. The parent-powdered zeolite (5 g) was converted to the sodium form by ion exchanging with NaCl solution (0.1M, 500 mL) under stirring at room temperature for 24 h. The zeolite was filtered and washed until the filtrate was free from chloride ions. The NaY so obtained was stored for further use after drying at 120⁰C for 2 h.

For introducing Mn²⁺, Co²⁺, Ni²⁺ and Cu²⁺ ions, the sodium exchanged Y zeolite (5 g) was stirred in a solution of the respective metal chlorides (0.05M, 500 mL) at room temperature for 24 h. At these very low concentrations it is assumed that all the metal ions are exchanged and situated in the super cage only. It was then filtered and made free from chloride ions. The metal exchanged zeolite samples so obtained were made active by calcining at 450⁰C for 2 hours.

2.3.2. Preparation of the Y zeolite encapsulated metal Schiff base complexes

The complexes were prepared using metal template method [2]. Here the Schiff base complexes were synthesized from the smaller components- aldehyde and amine- by assembling them around the transition metal ions already in the zeolite super cage. A general procedure for the preparation is as follows:

Metal exchanged Y zeolite (5g) was refluxed with the aldehyde (2 M) in appropriate solvent. The aldehyde chelates so obtained were purified by soxhlet extraction with one or more suitable solvents. These chelates were then condensed with a molar solution of the respective amines. The resulting Schiff base complexes were purified by soxhlet extraction to colourless washings. This ensures the complete removal of surface species. They were re-exchanged with 0.01M NaCl at room temperature for 24 h to remove any surface adsorbed metal ions remaining after soxhlet extraction. After filtration it was washed free of chloride ions and dried at 120⁰C for 2 h. before storing in vacuum over anhydrous calcium chloride.

2.4. ANALYTICAL METHODS

2.4.1. Analysis of the zeolite samples for Si, Al, Na and transition metal ions by the complete dissolution method

The chemical analysis of the zeolites and the zeolite encapsulated metal complexes were done according to the following procedure:

The zeolite sample was dried by keeping it at 120⁰ C for 2 hours. A known weight of the dried zeolite sample (w_1 g) was transferred to a beaker and treated with conc. sulphuric acid (40 mL, 98%) and heated until SO₃ fumes were evolved. This is to destroy the zeolite framework. It was cooled and diluted with water (200 mL) and filtered through an ashless filter paper in to a standard flask. The residue was dried at 1000⁰C in a

platinum crucible, cooled and weighed (w_2 g). Hydrofluoric acid (5 mL, 40%) was added and evaporated to dryness on a sand bath. This process was done for five or six times for each sample. All the silicon is removed in the form of H_2SiF_6 [3]. The residue was then ignited to 1000°C (w_3 g). The percentage of silica (SiO_2) was calculated by using the equation,

$$\% \text{SiO}_2 = (w_3 - w_2) \times 100 / w_1$$

Potassium peroxodisulphate was added to this residue and heated until a clear melt was obtained. This melt was dissolved in water and was combined with the filtrate in the standard flask. The sodium, aluminium and transition metal ions in this solution were determined by ICP analysis. The unit cell formula of the zeolite was calculated from the Si/Al ratio [4].

2.4.2. CHN analysis

Microanalyses for C, H and N in the zeolite samples were done on a Carto Erba Analyzer Model 1108 at Central Drug Research Institute, Lucknow

2.5. PHYSICO - CHEMICAL METHODS

2.5.1. Magnetic susceptibility measurements

Magnetic susceptibility measurements were done at room temperature on a simple Gouy-type magnetic balance. The Gouy tube was standardised using $\text{Co}[\text{Hg}(\text{SCN})_4]$ as the standard [5].

2.5.2. Surface Area Analysis

Surface area of the samples was measured by multipoint BET method using a Micromeritics Gemini 2360 surface area analyzer. Nitrogen gas was used as the adsorbate.

2.5.3. Infrared Spectra

Infrared spectra of the ligands and encapsulated complexes in the region 4600cm^{-1} – 400 cm^{-1} were taken by the KBr pellet technique using Shimadzu 8000 Fourier Transform Infrared Spectrophotometer.

2.5.4. Diffuse reflectance spectra

The diffuse reflectance spectra were recorded at room temperature between 200-2000 nm against MgO as standard. In order to make these reflectance data more meaningful and to remove the effect of scattering, a Kubelka-Munk analysis [6,7] was performed on the reflectance data. The Kubelka-Munk equation is,

$$F(R) = (1-R)^2/2R = k/s \text{ where,}$$

R is the diffuse reflectance of the sample compared to a non-absorbing standard such as MgO, k is the molar absorption coefficient and s is the scattering coefficient of the sample. In the case of s remaining constant with wavelength, e.g. in weakly absorbing materials, F(R), the emission factor or Kubelka-Munk (KM) factor, is directly proportional to the molar absorbance coefficient.

2.5.5. EPR Spectroscopy

The X-band EPR spectra of some of the zeolite encapsulated complexes were recorded at liquid nitrogen temperature using a Varian E-109 X/Q band spectrophotometer. The g values were estimated relative to the tetracyanoethylene (TCNE, $g = 2.0027$). The density of the unpaired electrons at the central copper ion can be calculated using the equation,

$$\alpha_{\text{Cu}}^2 = (A/P) + (g - 2) + 3/7 (g - 2) + 0.04,$$

where $1-\alpha_0^2$ measures the covalency associated with the binding of the metal ions to the ligand and $P= 0.036\text{ cm}^{-1}$.

2.5.6. X-ray diffraction studies

The powder XRD patterns of the Y-zeolite and the zeolite encapsulated metal complexes were recorded using 'Rigaku D-Max C' X-ray diffractometer. The measurements were carried out with a stationary X-ray source of Ni filtered Cu K_{α} radiation ($\lambda_0 = 1.5404$). The detector that is movable scans the intensity of the diffracted radiation as a function of the angle 2θ between the incident and the diffracted beams. .

2.5.7. Scanning electron microscopy

Scanning electron microscopy of a representative zeolite complex after and before Soxhlet extraction was performed on a Leica Stereoscan-440 microscope. The secondary electron probe is used for the analysis. Before exposing to the electron beam it was made conducting by coating with gold.

2.5.8. TG Analysis

Thermogravimetric analyses were done on a Shimadzu TGA-50 at a heating rate of $10^{\circ}\text{C}/\text{min}$ in the temperature range $30\text{-}800^{\circ}\text{C}$ in inert atmosphere.

2.6. CATALYTIC STUDIES

The detailed procedure regarding the catalytic activity studies is presented in Chapters VII and VIII. The following instruments were used for the screening studies.

2.6.1. Gas Chromatography

The progress of the reaction was monitored by checking the product formation by GLC using a Chemito 8510 GC coupled with PC using 2m long, 3mm ID, 4mm OD stainless steel column packed with SE30, 5% mesh size 60 to 80 with FID detector. A pure sample of the epoxide was used to determine yields by comparison of the peak height and area. The optical purity of the product was checked with chiral capillary column (chiraldex GTA). The analyses were done at Central Salt and Marine Chemicals Research Institute, Bhavnagar, Gujarat.

2.6.2. Polarimeter

The optical rotation of the epoxides was measured using a polarimeter (Atago, Japan.)

REFERENCES

- [1] D.D. Perrin, W.L.F. Armarego, D.R. Perrin, *Purification of Laboratory Chemicals*, 2nd Edn., Pergamon Press, New York, 1980, 417.
- [2] G. Meyer, D. Wohrle, M. Mohl, G. Schulz-Ekloff, *Zeolites* 4 (1984) 30.
- [3] A.I. Vogel, *A Text Book of Quantitative Inorganic Analysis*, 3rd Edn., ELBS, London, 1978.
- [4] C. Tollmann, N. Herron, *Symposium in Hydrocarbon Oxidation*, 194th National Meeting of The Am. Chem. Soc., New Orleans, LA, Aug. 30 - Sept. 4 (1987).
- [5] B.N. Figgis, R.S. Nyholm; *J. Chem. Soc.* (1958) 4190.
- [6] H.G. Hecht, in :W.W. Wendlandt (Ed.), *Modern Aspects of Reflectance Spectroscopy*, Plenum Press, New York, 1968.
- [7] S.K. Tiwary, S. Vasudevan, *Inorg. Chem.* 37 (1998) 5329.

CHAPTER III

STUDIES ON Y ZEOLITE ENCAPSULATED TRANSITION METAL COMPLEXES OF THE SCHIFF BASE *N,N'*-bis (SALICYLIDENE)-1,2-PHENYLENEDIAMINE

3.1 INTRODUCTION

During the past few years, considerable interest has been evolved on the synthesis and characterisation of transition metal complexes of Schiff bases [1-5]. The major goal of a coordination chemist is the fabrication of specifically designed complexes, and it can be achieved easily through the Schiff base ligands. Such complexes might help us to understand the chemistry of biological systems, particularly, enzymes and proteins. As the role and activity of a metal ion in a metallo-enzyme depends upon the coordination sphere around it, there has always been a growing interest on the studies of Schiff base complexes to obtain better knowledge of the factors that modify the coordination sphere and its electronic properties. Furthermore, better understanding of the biological systems can be obtained [6-9] through these studies.

Zeolites have been used as interactive supports for metal clusters and the ionic attachment of metal complexes [10,11]. A metal complex prepared inside zeolite can have substantially different reactivity than its solution analogue [12]. Such encapsulated complexes offer several advantages in catalytic reactions on account of their ruggedness, prevention of deactivation due to dimerisation or cluster formation and ease of separation from the reaction products. The Pd(Salen) complex encapsulated in X or Y zeolite has been found to be a good catalyst for the selective hydrogenation of hex-1-ene in the

presence of cyclohexane [13]. There are reports on the catalytic activity of Y zeolite encapsulated Cu(Salen) complex for the selective oxidation of cyclohexanol to cyclohexanone using H₂O₂ as the oxidant [14]. A Co(Salen) complex prepared inside the pore structure of Y zeolite shows affinity for dioxygen as the pyridine adduct [15]. These adducts show excellent resistance to autoxidation even at elevated temperatures. VO(Salen)-Y zeolite complex is reported to be active in the oxidation of toluene with H₂O₂ to give various oxidation products [16]. Recently different strategies have been developed for the encapsulation of metal complexes [17,18]. Using the ship in a bottle method, a complex can be prepared where all of the individual components (metal ions and various ligands as well) may easily pass in and out of the zeolite, but the final assembled coordination complex is too large and rigid to pass out once assembled inside [19]. But we have employed the metal template method for encapsulating the Schiff base complexes [20]

Studies on the preparation and characterisation of the zeolite encapsulated complexes of the Schiff base *N,N'*-bis(salicylidene)-1,2-phenylenediamine (SALOPH) are presented in this chapter. Various techniques like elemental analysis, X-ray diffraction studies, magnetic susceptibility measurements, FTIR, electronic and EPR spectral studies, surface area analyses and TG measurements were used in arriving at the coordination, composition and structure of the complexes.

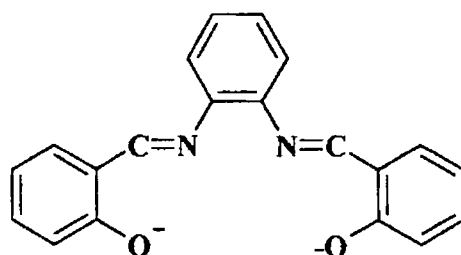


FIG III. 1. Structure of the ligand

3.2. EXPERIMENTAL

3.2.1. Materials:

The procedure for the preparation of metal exchanged zeolite is described in Chapter II. These metal exchanged zeolites were used for synthesizing the complex in the super cage.

3.2.2 Synthesis of zeolite encapsulated complexes of *N,N*-bis (salicylidene)-1,2-phenylenediamine

The general method used for the preparation of the complex within the zeolite cavity is given in Chapter II. The complexes were entrapped using metal template method. The metal exchanged zeolites were made to react with the required quantity of the components of the ligand, salicylaldehyde and 1,2-phenylenediamine, keeping the ligand to metal mole ratio ~ 4 . The corresponding metal exchanged zeolite (5 g) was refluxed with salicylaldehyde (4.3 mL, 0.04 M) in dichloromethane (15 mL) for 6 h. The chelates so formed were then soxhlet extracted with methanol to colourless washings and were dried. The salicylaldehyde complexes were then condensed with a molar solution of 1,2-phenylenediamine (2.2 g, 0.02 M) in methanol (15 mL) for 2 h. The complexes formed were filtered and washed several times with hot water. They were subjected to soxhlet extraction with methanol followed by acetone to remove the surface adsorbed ligand and complexes. Any uncomplexed metal ions remaining after the purification procedure could be removed by back exchange of the encapsulated complexes with NaCl (0.01 M) solution for 12 h. Accordingly, the complex was re-exchanged with NaCl (0.01 M) solution for 12 h. followed by washings with hot water to remove chloride ions, dried at 120°C for 2 h. and was stored in vacuum over anhydrous calcium chloride. Scanning electron micrograph of a representative complex before and after soxhlet extraction indicates that the extraction is effective in removing the surface adsorbed species. The complex so formed is confined internally and cannot be extracted due to its larger size than the window diameter.

3.2.3. Analytical methods

The analytical methods and other characterisation techniques used are described in Chapter II.

3.3. RESULTS AND DISCUSSION

3.3.1. METAL EXCHANGED ZEOLITE SUPPORTS

3.3.1.1. Chemical analysis

The analytical data of NaY and various metal exchanged zeolites are presented in Table III.1. It is clear from the data that the Si/Al ratio of NaY is around 2, which corresponds to a unit cell formula $\text{Na}_{58} [(\text{AlO}_2)_{58} (\text{SiO}_2)_{134}]$ [21]. Almost similar Si/Al ratio is found in all the metal exchanged zeolites indicating that there was no dealumination during the metal exchange to destruct the framework. It is reported that high concentration of metal chloride solution may affect the framework and to avoid the destruction of framework structure, dilute solutions have to be used [22]. In order to avoid dealumination, very low concentration of the metal chloride solutions (0.005 M) were used for ion- exchange and pH of the solution was adjusted to 4.0~4.5.

Table III.1 Analytical data of metal exchanged zeolites

Sample	%Si	%Al	%Na	% Metal
NaY	21.82	8.9	6.87	-
MnY	21.67	8.8	3.34	2.96
CoY	21.43	8.62	2.97	3.19
NiY	21.71	8.85	2.75	3.56
CuY	21.36	8.59	3.03	3.34

The degree of ion-exchange and unit cell formulae of the metal exchanged zeolites were derived from the analytical data and are given in Table III.2. The degree of ion exchange is represented as the percentage of Na⁺ ions replaced by metal ions from the total amount of the Na equivalent to Al content of the zeolite. The unit cell formula is a representation of the composition of a unit cell in the metal exchanged zeolites. The degree of ion exchange in various metal exchanged zeolites used in the present study are comparable to that reported earlier [23].

TABLE III.2. Composition of metal exchanged zeolites

Sample	Degree of ion exchange	Unit cell formula
NaY		Na ₅₈ [(AlO ₂) ₅₈ (SiO ₂) ₁₃₄ .nH ₂ O
MnY	49.68	Na _{49.68} Mn _{8.29} [(AlO ₂) ₅₇ (SiO ₂) ₁₃₅ .n H ₂ O
CoY	47.94	Na _{47.94} Co _{8.95} [(AlO ₂) ₅₇ (SiO ₂) ₁₃₅ .n H ₂ O
NiY	46.86	Na _{46.86} Ni _{9.66} [(AlO ₂) ₅₇ (SiO ₂) ₁₃₅ .n H ₂ O
CuY	46.82	Na _{46.82} Cu _{9.27} [(AlO ₂) ₅₇ (SiO ₂) ₁₃₅ .n H ₂ O

3.3.1.2. X-ray diffraction pattern

X-ray diffraction patterns of the zeolite samples are given in Fig.III.2. They are very similar to that of NaY. Moreover, the XRD patterns are very similar to those reported in the literature [24]. So it is a clear evidence that the crystalline structure was almost preserved in the metal exchanged zeolites. There are reports about the loss of crystallinity of Y-zeolite by metal exchange using metal salt solutions of concentration higher than 0.02 M and pH less than 4 [22].

3.3.1.3. Surface area analysis

The surface area of the zeolite samples determined by the BET method is presented in Table III.5. NaY zeolite has a surface area of 549 m²/g. It can be seen that there is only

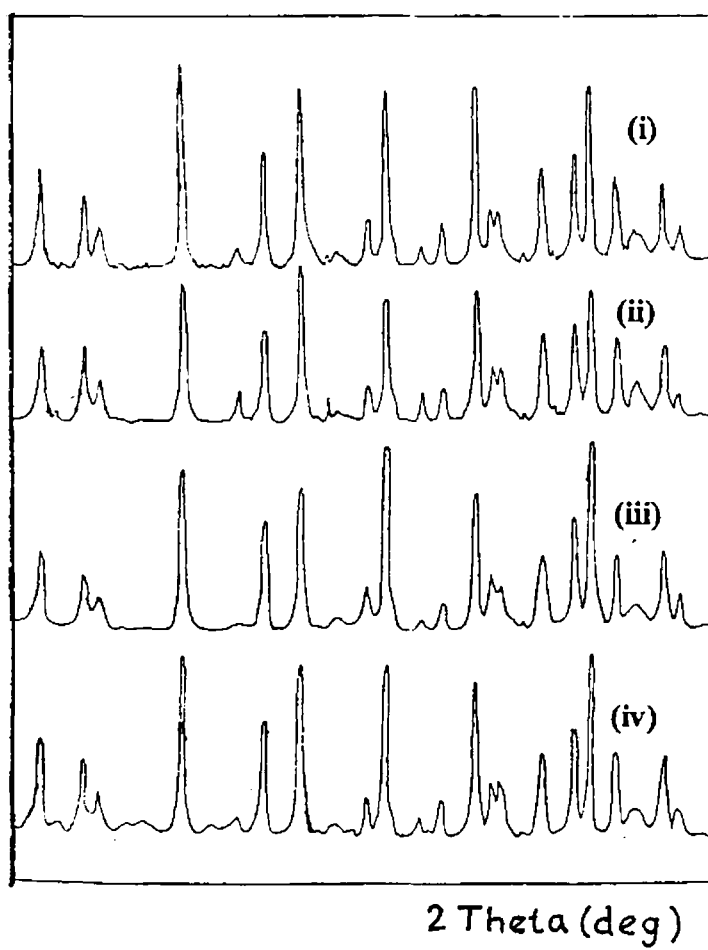


Fig.III.2 XRD Patterns of (i) MnY (ii) CoY
(iii) NiY (iv) CuY

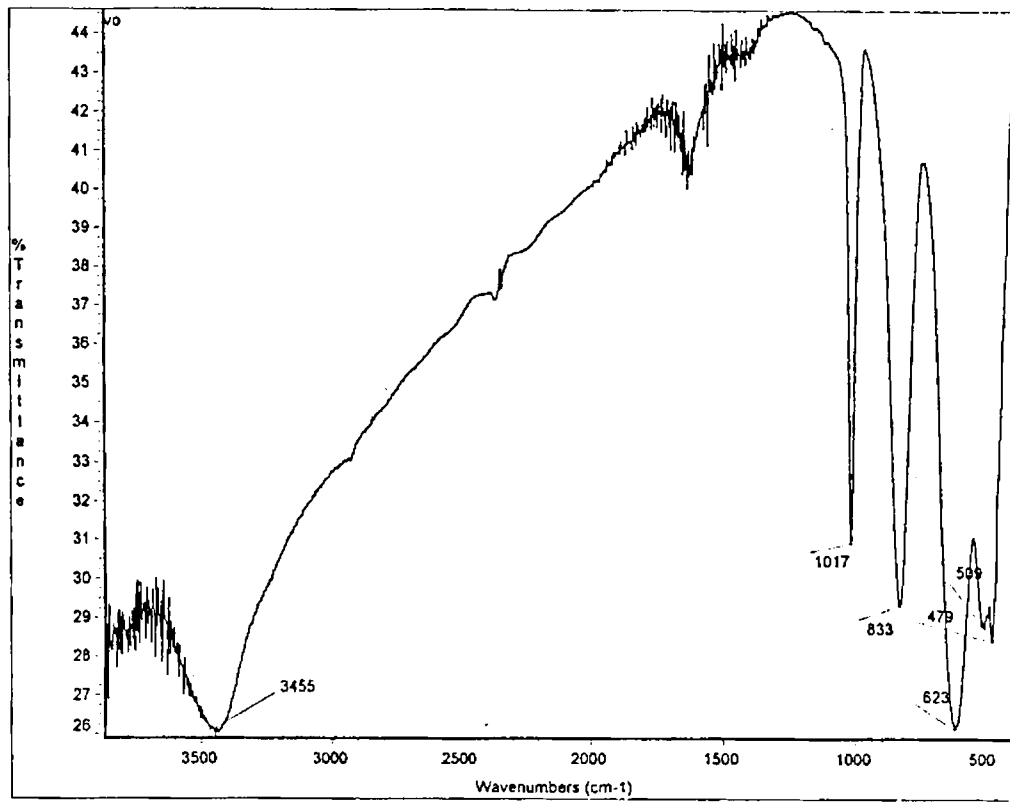
a small decrease in surface area as a result of metal exchange. This can be considered as an ample proof for the retention of the structure. There would have been a drastic decrease in the surface area if the structure was collapsed. The surface area values obtained are in agreement with those reported for the metal exchanged zeolites [23].

3.3.1.4. FTIR spectra

FTIR spectra of NaY and other metal exchanged zeolite^{CoY} are shown in Fig.III.3. The IR bands are listed in Table III.3. The frequencies of these vibrations are sensitive to Si/Al ratio and framework structure. Moreover, the bands are almost in the same position as that of the parent Y zeolite. The IR bands are in agreement with those reported for the Y Zeolite [24]. This observation further confirms that the zeolite framework is unaffected in the concentration range of the metal chloride solutions used. The mid infrared region of the spectrum (1300 to 200 cm^{-1}) reflects the framework structure as it contains the fundamental vibrations of the (Si,Al) O_4 tetrahedra. This region consists of two classes of vibrations:

- 1) The internal vibrations due to the framework TO_4 tetrahedron, which is the primary building unit in all zeolite frame work. These vibratins are, insensitive to the framework structure.
- 2) The vibrations due to external linkages between tetrahedra , which are sensitive to the frame work structure.

The two most intense bands in the spectrum of the metal exchanged zeolite and the parent NaY at 1050 cm^{-1} and 450 cm^{-1} come under the first class of vibration, and these bands are assigned as the internal tetrahedron vibrations. The strongest vibration, at 1050 cm^{-1} might be due to the asymmetric T-O stretching mode. The band at 450 cm^{-1} with a higher energy shoulder can be attributed to the T-O bending mode[23]. The symmetric stretching of the internal tetrahedron gives rise to a band at 580 cm^{-1} . The symmetric stretch of the external linkage appears in the spectrum as a broad band around 750 cm^{-1} . The asymmetric stretching of these external linkages is seen as the shoulder at 1100 cm^{-1} .



oil.

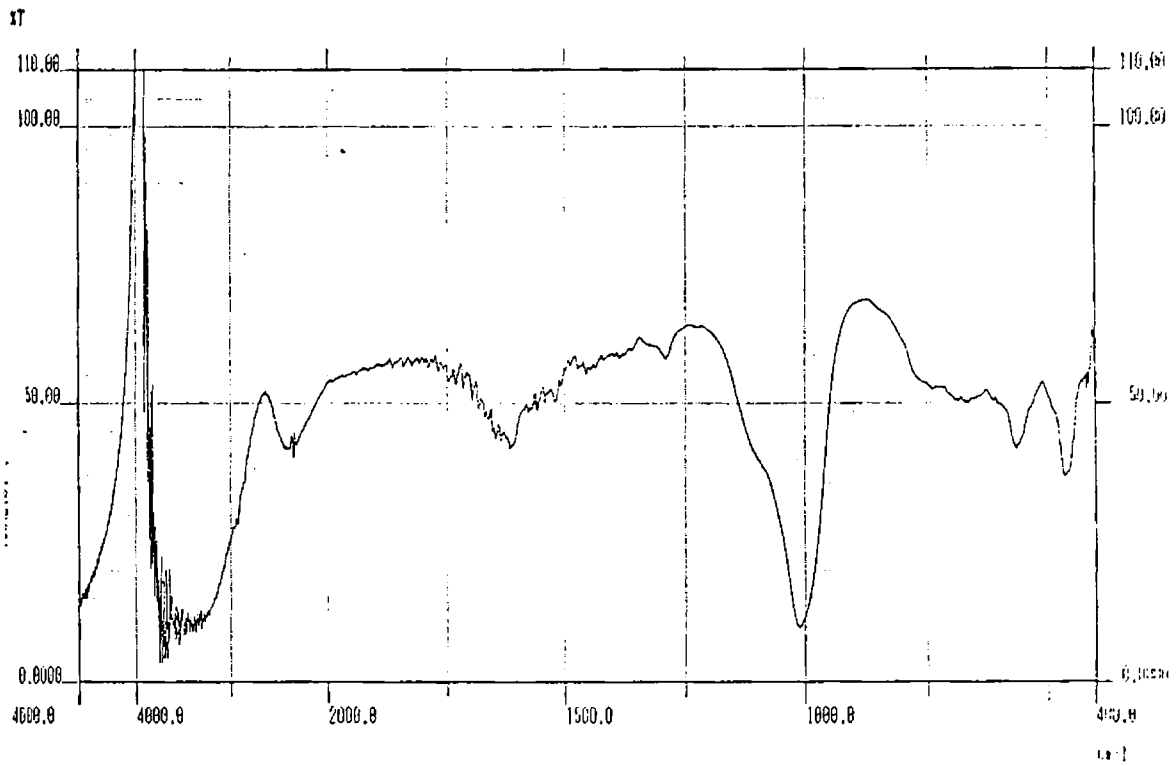


Fig III.3. FTIR of NaY and CoY

The water molecules will undergo stretching and bending vibrations at 3450 cm^{-1} and 1650 cm^{-1} respectively.

TABLE III.3. IR spectral data of metal exchanged zeolite (CoY).

Band Position (cm^{-1})	Tentative assignments
450	
580	γ_{sym}
750	γ_{sym} (external)
1050	$\gamma_{\text{asymmetric}}$ (internal)
1150	$\gamma_{\text{asymmetric}}$
1600	$\delta_{\text{H-O-H}}$
3450	$\gamma_{\text{O-H}}$

The above-mentioned studies were carried out with a view to make use of the data on the metal exchanged zeolites to understand the structural details of Y zeolite encapsulated metal complexes.

3.3.2. Y ZEOLITE ENCAPSULATED SALOPH COMPLEXES

Y zeolite encapsulated Saloph complexes of Mn(II), Co(II), Ni(II) and Cu(II), represented by the notation, MSOPY, were synthesised using the metal template method. The complexes were characterised using chemical analysis, SEM, XRD, surface area and magnetic moment measurements and electronic, FTIR and EPR spectroscopy. Thermal behaviour of the zeolite complexes in inert atmosphere was studied by TG analysis.

3.3.2.1. Chemical analysis

The analytical data of the zeolite complexes are given in Table III.4. The data shows that the Si/Al ratio is around 2.3 for the entrapped complexes. This proves that the

zeolite framework is unaltered even after encapsulation. The metal content of the encapsulated complexes is less compared to the corresponding metal exchanged zeolites, which suggests that a portion of the metal that remains uncomplexed is re-exchanged with the Na^+ ions. CHN data for the complexes suggest the presence of only one ligand around the central metal ion.

TABLE III.4 Analytical data of encapsulated complexes

Sample	% Metal	% Si	%Al	%Na	%C	%H	%N
MnSOPY	2.66	19.90	8.20	6.43	7.12	0.46	1.41
CoSOPY	2.70	18.70	7.60	5.71	6.60	0.39	1.22
NiSOPY	2.45	19.20	7.90	2.66	6.71	0.42	0.89
CuSOPY	2.82	18.31	7.40	3.21	6.94	0.36	0.92

3.3.2.2. T.G Studies

To have an idea about the influence of the zeolite framework on the thermal stability of the complexes, TG of all the samples were recorder at a heating rate of $10^\circ\text{C}/\text{min}$. in nitrogen atmosphere These curves are shown in Fig.III. 4. The data is summerised in TableIII. 5. All the encapsulated complexes show a different pattern of TG when compared to the metal exchanged zeolite and parent NaY. The first stage may be due to the loss of water. The sample isolated after the first stage of decomposition exhibits FTIR spectrum characteristic of the complex. Hence the encapsulated complexes decompose only after the first stage of decomposition. The weight loss during the second stage of decomposition is much higher than that due to the decomposition of the encapsulated complex alone. Therefore additional water loss may also be occurring at this stage. This observation indicates encapsulation of complexes in the super cage.

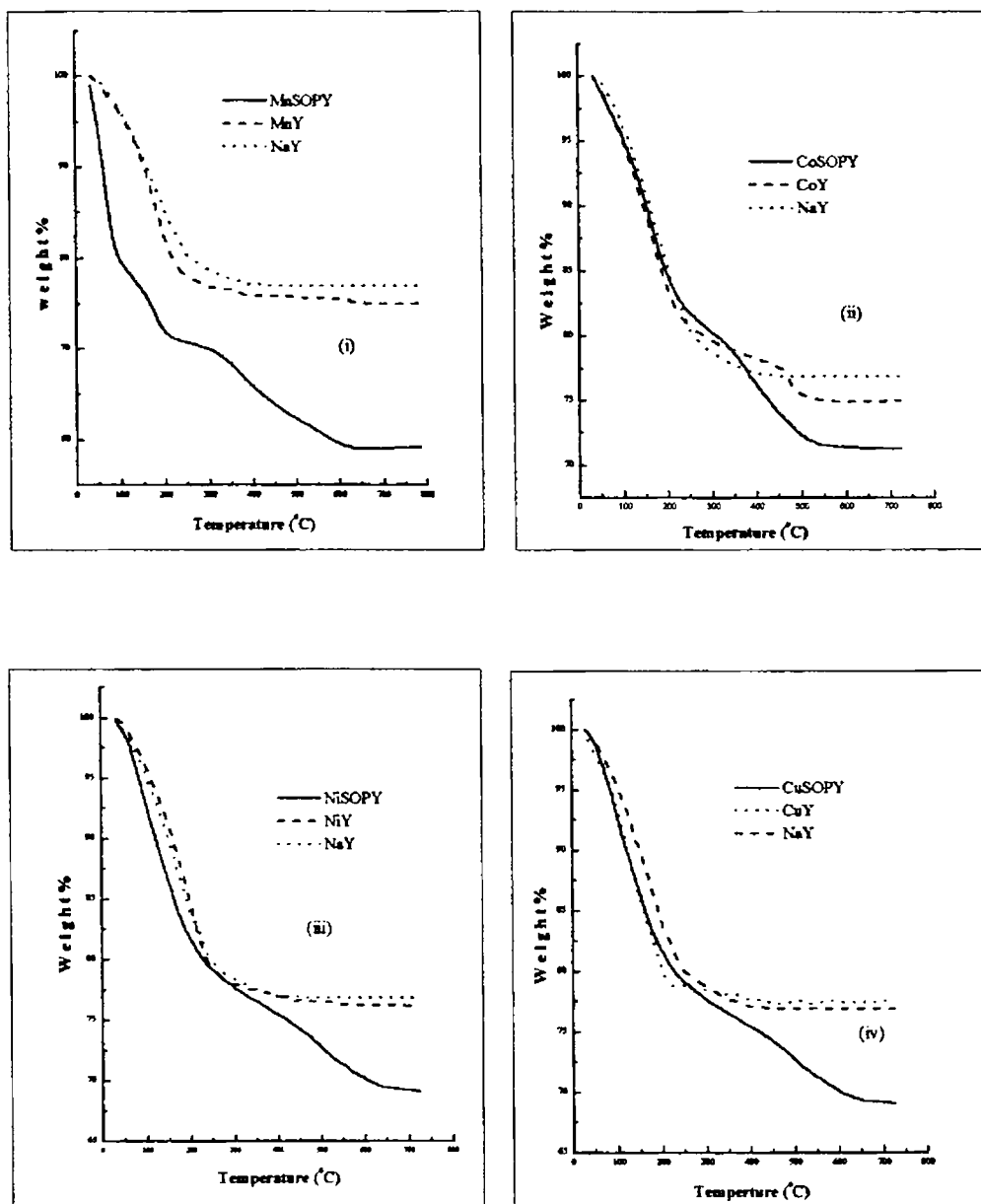


Figure III. 4. TG curves of zeolite complexes, metal exchanged zeolites and NaY.

(i) MnSOPY

(ii) CoSOPY

(iii) NiSOPY

(iv) CuSOPY

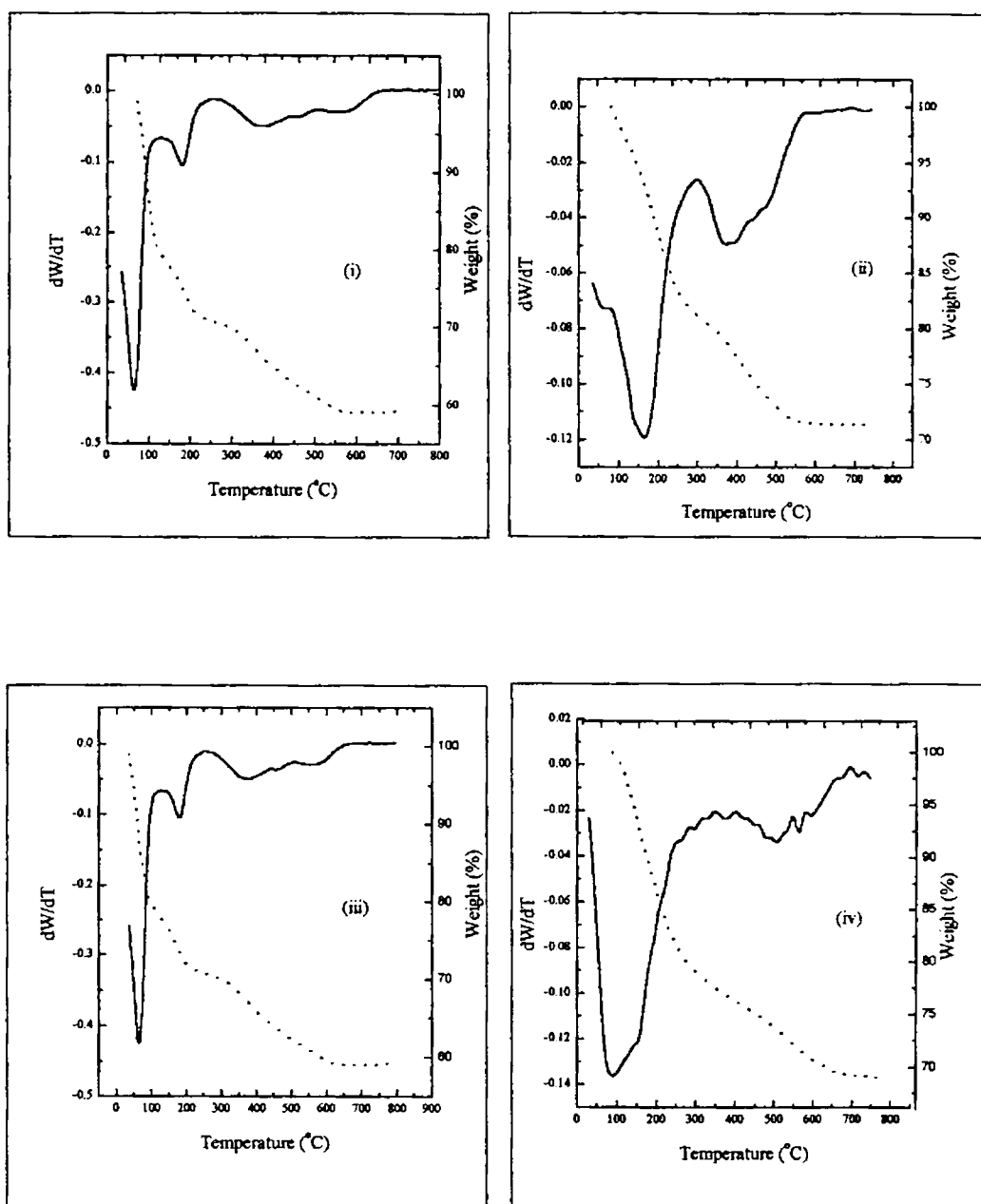


Figure III. 5. TG/DTG curves of encapsulated SOPY complexes

(i) MnSOPY

(ii) CoSOPY

(iii) NiSOPY

(iv) CuSOPY

Table III.5 TG/DTG data

Sample	Weight loss-Stage I			Weight loss-Stage II		
	Temp. range(°C)	Peak temp. (°C)	% mass loss	Temp. range(°C)	Peak temp. (°C)	% mass loss
MnSOPY	50-115	58	14.0	150-230	175	5.8
CoSOPY	75-210	160	13.5	300-550	350	8.5
NiSOPY	70-115	75	11.8	195-600	350	8.5
CuSOPY	50-216	90	17.0	250-650	500	7.5

3.3.2.3. SEM analysis

Scanning electron micrograph of MnSOPY before and after soxhlet extraction in different magnifications are given in Fig. III 6. In the SEM of the impure sample the surface boundaries of the lattice are not clear. But, after the soxhlet extraction the surface boundaries are clearly visible which indicates that the extraction is effective in removing the surface adsorbed species. So the same procedure was adopted for the purification of the rest of the complexes. From the micrograph, it can be inferred that the NaY has got an average particle size of 1 μ m. The same particle size has been retained in MnY and in the encapsulated complex. So the morphology of the parent zeolite Y is not changed as a result of encapsulation.

3.3.2.4. X-ray diffraction analysis

The XRD patterns of the encapsulated complexes are given in Fig.III 7. They appear similar to those of the corresponding metal exchanged zeolites and the parent zeolite. Therefore, the zeolite framework structure was not altered during the encapsulation of the complexes within the super cage. Similar observations have been reported in the literature [22,23].

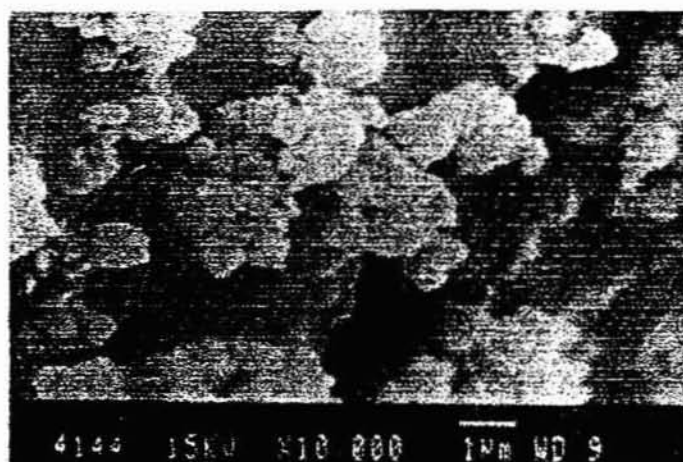


(i)

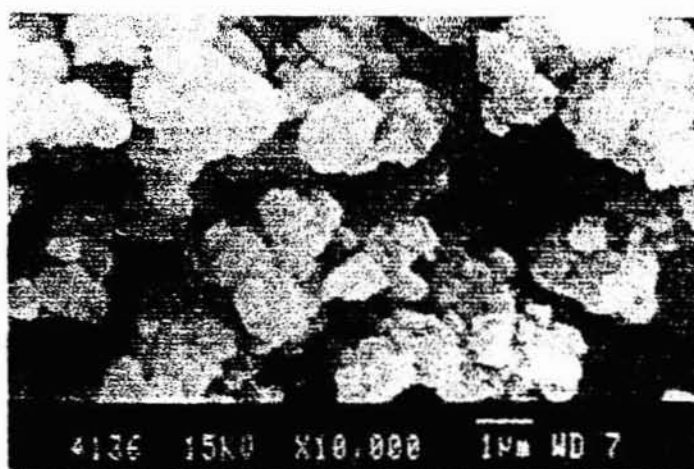


(ii)

Fig III.6. SE micrograph of (i) NiY (ii) MnY



(iii)



(iv)

Fig.III.6 SE micrograph of MnSoPY
(iii) before and (iv) after soxhlet extraction

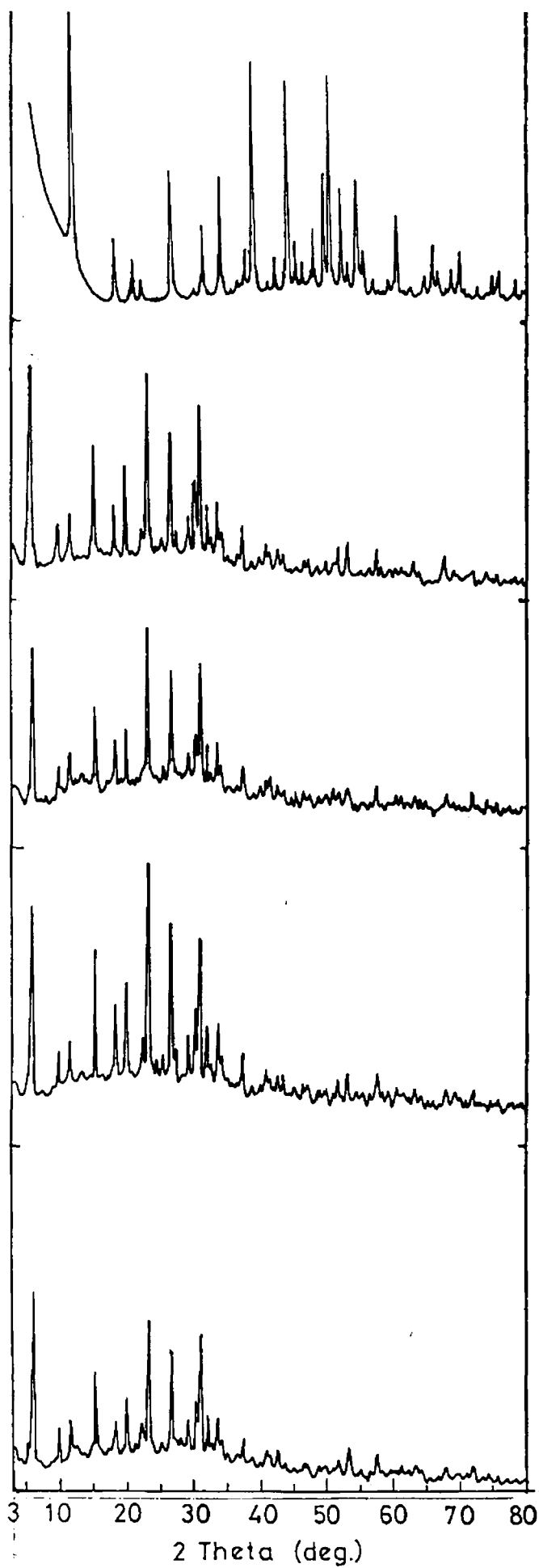


Fig. IIL7 XRD Patterns of

(i) MY

ii) MnSOPY

(iii) CoSOPY

(iv) NiSOPY

(v) CuSOPY

3.3.2.5. Surface area analysis

The surface area values of the Saloph complexes encapsulated in the cavity of Y-zeolite are given in Table III.6. The data has been represented as bar chart also (see Fig III.7). There is a marked decrease in surface area of the encapsulated complexes from the metal exchanged zeolites. Such lowering of the surface area values as a result of encapsulation has been reported by Balkus and Gabrielov [25]. The filling of the complexes within the zeolite pores might be a reason for the lowering of surface area.

TABLE III.6 Surface area data of the encapsulated metal complexes

Sample	Surface area (m ² /g)		
	MY	MSOPY	%Loss
NaY	549	-	-
MnSOPY	539	315	41.5
CoSOPY	532	399	25
NiSOPY	528	340	35.6
CuSOPY	528	335	36.55

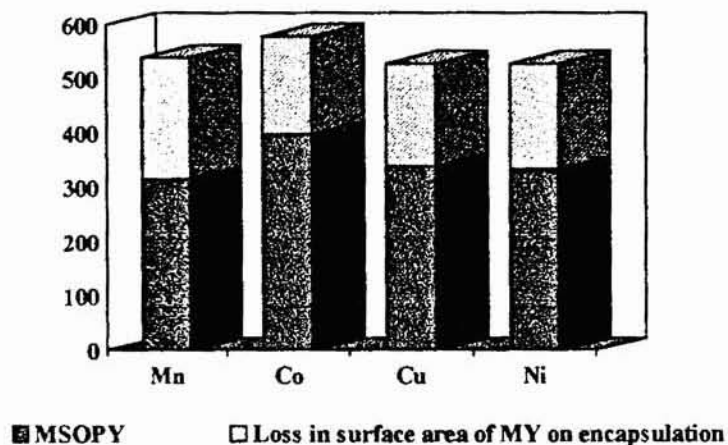


Fig III. 8. Decrease of surface area of metal exchanged zeolites on encapsulation

3.3.2.6. Magnetic moment

The magnetic moment values of zeolite complexes were measured using the Gouy method at room temperature. The magnetic moment determination by this method cannot be considered as very accurate, as the application of diamagnetic correction due to the zeolite support and the paramagnetic contribution of the traces of iron impurity are not perfect. In the present study, the magnetic susceptibility of the NaY zeolite was measured and its value was added to the magnetic moment of the encapsulated complexes after calculating the magnetic susceptibility per mole of the metal ion.

Room temperature magnetic moment values of the encapsulated metal complexes are given in Table III.7. The magnetic moment of the MnSOPY complex was found to be 5.9 BM, which corresponds to the presence of five unpaired electrons. The high spin Mn(II) complexes are reported to exhibit magnetic moment close to spin only values irrespective of their coordination in octahedral or tetrahedral fields or even in geometries of lower symmetries [26]. The room temperature magnetic moment of CoSOPY is 4.7. Usually tetrahedral Co(II) complexes have magnetic moment values in the range 4.4-4.8 BM which is higher than the spin only value. This is due to the mixing of the excited 4T_2 (F) term into the ground 4A_2 term as a result of spin-orbit coupling [27,28]. So the observed magnetic moment indicates a tetrahedral symmetry for the encapsulated complex.

TABLE III.7 Magnetic moment data

Sample	Magnetic moment (BM)
MnSOPY	5.9
CoSOPY	4.7
NiSOPY	3.2
CuSOPY	1.8

The NiSOPY has a magnetic moment value of 3.2 BM. This lies in the boarder of a distorted tetrahedral and a tetrahedral geometry [28]. As the distortion from the tetrahedral field increases, the magnetic moment value reduces towards the spin-only value of 2.83 BM [27]. So the magnetic moment value suggests a tetrahedral or a slightly distorted tetrahedral environment for the Ni(II) in NiSOPY complex.

A magnetic moment of 1.79 BM was observed for the CuSOPY complexes. Usually the magnetic moment values of the copper(II) complexes are in the range 1.75-2.2 BM [27]. It is not possible to arrive at the geometries for Cu complexes on the basis of room temperature magnetic moment values alone. However, square planar Cu(II) complexes have values closer to the lowest limit and the distortion from the planar structure results in higher magnetic moment values.

3.3.2.7. Electronic spectra

Optical reflectance spectra were recorded and plotted as percentage reflectance against wavelength. Kubelka-Munk analysis was done on the data using the procedure given in Chapter II. To have an idea, the $F(R)$ is plotted against wavelength in the corresponding diffuse reflectance spectrum.

Generally the intensity of the absorption band is very low as the complex is well buried inside the cavity. The ligand absorption and charge transfer transition may further complicate the interpretation of the electronic spectra. The electronic spectral data of the encapsulated complexes and their tentative assignments are given in Table III.8.

Being a d^5 system, the electronic transitions are both spin and orbitally forbidden for the high spin complexes of Mn(II). In an octahedral field, Mn(II) gives spin- as well as parity-forbidden transitions of very low intensity due to weak spin- orbit coupling. There is an excited "spin quadruplet" state for the d^5 ion with two paired electrons. In such complexes usually there is a broad band around $20,000\text{ cm}^{-1}$ with shoulder indicating that the two absorptions are very close together [29]. Generally, molecular vibrations and spin-orbit coupling are responsible for the broadening of absorption bands. It is clear from the

Tanabe-Sugano diagram that the degenerate ${}^4E_g(G)$ and ${}^4A_{1g}(G)$ terms of the octahedral d^5 ion are parallel to the ground ${}^6A_{1g}$ term. So the energy of the ground term will not be affected either by molecular vibrations or by spin-orbit coupling. At sufficiently high values of the crystal field splitting energy (Δ), a t_{2g}^5 configuration gives rise to a doublet ground state. For Mn(II), the pairing energy is high and only a few of the strongest ligand sets can accomplish this

It is evident from Fig. III. 9 that there is considerable change in the electronic spectra of the parent Y zeolite upon metal exchange. The exchanged metal as a result of coordination shows more bands in the visible region that may be due to the modified environment of the Mn(II) as a result of complexation. The absorption at $15,200\text{ cm}^{-1}$ in MnSOPY may be due the ${}^4T_{1g}(G) \leftarrow {}^6A_{1g}$ of an octahedral Mn(II). The ${}^4T_{2g}(G) \leftarrow {}^6A_{1g}$ occurs at $21,000\text{ cm}^{-1}$ in this complex. The broad band around $24,000\text{ cm}^{-1}$ may be the result of ${}^4E_g(G) \leftarrow {}^6A_{1g}$ and ${}^4A_{1g}(G) \leftarrow {}^6A_{1g}$ transitions. The ${}^4T_{2g}(D) \leftarrow {}^6A_{1g}$ occur at $28,500\text{ cm}^{-1}$ in MnSOPY. In the encapsulated complex, there is a band around $30,700\text{ cm}^{-1}$, which, may be ${}^4E_g(D) \leftarrow {}^6A_{1g}$ of an octahedral Mn(II). So spin and parity-forbidden ^{transitions} are observed in the present Mn(II) complex.

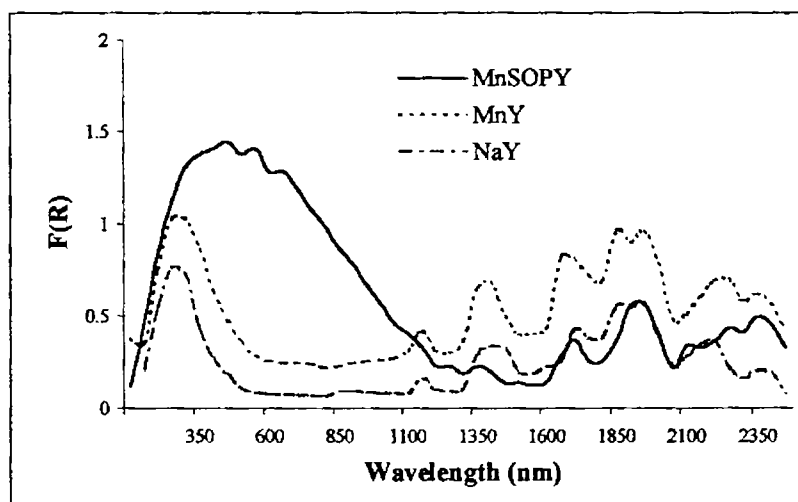


Fig.III.9. Diffuse reflectance spectrum of NaY, MnY and MnSOPY

A penta coordinated structure has been proposed for the Mn(II) Salen complex encapsulated in zeolite Y by Bowers and Dutta [30]. On the contrary, some other workers have reported octahedral coordinated Mn Salen complexes within the super cage of Y zeolite [16]. So spin, parity-forbidden transitions are observed in the present Mn(II) complex.

Fig.III.10 represents the diffuse reflectance spectrum of CoSOPY along with that of CoY and NaY. It clearly indicates encapsulation of the metal complex.

The high spin state of a d^7 ion in a tetrahedral field provides three spin-allowed d-d transitions ν_1 , ν_2 and ν_3 occurring from the quartet ground state to the excited quartet state. The ν_3 band is due to ${}^4T_1(P) \leftarrow {}^4A_2(F)$ transition and the ν_2 band due to the ${}^4T_1(F) \leftarrow {}^4A_2(F)$ transition. The ν_1 band, ${}^4T_2(F) \leftarrow {}^4A_2(F)$ is expected in the near IR region $3000-5000\text{ cm}^{-1}$.

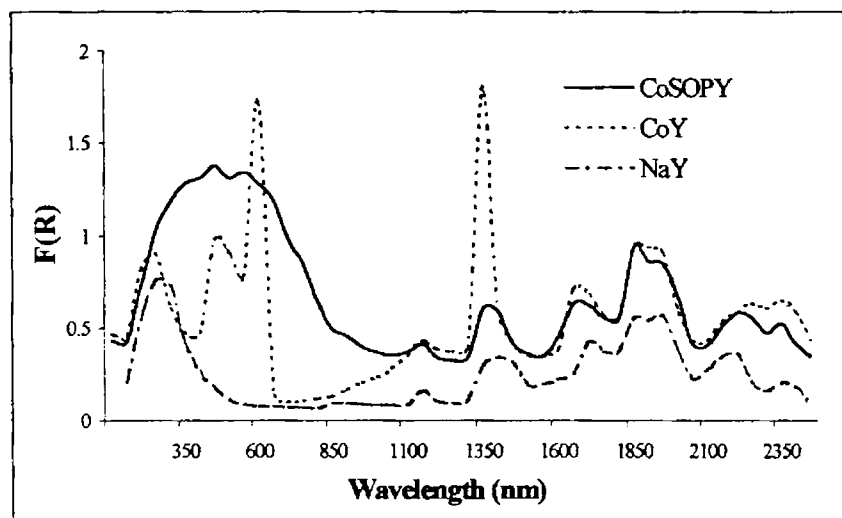


Fig.III.10. Diffuse reflectance spectrum of CoSOPY,CoY and NaY

As a general observation, the visible spectrum of the d^7 ion in a tetrahedral field is dominated by the highest energy transition, ν_3 [31]. In the case of CoSOPY complex, the ν_3 band appears as multiple peaks. The visible transition of the d^7 ion in the high spin

tetrahedral environment is with very complex envelopes as a result of a number of transitions due to doublet excited state occurring in the same region. Further this band acquires same intensity by means of spin-orbit coupling [30,32]. The band with absorptions around $21,270\text{ cm}^{-1}$, $16,660\text{ cm}^{-1}$ and $15,380\text{ cm}^{-1}$ may be due to the transition ${}^4T_1(P) \leftarrow {}^4A_2(F)$. the ${}^4T_1(F) \leftarrow {}^4A_2$ and ${}^4T_2 \leftarrow {}^4A_2$ transition data present in the near IR region may be masked by the bands due to the frame work of the zeolite. The simple Co(II) complex have been reported to have square planar structure [33]. The SALOPH ligand is very rigid. So the distortion from planarity may be induced by the frame work.

In a cubic field, three spin-allowed transitions are expected for Ni(II) due to the splitting of the free-ion, ground 3F term and the presence of the 3P term. The expected bands are:

$$\begin{aligned} \nu_1 &= {}^3T_2(F) \leftarrow {}^3T_1(F) \\ \nu_2 &= {}^3A_2(F) \leftarrow {}^3T_1(F) \text{ and} \\ \nu_3 &= {}^3T_1(P) \leftarrow {}^3T_1(F). \end{aligned}$$

These bands may be very often split by spin-orbit coupling. For a regular or nearly regular tetrahedral Ni(II), ν_3 occur in the visible region around 15000 cm^{-1} [31].

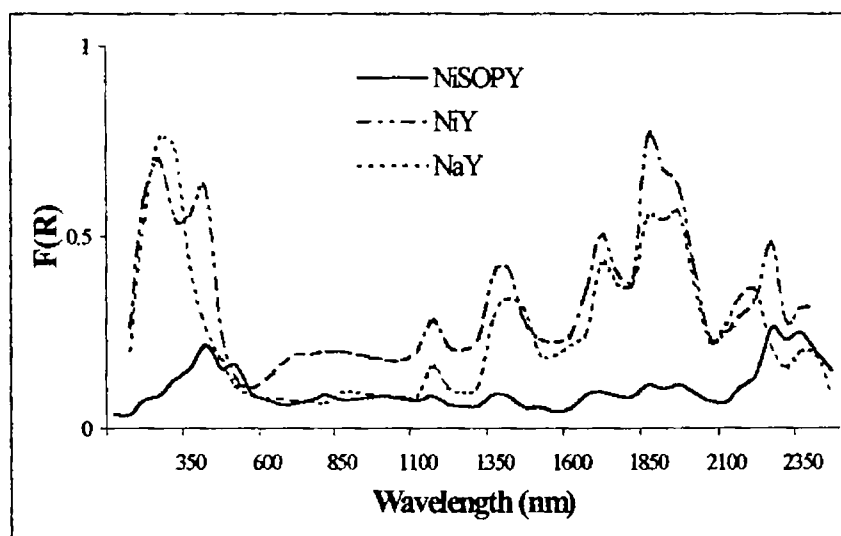


Fig. 11.11. Diffuse reflectance spectrum of NiSOPY, NiY and NaY.

The band around 6700 cm^{-1} in the spectrum of NiSOPY may be the ${}^3A_2(F) \leftarrow {}^3T_1(F)$ transition of a tetrahedral Ni(II) complex with distortion. In the present complex, the ${}^3T_1(P) \leftarrow {}^3T_1(F)$ transition is occurring at $12,340\text{ cm}^{-1}$. The ${}^3T_2(F) \leftarrow {}^3T_1(F)$ transition in the near IR region may be masked in the complex. The magnetic moment also suggests a distorted tetrahedral structure for NiSOPY.

The Cu(II) systems, due to the Jahn-Teller distortion exhibit large distortions from octahedral symmetry and give rise to more bands. The broad or double band around $15,000\text{ cm}^{-1}$ is normally assumed to represent one rather than two transitions [29]. The bands are often split by spin-orbit coupling to an extent, which can make unambiguous assignments difficult. The expected transitions are:

$$\nu_1 = {}^3T_2(F) \leftarrow {}^3T_1(F)$$

$$\nu_2 = {}^3A_2(F) \leftarrow {}^3T_1(F) \text{ and}$$

$$\nu_3 = {}^3T_1(P) \leftarrow {}^3T_1(F)$$

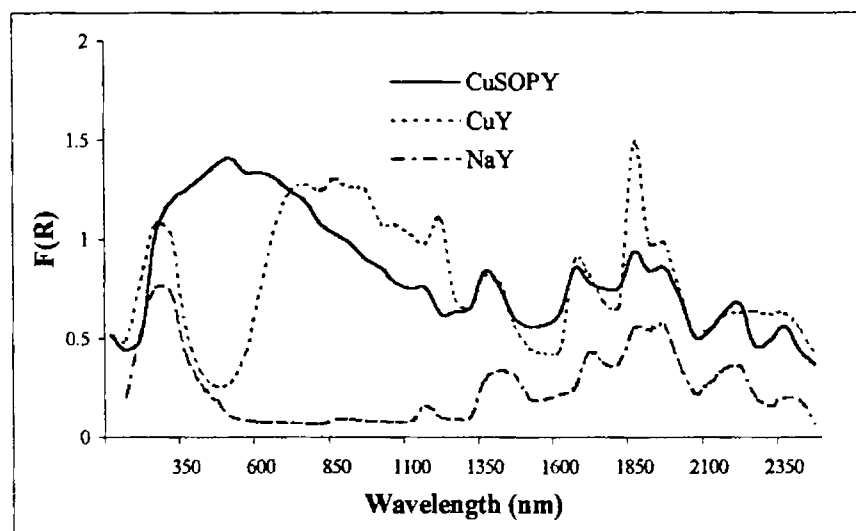


Fig. III.12. Diffuse reflectance spectrum of CuSOPY, CuY and NaY.

TABLE III.8 Electronic spectral data

Sample	Abs. Max (cm^{-1})	Tentative assignments
MnSOPY	15,200	${}^4T_{1g}(G) \leftarrow {}^6A_{1g}$
	21,000	${}^4T_{2g}(G) \leftarrow {}^6A_{1g}$
	24,000	${}^4E_g(G) \leftarrow {}^6A_{1g}$
		${}^4A_{1g}(G) \leftarrow {}^6A_{1g}$
	28,500	${}^4T_{2g}(D) \leftarrow {}^6A_{1g}$
	30,700	${}^4E_g(D) \leftarrow {}^6A_{1g}$
CoSOPY	15,380	
	16,660	${}^4T_1(P) \leftarrow {}^4A_2(F)$
	21,270	
NiSOPY	6,700	${}^3A_2(F) \leftarrow {}^3T_1(F)$
	12,340	${}^3T_1(P) \leftarrow {}^3T_1(F)$
CuSOPY	13,800	d-d band

As seen from Fig.III.12, in the encapsulated Cu(II) complex, the band in the visible region has too many unsymmetrical envelopes seeing to encompass several overlapping transitions but resolution into proper number of sub bands with correct location is difficult. This is noted as a characteristic feature of Cu²⁺ in a field of lower symmetry than cubic [29]. So CuSOPY complex may be assigned as having a tetragonal geometry as the band around 13,800 cm⁻¹ appears as a multiple band. The electronic transitions of the above mentioned encapsulated metal complexes are summarized in the following table:

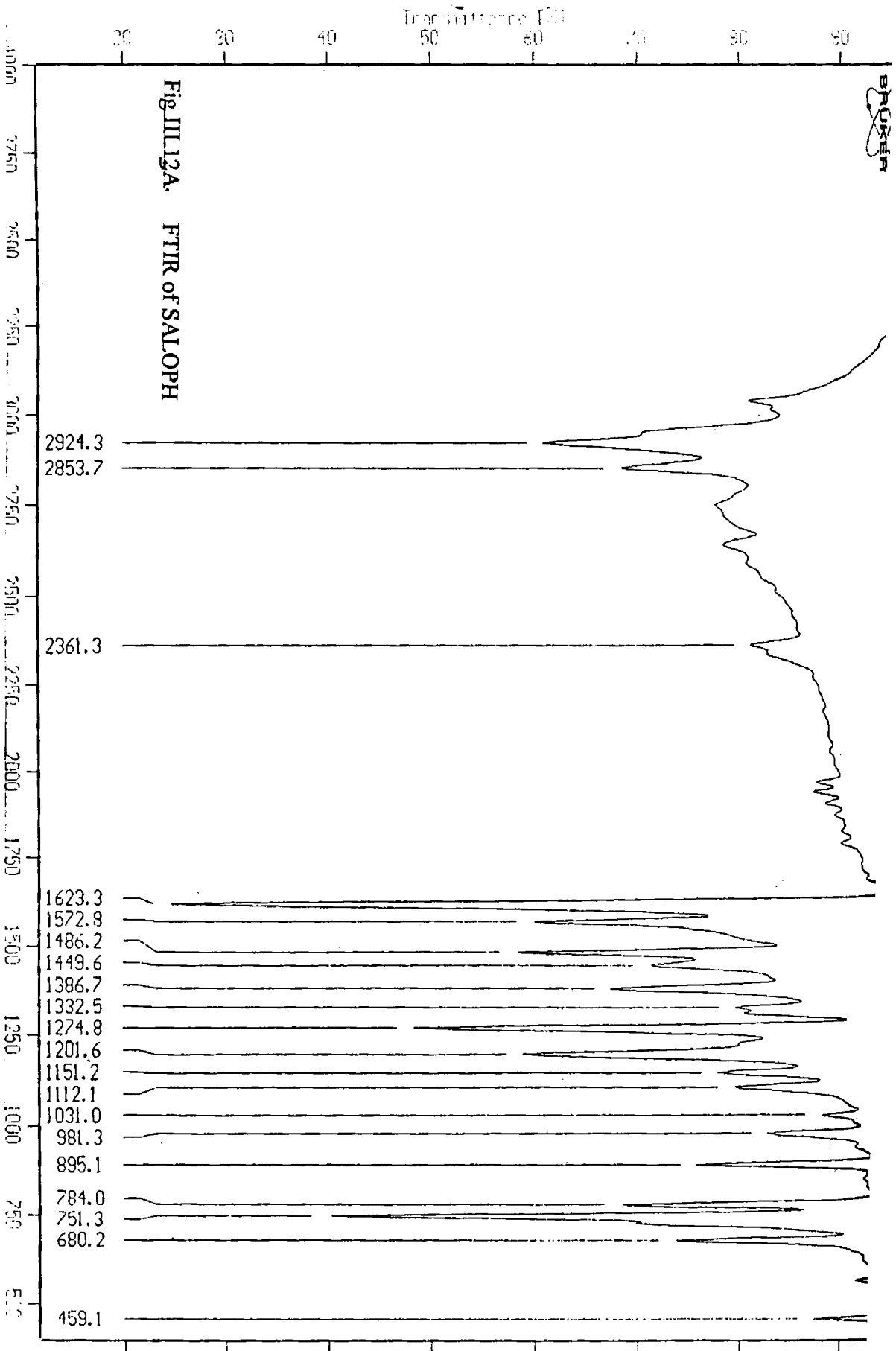
3.3.2.8. Infrared Spectra

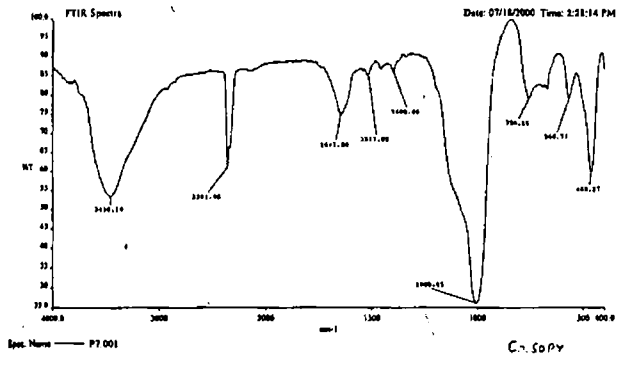
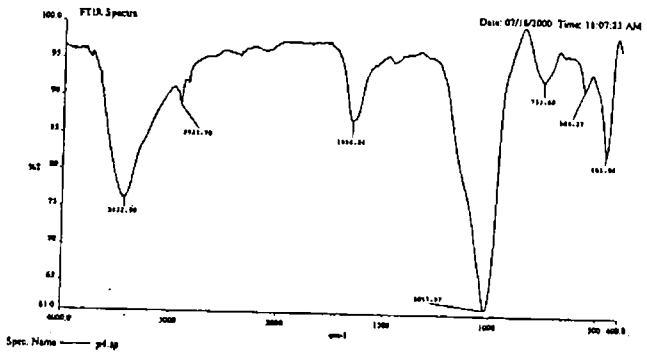
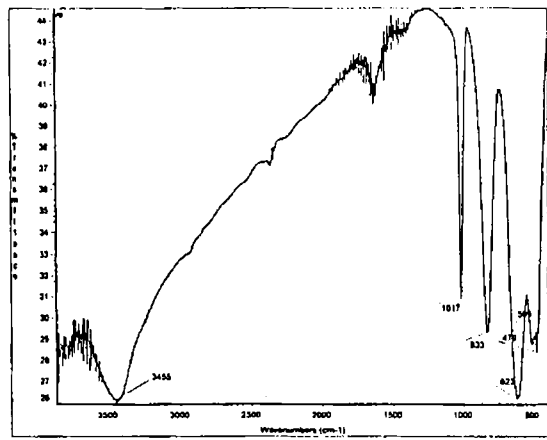
Infrared spectroscopy can be used for the identification of the complex formation within the zeolite cavity. The IR spectra of the ligand and the encapsulated complexes are given in Fig.III.13. A comparison of the vibrational bands is given in Table III.9.

In the Saloph ligand, the azomethine group stretching vibration is occurring at 1624 cm⁻¹. In all the complexes, the frequency of $\nu_{C=N}$ has undergone a shift to higher wave numbers. Such a shift to higher wave numbers has been reported by earlier workers also [33]. But in the hydrated zeolite sample there is a very sharp peak around 1600 cm⁻¹ that may be due to the δ_{H-O-H} . So the vibrational spectra of the metal exchanged as well as the parent zeolite Y samples were taken after dehydration and compared. This peak is absent in the dehydrated NaY sample. The FTIR spectrum of the complex, which was heated upto 400°C showed the presence of azomethine group vibration around 1640 cm⁻¹. The retention of this peak even at this high temperature indicates that this band is due to the $\nu_{C=N}$ of the ligand (which has undergone a blue shift after complexation.)

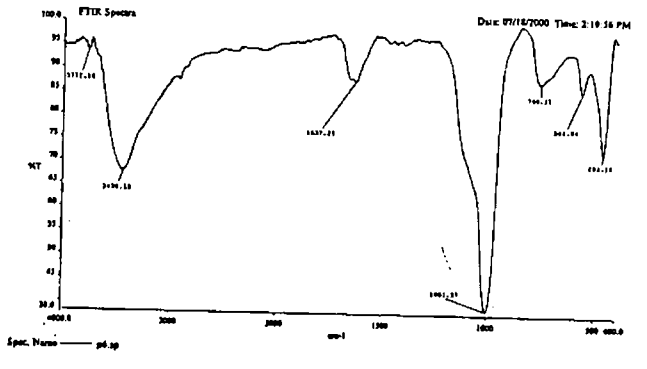
3.3.2.9. EPR spectroscopy

EPR spectroscopy is a very important tool in arriving at the coordination geometry of the metal ion in the zeolite. In the present study the EPR parameters were calculated manually for the Cu and Mn complexes and the information obtained from this could provide a qualitative idea about the nature of the coordination sphere in the encapsulated complexes. The EPR of the Cu(Saloph) encapsulated in Y zeolite at liquid nitrogen

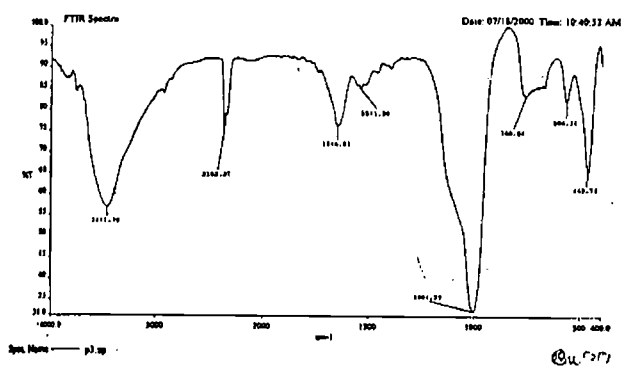




CoSOPY



pd.sp



CoSOPY

Fig.III.12B. FTIR of (i) MY
 (ii) MnSOPY
 (iii) CoSOPY
 (iv) NiSOPY
 (v) CuSOPY

Table III.9 IR Spectral data of MY, SALOPH and zeolite complexes

MY	SALOPH	MnSOPY	CoSOPY	NiSOPY	CuSOPY
460	459	459	450	452	460
					566
570	573				
680	680				
750	751	749	752		760
	784				
	895				
	981		1014	1003	1004
1000					
	1031	1042			
	1112				
	1151				
	1202				
	1275				
	1333				
	1387				
	1450				
	1486				
	1573				
1600	1623	1637	1642	1640	1647
	2361	2362	2362	2362	2363
	2854	2921			
	2924				
			3400		
3456		3437		3432	3447

temperature is given in Fig. III/4. The EPR data are given in Table III.10. The $A_{||}$ value obtained is 133.3 G. The value is indicative of an axial symmetry around the copper ion. This may be due to the ionic nature of the bonding in the CuSOPY that may be expected for zeolite encapsulated complexes generally. Furthermore, $g_{||} > g_{\perp} > 2$ and $G = (g_{||}-2) / (g_{\perp}-2) > 4.4$, which suggest a $d_{x^2-y^2}$ ground state with a large exchange coupling for the complex [36]. The $g_{||}$ value obtained is greater than 2.3. The ratio $g_{||}/A_{||}$ is 179 indicating a high degree of distortion. This distortion may be due to the interaction of zeolite framework on the encapsulated complex.

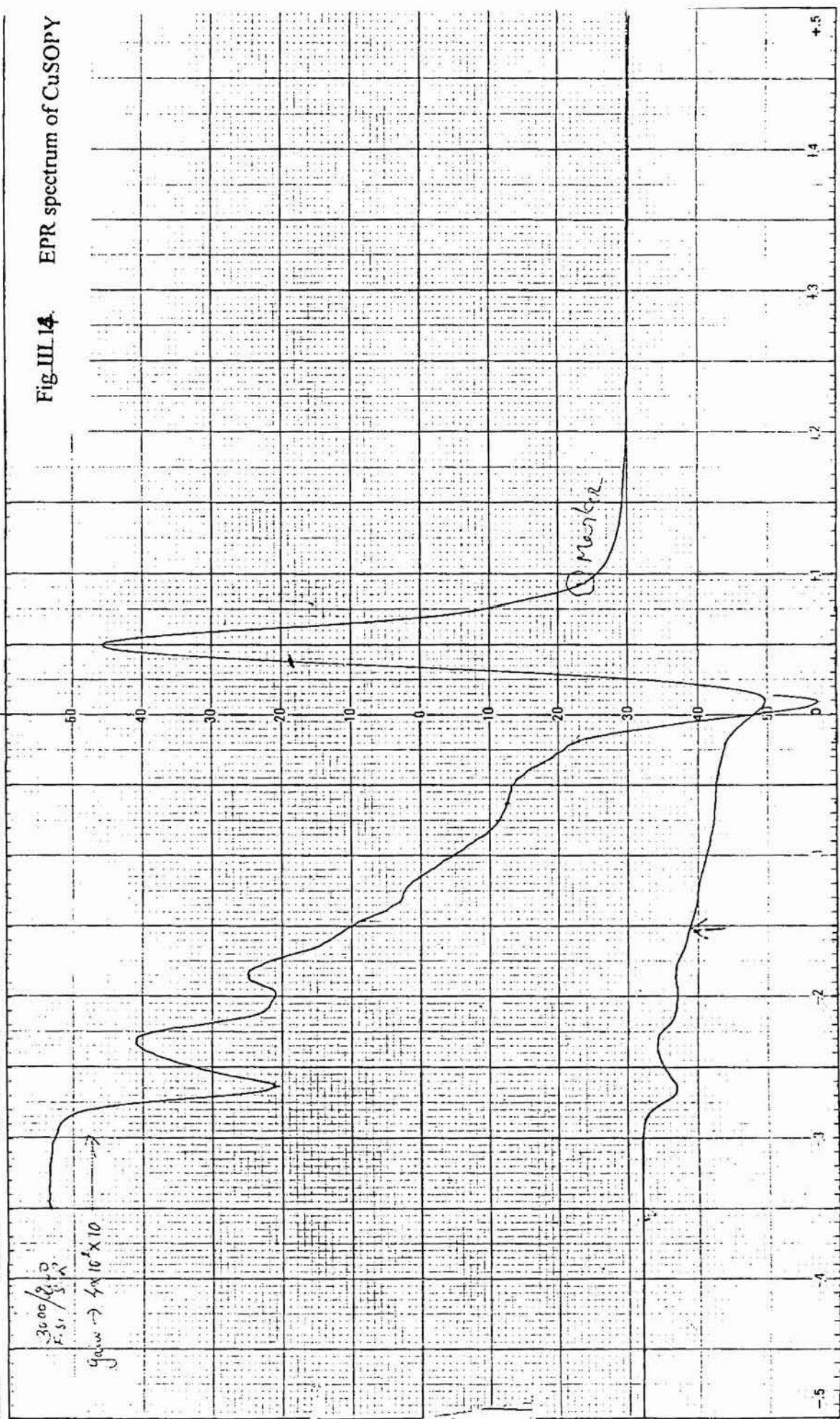
TABLE III.10 EPR spectral data of CuSOPY

EPR parameter	CuSOPY
$g_{ }$	2.38
$A_{ }$	$14.354 \times 10^3 \text{ cm}^{-1}$
$g_{ } / A_{ }$	178.95
g_{\perp}	2.07
α^2	0.4541

The CoSOPY is also found to be EPR active. However the spectra is very broad at LNT, which indicates that Co(II) is in the high spin state. This may be an indication of the fact that the Co(II) is in the high spin state. Any further conclusion regarding the structure could not be arrived from the spectra. The EPR spectrum of MnSOPY is presented in Fig. III. 15. The spectrum shows six peaks characteristic of $I = 5/2$ of Mn(II) ion. The g value was found to be 1.99 G. Mn(II) exchanged zeolites has been reported to have an A value of 87G. In the present case A values is found to be 110G. Such increase in A value has been observed by earlier workers also [35, 36].

Field Set: 3000 Gauss, Scan Time: 5 min, Modulation Frequency: 50 kHz, Modulation Amplitude: 0.5 G, Microwave Frequency: 9.1 GHz, Date: 3/11, Remarks: 1-3

Fig. III 14. EPR spectrum of CuSO₄



SCAN RANGE

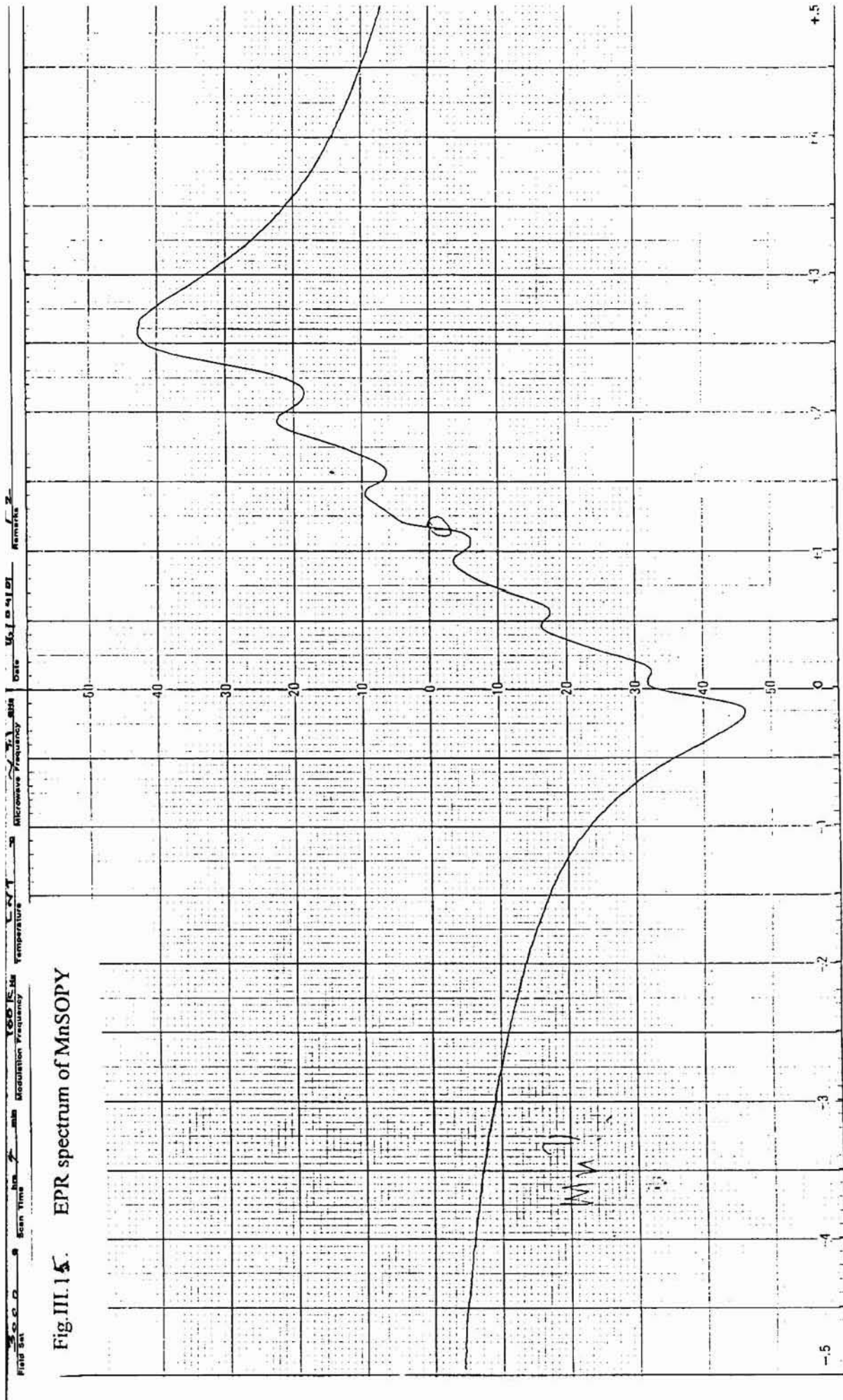


Fig. III. 15. EPR spectrum of MnSO₄

REFERENCES:

- [1] D.X. West, S.B. Padhye, P.B. Sonawane, *Struct. Bonding* **76** (1991) 1.
- [2] M.A. Ali, S. E. Livingstone, *Coord. Chem. Rev.* **13** (1974) 101.
- [3] D.H. Jones, R. Slack, S. Squires, K.R.H. Wooldridge, *J.Med.Chem.* **8** (1965) 676.
- [4] J. Lasada, I. Del Peso, L. Beyer, *Inorg.Chim. Acta* **321** (2001) 107.
- [5] A.F. Marinovich, R.S. O' Mahony, J.M. Waters, T.N.M. Waters, *J.Croat. Chem. Acta* **72** (1999) 685.
- [6] E.V. Lovecchio, E.S. Gore, D.H. Bucch, *J.Am.Chem.Soc.* **96** (1974) 3109.
- [7] G.S. Patterson, R.H. Holm, *Bio. Inorg.Chem.* **161** (1978) 109.
- [8] T. Jeeworth, H. Li Kam Wah, M.G. Bhowon, D.B.K. Ghoorohoo, *Synth. React. Inorg. Met. -org. Chem.* **30** (2000) 1023.
- [9] T.D. Thangadurai, K. Natarajan, *Trans. Met. Chem.* **26** (2001) 712.
- [10] P. Gallezot, in M. Moskovits (Ed), *Metal Clusters*, John Wiley, New York, 1986, p.219.
- [11] J.H. Lunsford, *Rev. Inorg. Chem.* **9** (1987) 1.
- [12] J.M. Basset, A. Theolier, D. Commereue, Y. Chauvin, *J.Organomet.Chem.* **279** (1985) 147.
- [13] S. Kowalak, R.C. Weiss, K.J. Balkus, Jr. *J.Chem.Soc., Chem.Comm.* (1991) 57.
- [14] C. Ratnasamy, A. Murugkar, S. Padhye, *Ind. J. Chem.* **36A** (1996) 1
- [15] N. Herron, *Inorg. Chem.* **25** (1986) 4714.
- [16] N. Ulagappan, V. Krishnasamy, *Ind. J.Chem.* **35A** (1996) 787.
- [17] R. Parton, D. De Vos, P.A. Jacobs, in E.G. Deroune (Ed), *Zeolite microporous solids: Synthesis, structure and reactivity*, Kluwer, Netherlands, 1992, 555.
- [18] N. Herron, *Chem Tech* (1989) 542.
- [19] C. Naacache, Y. B. Taarit, *Pure. Appl. Chem.* **52** (1980) 2175.
- [20] N. Herron, G.D. Stucky, C.A. Tolman, *J. Chem. Soc. Commun.*, 1986, 1521.
- [21] C. Tolman, N. Heron, Symposium in Hydrocarbon Oxidation, 194th National Meeting of the Am. Chem. Soc., New Orleans, LA, Aug. 30-Sept. 4, 1987.

- [22] P.G. Menon in S.Ramasheshan (Ed.), Lectures on Catalysis, 41st Ann. Meet. Ind. Acad. Sci., 1975.
- [23] M. Diegruber, P.J. Plath, G. Schulz-Ekloff, M. Mohl, *J. Mol. Catal.*, 24 (1984) 115
- [24] E. Paez-Mozo, N. Gabriunas, F. Lucaccioni, D.D. Acosta, P. Patrono, A. La Ginestra, P. Ruiz, B. Delmon, *J. Phys. Chem.*, 97 (1993) 12819.
- [25] K.J. Balkus, Jr, A.G. Gabrielov, *J. Inclus. Phenom. Mol. Reagn. Chem.*, 21(1995) 159 (1959) 3997.
- [26] B.N. Figgis, J. Lewis, *Progr. Inorg. Chem.* 6 (1964) 97.
- [27] N.N. Greenwood, A. Earnshaw, The Chemistry of the Elements, Pergamon Press, New York, 1989.
- [28] L.J.Heidt, G.F. Koster, A.M. Johnson, *J.Am. Chem. Soc.* 80, 6471.
- [29] F.A. Cotton, G. Wilkinson, Advanced Inorganic Chemistry, 5th Edn., John Wiley and Sons. New York, 1988.
- [30] C. Bowers, P.K. Dutta, *J. Catal.* 122 (1990) 271.
- [31] A.B.P. Lever, Inorganic Electronic spectroscopy, 2nd Edn., Elsevier, New York, 1984.
- [32] C. Daul, C.W. Schlapfer, A.von Zelewsky in structure and Bonding, 36
- [33] M. P. Vinod, T. Kr Das, A.J. Chandwadkar, K. Vijaymohanan, J.G. Chandwadkar, Materials Chemistry and Physics, 58 (1999) 37.
- [34] M.J.Bew, B.J. Hathway, R.F. Faraday, *J. Chem. Soc. Dalton Trans.* (1972) 1229.
- [35] N. Ulagappan , V. Krishnasamy, *Ind. J. Chem.*, 35A (1996) 787.
- [36] S.K. Sur, R.G. Bryant, *J. Phys. Chem.*, 97 (1993) 2686.

CHAPTER IV

STUDIES ON Y ZEOLITE ENCAPSULATED TRANSITION METAL COMPLEXES OF *N,N'*-Bis(2-HYDROXYMETHYLBENZYLIDENE) 1,2-PHENYLENEDIAMINE

4.1. INTRODUCTION

Tetradentate Schiff bases with an N_2O_2 donor set have been widely studied due to their ability to coordinate metal ions. It is very attractive that the properties of these complexes are largely dependent on the electronic nature and the conformational behaviour of the ligand. The importance of tetradentate Schiff base complexes in modeling oxygenase enzymes has been widely discussed [1]. The absorption of molecular oxygen from atmosphere and the subsequent darkening of the Co Salen are well known [2]. Such dibasic ligand can form neutral complexes with vacant coordination sites making it potentially viable catalysts. The metal complexes of Salen are of appropriate size (10-11Å) and once formed in the super cage of zeolite Y (13Å), the complex cannot escape through the 7Å ring opening [3]. Therefore it is very motivating to carry out studies on similar systems.

In this chapter, the details regarding the encapsulation of Mn(II), Co(II), Ni(II) and Cu(II) complexes of *N,N'*-bis(2-hydroxymethylbenzylidene)-1,2-phenylenediamine and the further characterisation of the complexes using the various physico-chemical techniques are presented.

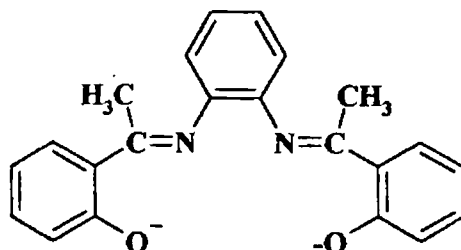


FIG IV. 1. Structure of the ligand

4.2. EXPERIMENTAL

4.2.1. Materials

Details regarding the preparation of the metal exchanged zeolites are given in Chapter II. These metal exchanged zeolites are further used for the encapsulation of the Schiff base complexes using the metal template method. The general procedure for the preparation of the encapsulated complexes is given in Chapter II.

4.2.2. Synthesis of zeolite encapsulated metal complexes

The metal exchanged zeolite (5.0 g) was refluxed with 2-hydroxyacetophenone (4.9 mL, 0.08 M) in dichloromethane (10 mL). The complex so formed was then soxhlet

extracted with methanol. The purified 2-hydroxyacetophenone complex encapsulated in Y zeolite was then complexed with 1,2-phenylenediamine (2.2 g, 0.04M) in methanol (10 mL) for 2 h. The encapsulated complex so formed were purified by soxhlet extraction first with dichloromethane and then with methanol. Then the complex was re-exchanged with 0.01M NaCl solution as mentioned in the previous chapter. The complexes was made free from chloride ions, dried at 120^o C for two hours and stored in vacuum over anhydrous calcium chloride. By adopting the above mentioned procedure zeolite Y encapsulated Mn(II), Co(II), Ni(II) and Cu(II) complexes of the Schiff base *N,N'*- bis(2-hydroxymethylbenzylidene)-1,2-phenylenediamine (MOHOPY) were prepared.

4.2.3. Analytical Methods

A detailed account of the various analytical methods and characterisation techniques employed are given in Chapter II. .

4.3. RESULTS AND DISCUSSION

The Mn(II), Co(II), Ni(II) and Cu(II) complexes synthesised in Y zeolite were characterised by chemical analysis, XRD, surface area and magnetic moment measurements, electronic, FTIR and EPR spectroscopy and TG analysis.

4.3.1. Chemical Analysis

The results of chemical analysis of the complexes are given in Table IV.1. The Si/Al ratio of zeolite complexes were found to be around 2.4 which is found to be the same

for the metal exchanged zeolites. So dealumination was not found to occur in the encapsulated complexes. A good amount of the metal initially present in the metal exchanged zeolites was present in the complexed state and the rest removed as a result of the final ion exchange with NaCl solution.

Table IV.1. Analytical data of encapsulated complexes

Sample	%Metal	%Si	%Al	%Na	%C	%H	%N
MnOHOPY	2.84	18.51	7.53	2.86	6.92	0.49	0.91
CoOHOPY	2.08	19.24	7.83	2.70	7.34	0.32	1.01
NiOHOPY	2.48	18.64	7.64	2.36	7.41	0.53	0.86
CuOHOPY	2.61	19.15	7.73	2.79	6.51	0.41	0.89

The CHN data suggests the presence of only one ligand around the metal ion. So the metal to ligand mole ratio is around 1:1 in these complexes. However the data indicate the presence of trace amount of uncomplexed metal ion, which, cause of the shielding by the encapsulated complexes, might not have been ion-exchanged with Na⁺ ions. These traces of uncomplexed metal ion would not interfere with the properties of the encapsulated complexes.

4.3.2. TG Studies

TG studies of the complexes were carried out in inert atmosphere. The results are summarized in Table IV.2. The TG curves are given in Fig IV.2 and IV.3

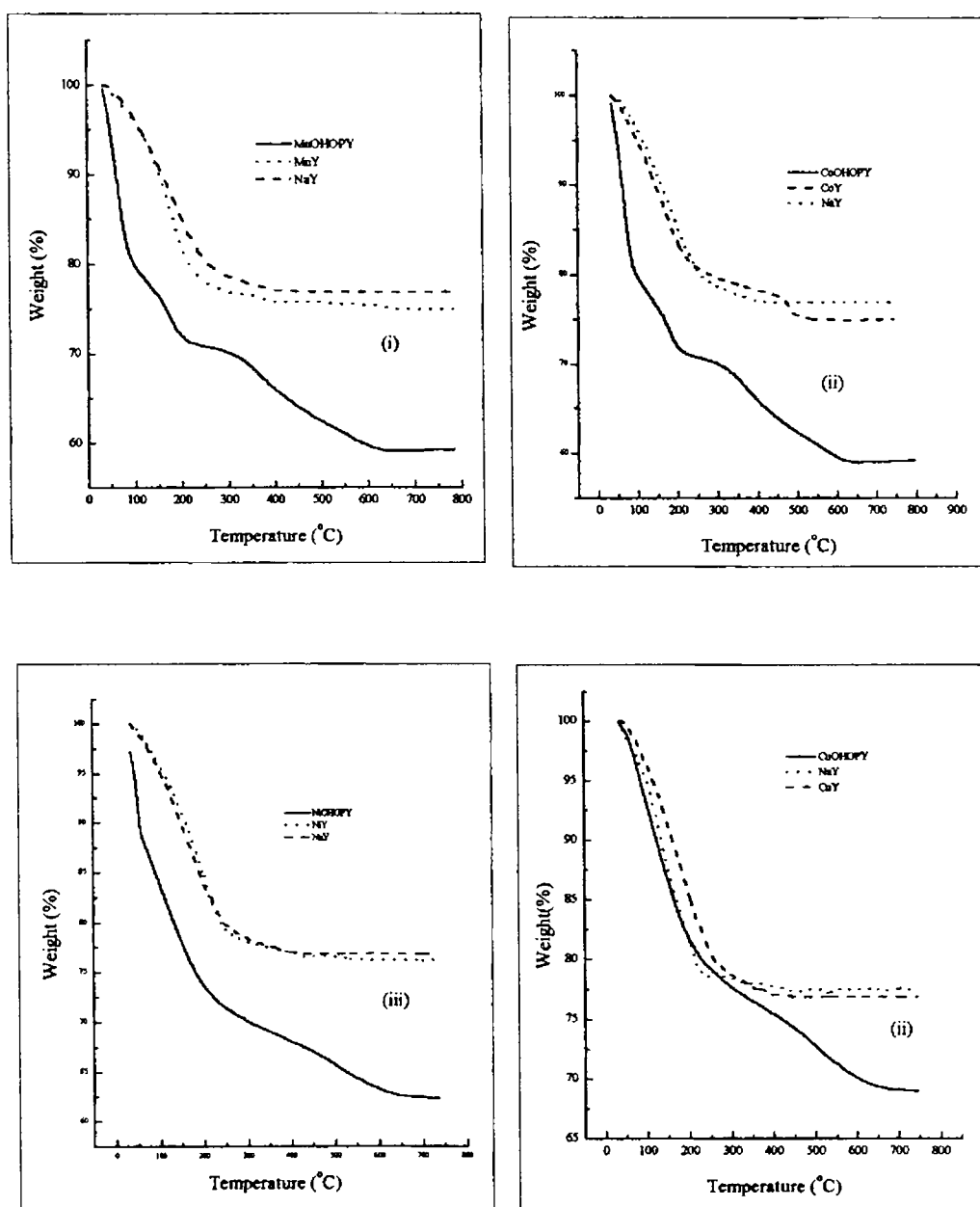


Figure IV. 2. TG curves of zeolite complexes, metal exchanged zeolites and NaY.

(i) MnOHOPY

(ii) CoOHOPY

(iii) NiOHOPY

(iv) CuOHOPY

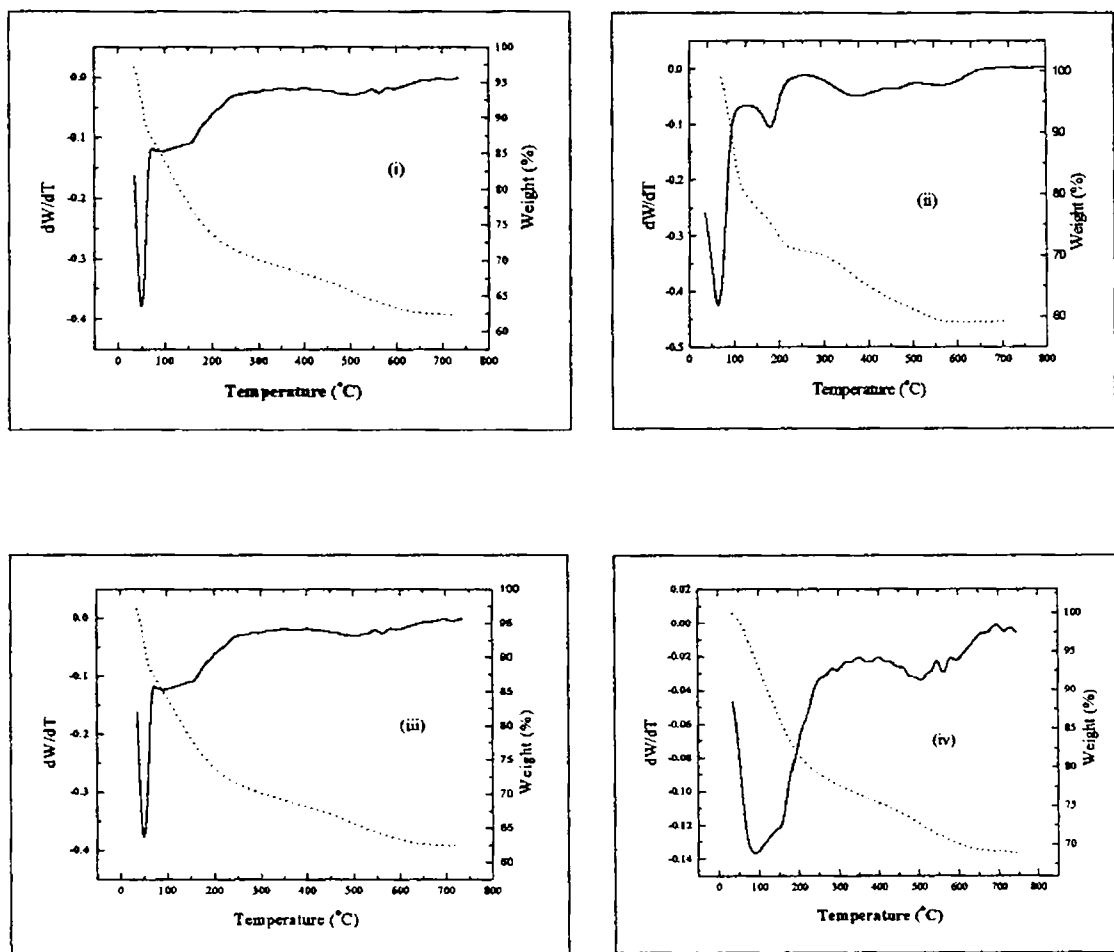


Figure IV. 3. TG/DTG curves of encapsulated complexes

- | | |
|---------------|--------------|
| (i) MnOHOPY | (ii) CoOHOPY |
| (iii) NiOHOPY | (iv) CuOHOPY |

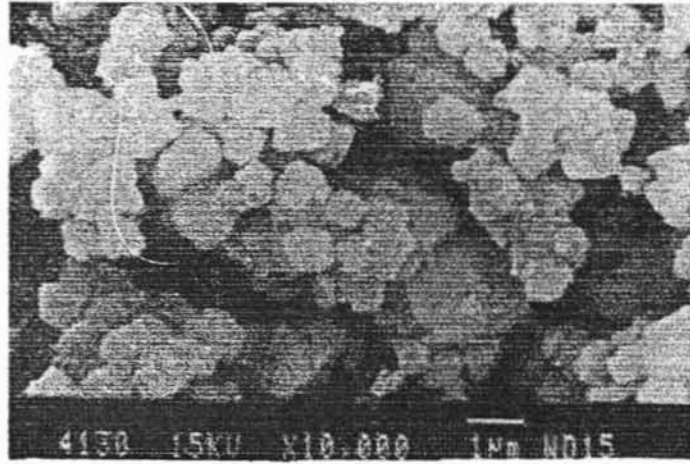
There are two main stages of decomposition. The first stage corresponds to removal of water. The FTIR spectrum of the complex taken at the end of this stage contains characteristic peaks of the encapsulated complex. Therefore the decomposition of the encapsulated complex might be happening only after this stage. However the weight loss occurring in the second stage is not entirely due to the decomposition of the encapsulated complex.

Table IV.2 TG/DTG data

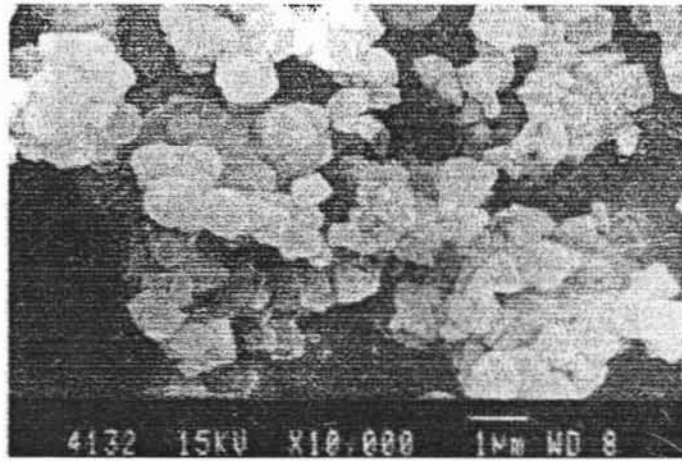
Sample	Weight loss-Stage I			Weight loss-Stage II		
	Temp. range (°C)	Peak temp. (°C)	% mass loss	Temp. range (°C)	Peak temp. (°C)	% mass loss
MnOHOPY	93-210	50	12.8	310-630	500	10
CoOHOPY	80-200	170	11.5	300-620	350	11.5
NiOHOPY	50-190	150	14.6	230-600	490	8.5
CuOHOPY	70-190	100	13.8	250-640	500	9.0

4.3.3. SEM Analysis

The SEM analysis was carried out to check whether the soxhlet extraction is effective in removing surface adsorbed specie. In Fig.IV.4., the micrographs of the MnOHOPY before and after soxhlet extraction is given. It is noticeable that the surface of the zeolite encapsulated complex *after* soxhlet extraction is almost clean. The morphology of the parent NaY has been retained in the encapsulated complex.

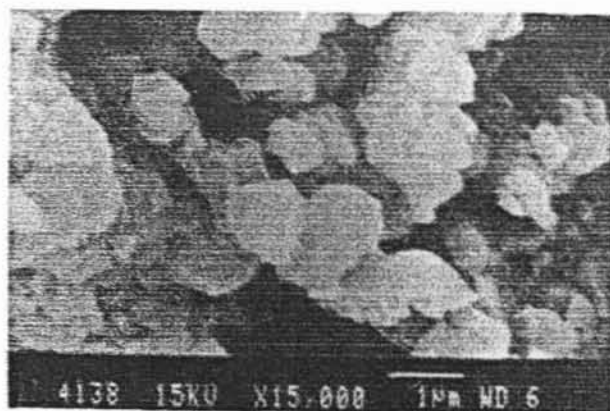


(i)

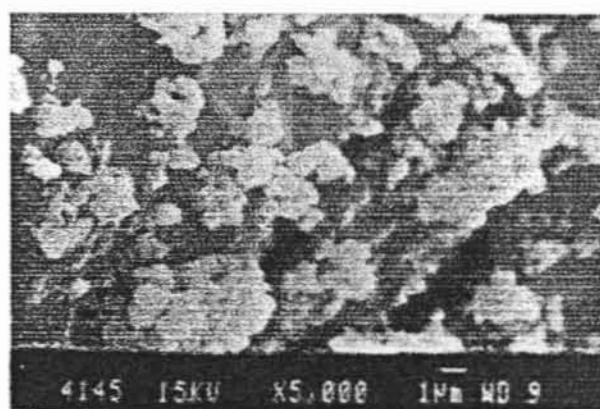


(ii)

Fig. IV.4. SE Micrograph of (i)NiY (ii)MnY



(iii)



(iv)

Fig. IV.4. SE Micrograph of MnOHOPY
(iii) before and (iv) after Soxhlet extraction

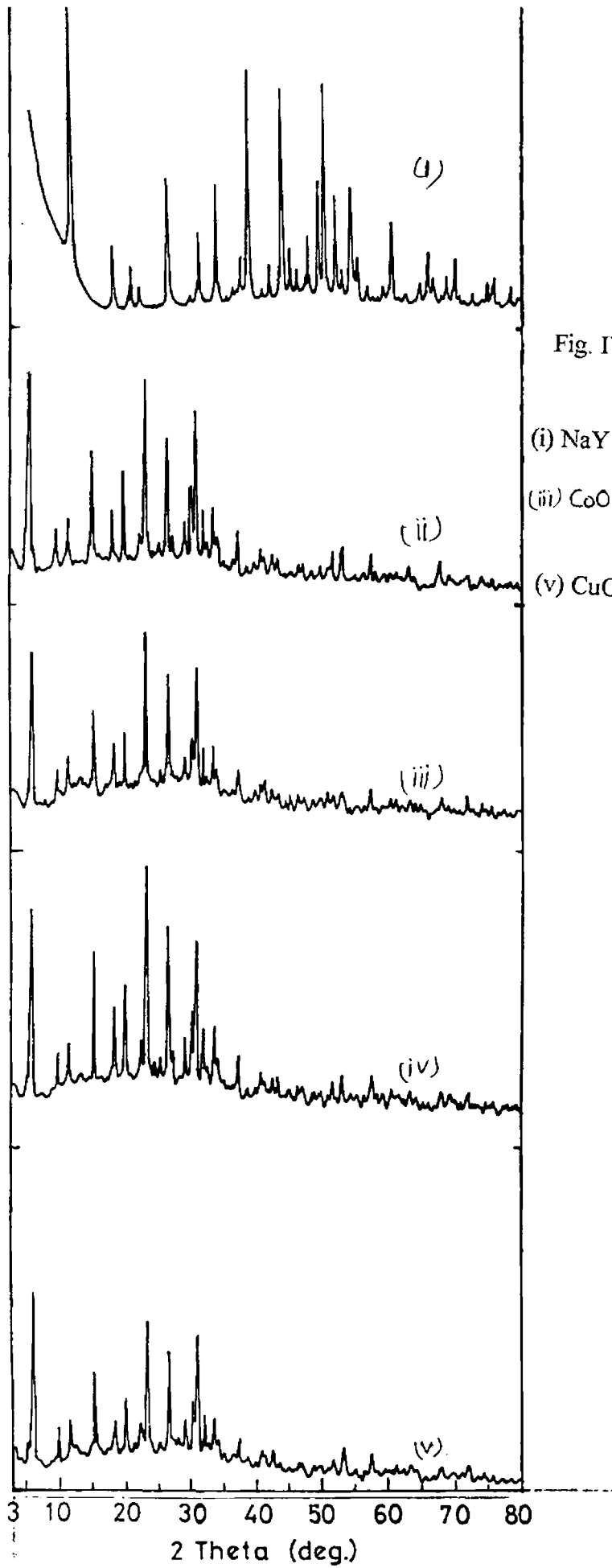


Fig. IV.5. XRD Patterns of

(i) NaY (ii) MnOHOPY

(iii) CoOHOPY (iv) NiOHOPY

(v) CuOHOPY

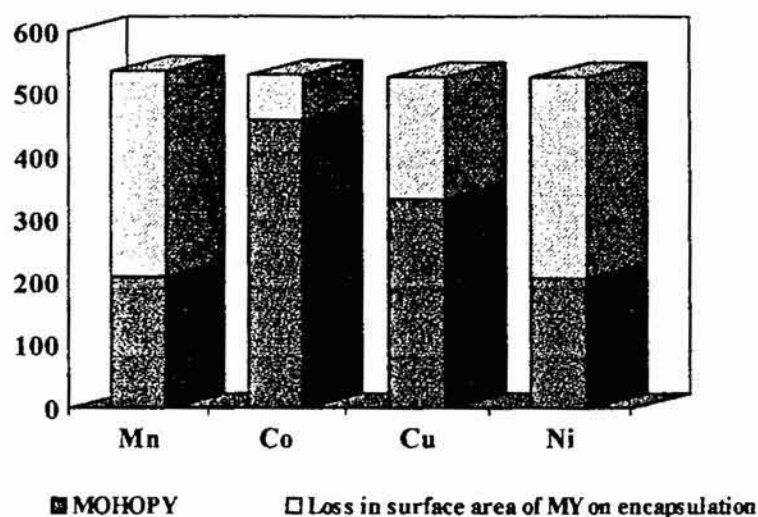


Fig.IV.6. Decrease of surface area of encapsulated complexes.

The very sharp decrease in surface area may be an indication that the encapsulated complexes are in the super cage. Such sharp decrease of surface area during encapsulation has been observed for other zeolite encapsulated complexes [5,6]. Since the XRD patterns suggest the retention of the zeolite framework even after encapsulation, this decrease is due to the encapsulation of the complex.

4.3.6. Magnetic susceptibility Measurements

The room temperature magnetic moment values using the Gouy method are given in Table IV.4.

Table IV.4. Magnetic moment values of the encapsulated complexes.

Sample	Magnetic susceptibility (BM)
MnOHOPY	6.1
CoOHOPY	4.4
NiOHOPY	3.2
CuOHOPY	1.9

The encapsulated Mn(II) complex has a magnetic moment value of 6.1. This is close to the spin only value of 5.92 of a d^5 ion in the high spin state. No special information about the structure of the complex can be arrived from this value [7].

The Co(II) and Ni(II) complexes have magnetic moment values 4.4 BM and 3.2 BM. These values come in the range for a tetrahedral environment for both the metal ions [8,9]. The magnetic moment value of 1.9 BM for the Cu(II) complexes indicate a d^9 ion in axial symmetry [10].

4.3.7. Electronic Spectra

The Kubelka-Monk (KM) factor $F(R)$ is obtained from the reflectance data as a result of the KM analysis. After that, $F(R)$ is plotted against wavelength. The electronic transitions and their tentative assignments are given in Table IV.5. The electronic spectrum of the MnOHOPY is compared to that of MnY and NaY in Fig. IV.7.

The d-d bands of a Mn(II) complex with an organic ligand is very difficult to identify as these bands are due to ${}^6A_1 \rightarrow {}^6A_1$ spin forbidden transition. Even the very weak tail of the UV organic absorption tailing into the visible region can obscure them. There can be rich spin allowed transitions for low spin Mn(II) complexes if the charge transfer bands are not masking the d-d bands. Room temperature magnetic moment values also indicate a high spin state for the d^5 ion. The d-d absorption is seen as a broad band in the region 26,670-13,800 cm^{-1} in the spectrum of MnOHOPY. This may be the result of the five transitions, ${}^4T_{1g}(G) \leftarrow {}^6A_{1g}$, ${}^4T_{2g}(G) \leftarrow {}^6A_{1g}$, ${}^4E_g(G) \leftarrow {}^6A_{1g}$, ${}^4A_{1g}(G) \leftarrow {}^6A_{1g}$, ${}^4T_{2g}(D) \leftarrow {}^6A_{1g}$ of an octahedral Mn(II) [6]. So the electronic spectra suggest an octahedral geometry for MnOHOPY complex.

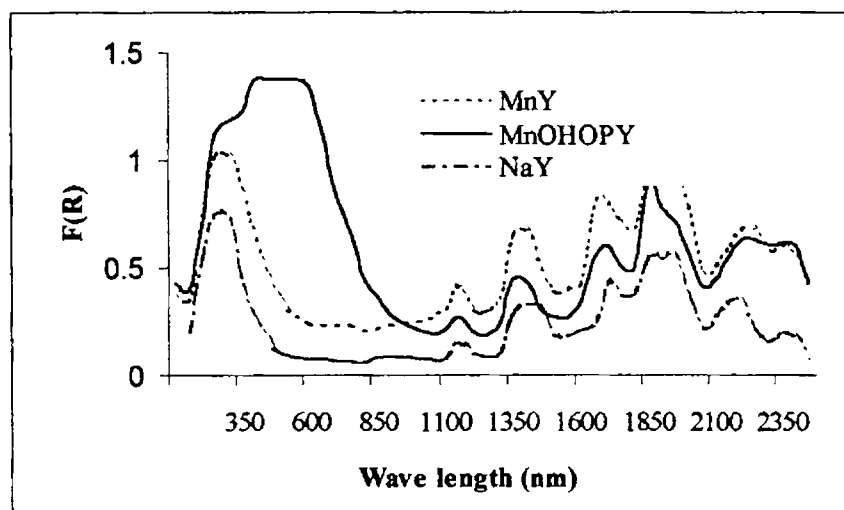


Fig.IV.7 Diffuse reflectance spectrum of MnOHOPY, MnY and NaY.

It clearly indicates that there is complexation of the ligand with Mn(II). The bands representative of the complex appeared in the visible region where there is no band in the diffuse reflectance spectrum of MnY. So there is coordination to the Mn(II) by the chelating ligand.

The diffuse reflectance spectrum of CoOHOPY along with CoY and NaY is given in Fig. IV.8. Both the tetrahedral and octahedral Co(II) species exhibit rich spin forbidden transitions whose intensity is often enhanced by intensity stealing. Tetrahedral species exhibit three transitions. The bands occurring at $22,000\text{cm}^{-1}$, $19,230\text{ cm}^{-1}$ and $16,660\text{ cm}^{-1}$ in the electronic spectrum of CoOHOPY may be assigned as due to the ${}^4\text{T}_1(\text{P}) \leftarrow {}^4\text{A}_2(\text{F})$. Such a band with multiple absorption has been reported as characteristic feature for the Co(II) in a tetrahedral geometry [11]. The band in the low energy near IR region arising from the ${}^4\text{T}_2(\text{F}) \leftarrow {}^4\text{A}_2(\text{F})$ has been masked in the CoOHOPY complex due to the transitions from the zeolite framework.

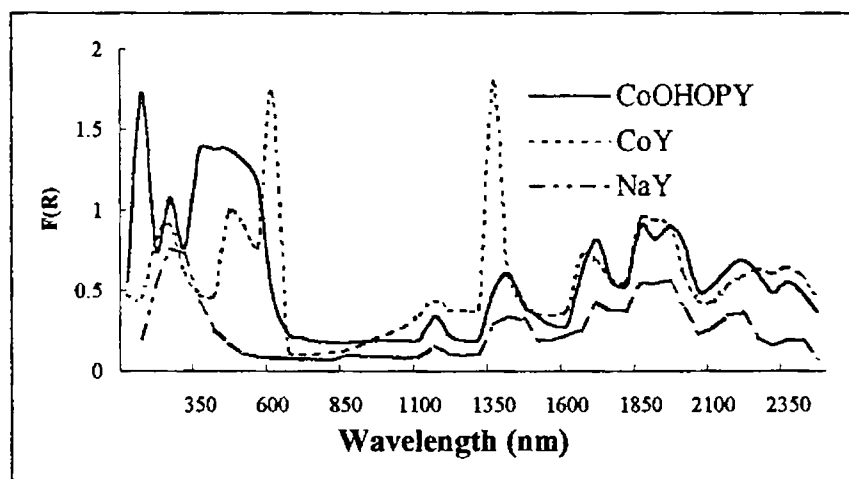


Fig. IV.8. Diffuse reflectance Spectrum of CoOHOPY ,CoY and NaY.

The diffuse reflectance spectra of NiOHOPY, NiY and NaY are given in Fig.IV.9. For tetrahedral Ni(II) complexes, the spectrum is similar in intensity and band energies to those of cobalt(II). On close examination of the table it can be seen that the band energies are similar. The visible band ${}^3T_1(P) \leftarrow {}^3T_1(F)$, which occurs in the spectrum of NiOHOPY around $12,270\text{ cm}^{-1}$ exhibit multiple structures. The low energy transition ${}^3A_2(F) \leftarrow {}^3T_1(F)$ is seen at $6,600\text{ cm}^{-1}$ [10]. Magnetic moment value for this complex also suggests a tetrahedral structure [7].

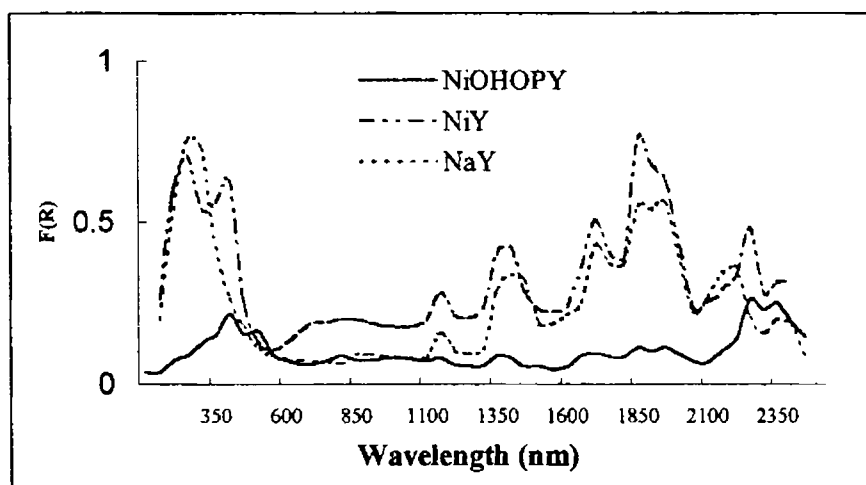


Fig.IV.9. Diffuse reflectance spectrum of NiOHOPY, NiY and NaY.

The diffuse reflectance spectra for the copper(II) complex is given in Fig.IV.10. A broad absorption band is observed at $16,000\text{ cm}^{-1}$. A regular tetrahedral Cu(II) complex should yield a single transition, the d^9 configuration can be thought of as an inversion of d^1 , relatively simple spectra might be expected, and it is indeed true that the great majority of

Cu(II) compounds are blue or green because of a single broad absorption in the region 11,000-16,000 cm^{-1} however, as already noted the d^9 ion is characterised by large absorption from octahedral symmetry and the band is unsymmetrical, being the result of a number of transition which are by no means easy to assign unambiguously. The relevant absorption bands in the electronic spectrum of the encapsulated complexes are given in TableIV.5.

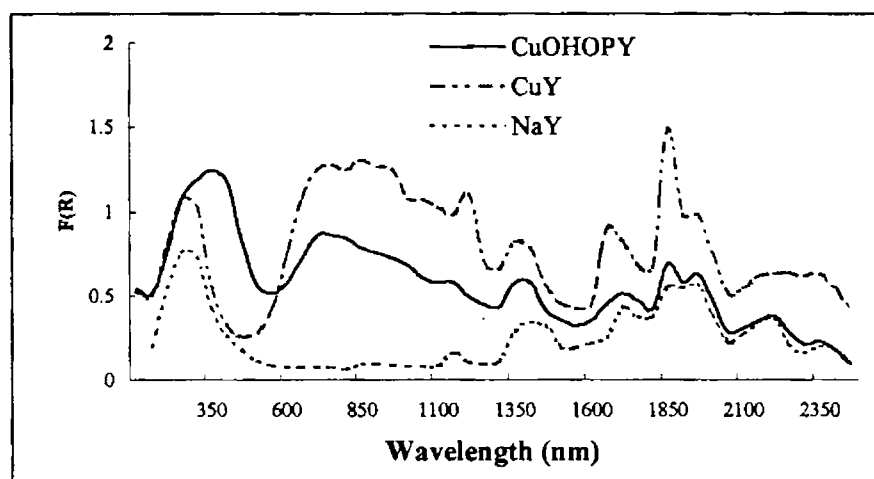


Fig.IV.10. Diffuse reflectance spectrum of CuOHOPY, CuY and NaY.

TABLE IV.5 Electronic spectral data

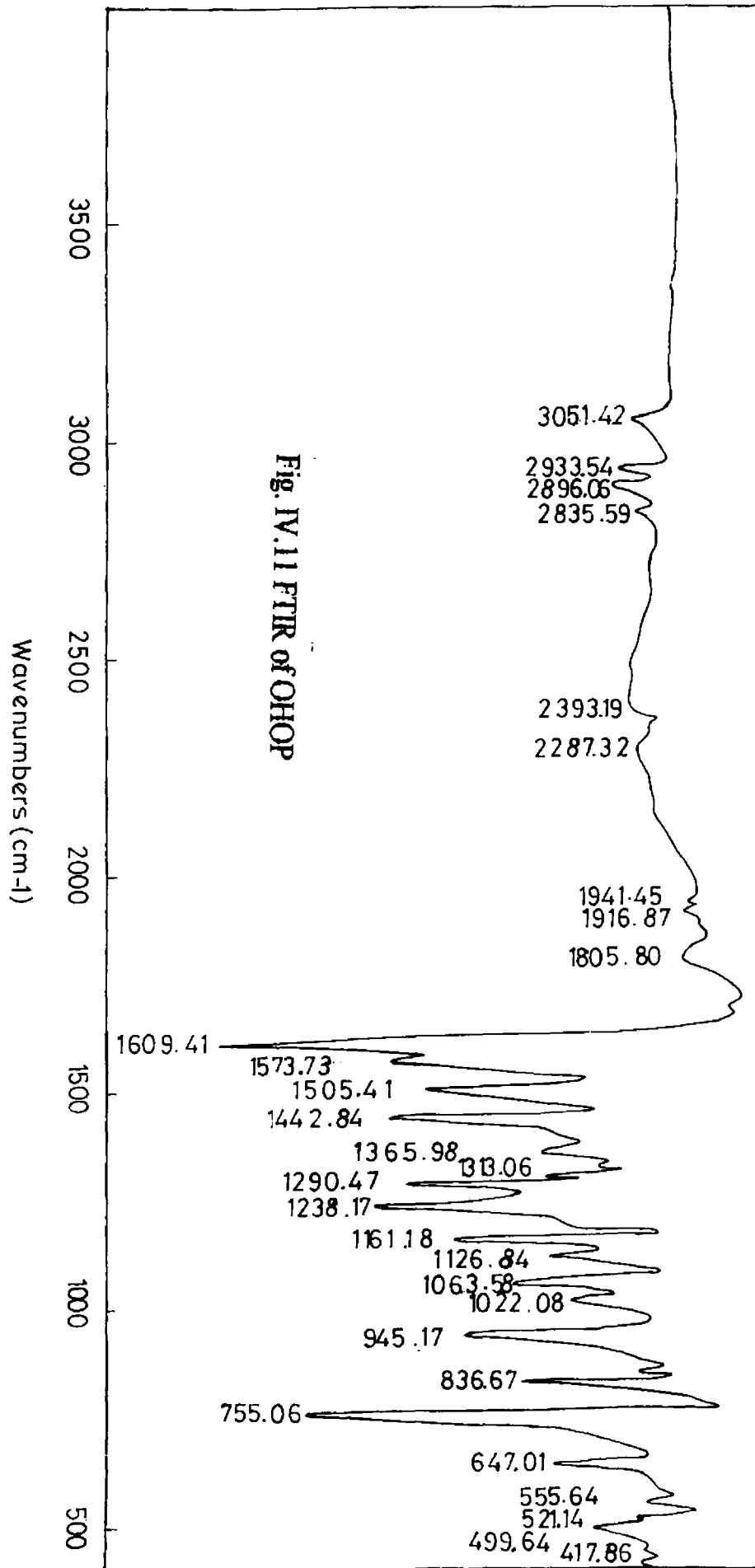
Sample	Abs. Max (cm^{-1})	Tentative assignments	
MnOHOPY	26,670-	${}^4T_{1g}(G) \leftarrow {}^6A_{1g}$	
	13,800	${}^4T_{2g}(G) \leftarrow {}^6A_{1g}$	
	(broad band)	$\left\{ \begin{array}{l} {}^4E_g(G) \leftarrow {}^6A_{1g} \\ {}^4A_{1g}(G) \leftarrow {}^6A_{1g} \\ {}^4T_{2g}(D) \leftarrow {}^6A_{1g} \\ {}^4E_g(D) \leftarrow {}^6A_{1g} \end{array} \right.$	
22,000			
CoOHOPY	19,230	${}^4T_1(P) \leftarrow {}^4A_2$	
	16,660		
NiOHOPY	12,270	${}^3T_1(P) \leftarrow {}^3T_1(F)$	
	6,600	${}^3A_2(F) \leftarrow {}^3T_1(F)$	
CuOHOPY	16,000	d-d transitions.	
	(broad band)		

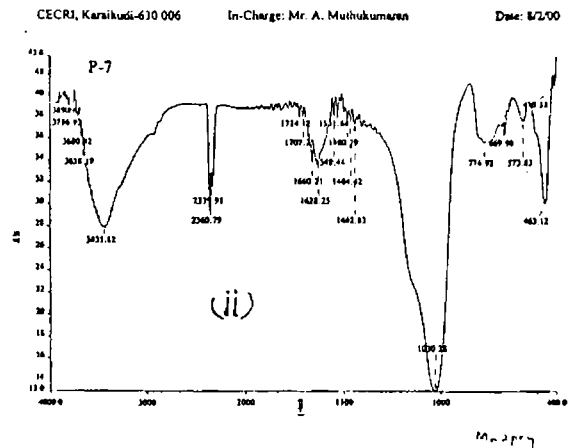
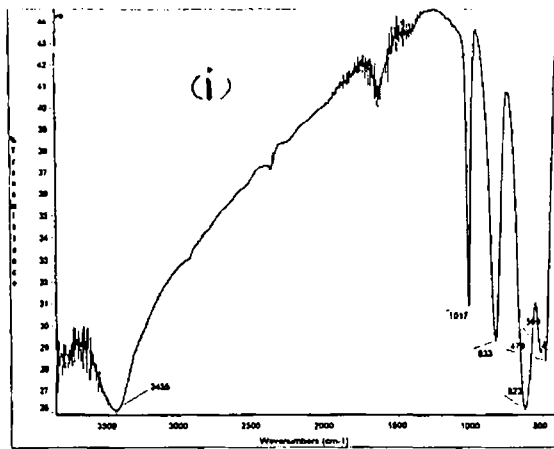
4.3.8. Infrared Spectra

The IR bands of the metal exchanged zeolite, OHOP ligand and the encapsulated complexes are presented in Table IV.6. The FTIR spectrum of the ligand is given in Fig. IV.11. The FTIR spectra of the encapsulated complexes are presented in Fig. IV.12 along with that of the metal exchanged zeolite.

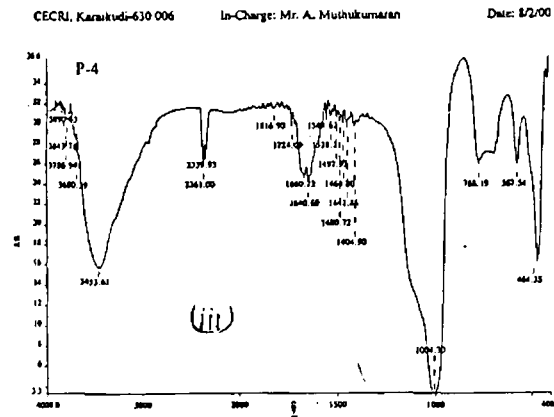
The azomethine group vibration in the ligand at 1609 cm^{-1} is shifted to higher wavelength in all the complexes. Similar shifts have been reported for other intrazeolitic complex such as Salen complexes, cobalt phthalocyanine complexes etc [9]. Any physical mixture of NaY zeolite and the Schiff base are not at all giving this type of a shift and this can be used as a diagnostic criteria for the intrazeolitic complex formation. Eventhough many of the peaks were obscured by the broad bands of the zeolite framework, the azomethine group vibration is seen as a separate sharp peak in all the complexes. This peak was retained even after heating upto 400°C and was appearing on the FTIR of the residue obtained at this temperature. So, this may not be the $\delta_{\text{H-O-H}}$ of the water molecule present in the zeolite molecule. Some of the $\nu_{\text{C-H}}$ frequencies of the aromatic ring of the ligand have not been masked by the framework. This also can be considered as a proof for the presence of the ligand around the metal.

Transmittance

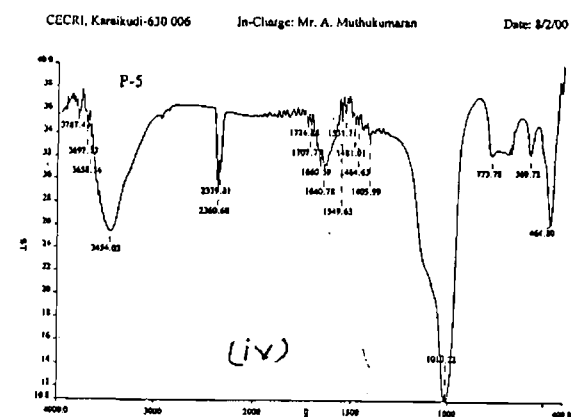




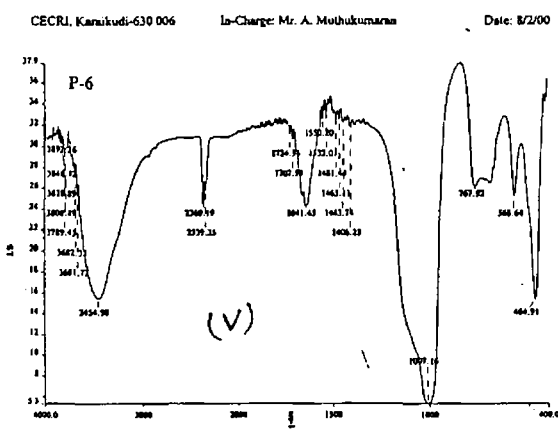
P7.PK



P4.PK



P5.PK



P6.PK

Fig. IV.12 FTIR of (i) MY (ii) MnOHOPY (iii) CoOHOPY (iv) NiOHOPY (v) CuOHOPY

Table IV.6. IR spectral data (cm⁻¹) of MY, OHOP and the encapsulated metal complexes.

MY	OHOP	MnOHOPY	CoOHOPY	NiOHOPY	CuOHOPY
450	418				
	500	463	463	461	463
	556	567	565	566	567
615	647				
	755				
	837				
	945				
	1023	1008		1009	1006
1050	1064		1040		
	1127				
	1161				
	1238				
	1291				
	1443				
	1505				
	1573	1543			
1600	1609	1647	1629	1648	1639
	1806				
2300		2360	2324	2324	2363
	2934				
	3051				
3250					

4.3.9. EPR spectroscopy

The EPR of MnOHOPY at room temperature is given in Fig. IV.13. It has six peaks characteristic of $I=5/2$ of Mn(II) ion. The calculated g value is 2.0095. This value is very close to the g value reported for Mn(Salen) in zeolite Y [13]. The calculated value of A is 83.33G. This value is lower than that reported for the above said complex. No hyperfine splitting or spin forbidden transitions have been observed in the signal. Very broad signals are exhibited by CoOHOPY at LNT. Therefore the Co(II) complex should be in the high spin state. No further information could be obtained from the spectrum. CuOHOPY exhibits EPR spectrum characteristic of an axially symmetrical d^9 ion. (Fig.IV.14) The various EPR parameters of CuOHOPY are given in Table IV.7.

Table IV.7. EPR Parameters of CoOHOPY.

EPR parameter	CuOHOPY
$g_{ }$	2.23
$A_{ }$	104cm^{-1}
$g_{ } / A_{ }$	114.4
g_{\perp}	2.056

TEMP (°C) 114.0
FREQ (MHz) 100.0
POWER (mW) 100.0
MOD 3.0
GAIN 10.0
SCAN TIME 1.0
GAIN X 10.0
MODE 1.0
UNIT G

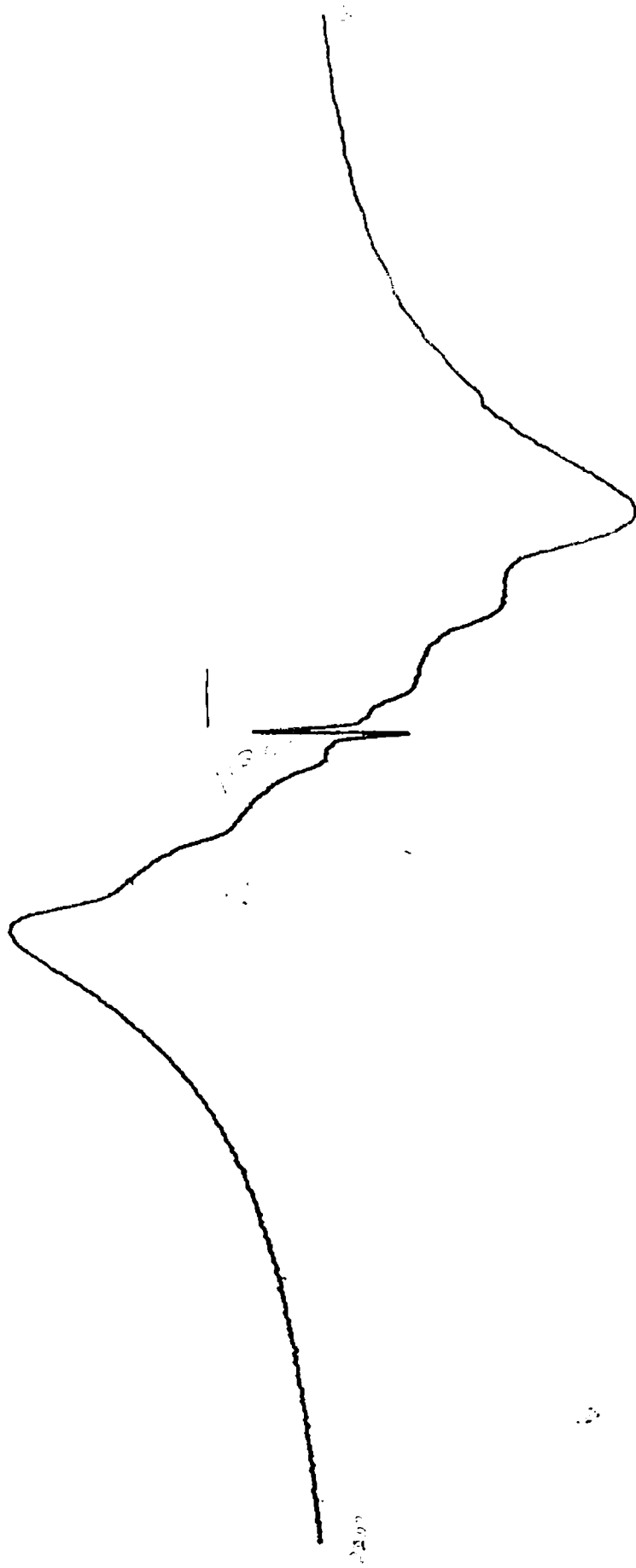
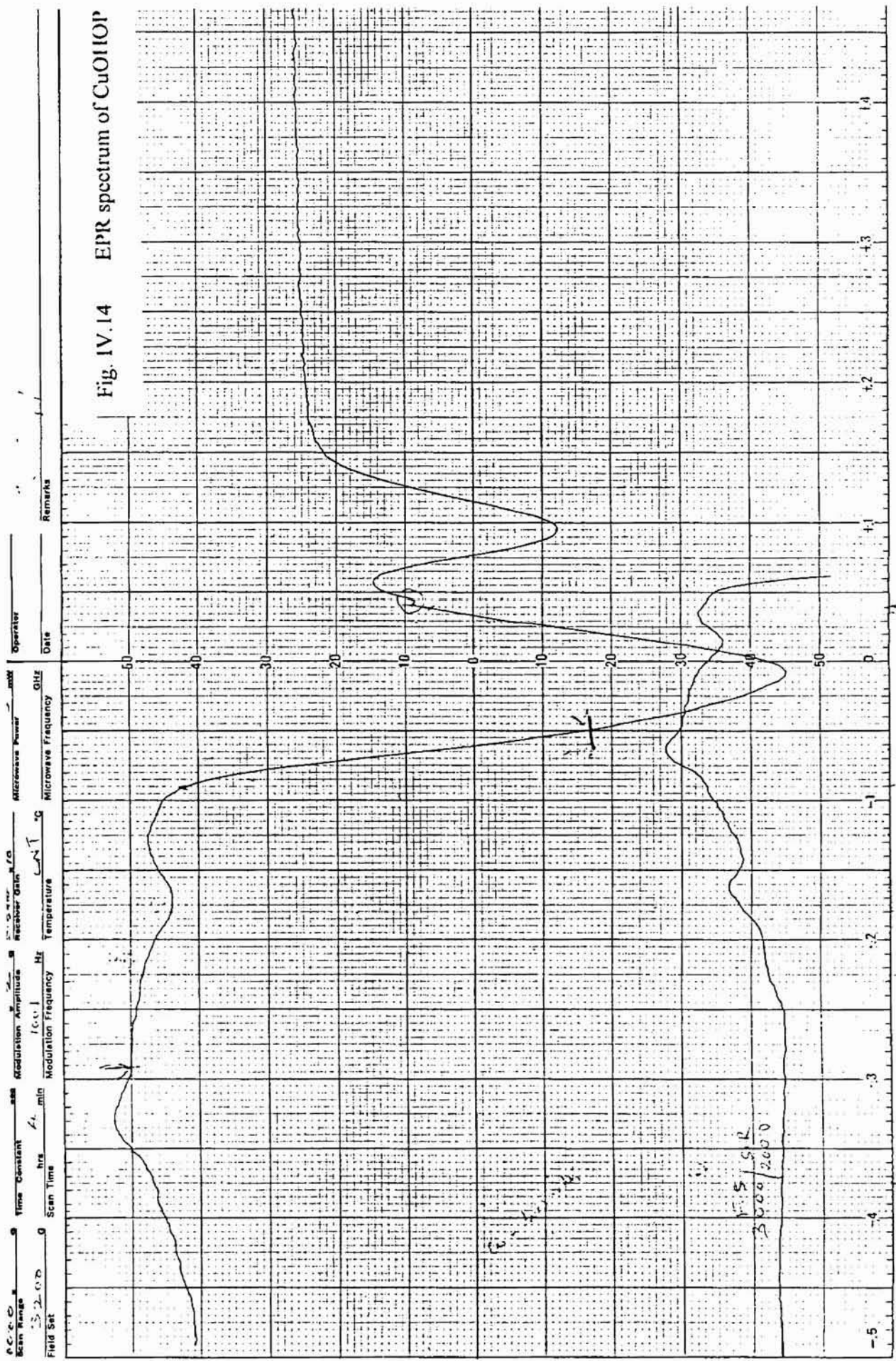


Fig. IV.13 EPR spectrum of MnOHOPY



REFERENCES

- [1] J.C. Stevens, D.H. Busch, *J.Am.Chem.Soc.* **102** (1980) 3285.
- [2] Pfeiffer, Breith, Lubbe, Tsumaki, *Ann.* **503** (1933) 84.
- [3] C. Bowers, P.K. Dutta, *J.of Catal.* **122** (1990) 271.
- [4] W.H. Qualye, J.H. Lunsford, *Inorg. Chem.* **21** (1982) 97.
- [5] S.P. Varkey, C.R. Jacob, *Ind.J.Chem.* **37** (1998) 407.
- [6] K.J. Balkus, A.G. Gabrielov, *J. Incl. Phenom. Mol. Rec. Chem.* **21** (1995) 159.
- [7] A. Earnshaw, *Introduction to Magneto Chemistry*, Academic Press, New York, 1968.
- [8] B. N. Figgis, J. Lewis, in F.A. Cotton (Ed), *Progr. Inorg. Chem.*, Vol. 4 Interscience, New York, (1964).
- [9] N.N. Greenwood, A. Earnshaw, *The Chemistry of the Elements*, Pergamon Press, New York, 1989.
- [10] F.A. Cotton, G. Wilkinson, *Advanced Inorganic Chemistry*, 5th Edn. John Wiley and Sons, New York, 1988.
- [11] A.B.P. Lever, *Inorganic Spectroscopy*, Elsevier, New York, 1984.
- [12] L. Gaillon, N. Sajot, F. Bedioui, J. Debynk, K.J. Balkus, Jr., *J. Electroanal. Chem.*, **315** (1993) 157.
- [13] N. Ulagappan, V. Krishnasamy, *Ind. J. Chem.*, **35A** (1996) 787.

CHAPTER V

STUDIES ON Y ZEOLITE ENCAPSULATED TRANSITION METAL COMPLEXES OF *N,N'*-Bis-(2-PYRIDINEMETHYLENE)-1,2-DIAMINOETHANE

5.1. INTRODUCTION

There are so many dioxygen binding complexes formed inside zeolites [1,2]. The zeolite framework retards the formation of binuclear complexes and there by enhances the reversibility of oxygen binding [3]. A major disadvantage of such systems is the lack of control of the number of mono- or bi- dentate species coordinating to the cation. The use of polydentate ligands can offer solution to this by forming more stable complexes and the nature of coordination is expected to be controlled by the assembly of them in a single ligand molecule.

The ligand field of the Schiff bases containing heterocyclic ring systems are usually weaker than the corresponding one with aromatic systems. So such systems exhibit interesting structural features. The multi dentate Schiff bases obtained from the condensation of pyridine-2-carboxaldehyde with diamines [4], triamines [5] and certain amino compounds [6] can give rise to structurally attractive complexes. It has been found that some of the Schiff base complexes of pyridine-2-carboxaldehyde have the same structure when compared to that of the salicylaldimine with the same amine [7]. The introduction of the tertiary nitrogen group in the tetradentate ligand that occupies a position structurally intermediate between Salen and bipyridine [2,8]. The zeolite complexes of these ligands find application as oxygen binders in many

synthetically important organic reactions. So, it is interesting to explore the vistas in the structural aspects and also the reactivity that the tertiary nitrogen can impart.

In this chapter, our studies on the encapsulation and characterization of the Mn(II), Co(II), Ni(II) and Cu(II) Schiff base complexes of *N,N'*-bis(pyridinemethylene)-1,2-diaminoethane (2PyEn) in Y zeolite are presented.

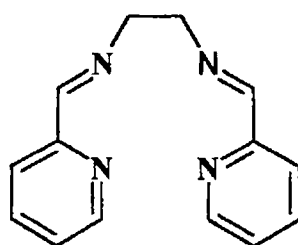


FIG V. 1. Structure of the ligand

5.2. EXPERIMENTAL

5.2.1. Materials

The procedural details regarding the preparation of the metal exchanged zeolites are given in Chapter II.

5.2.2. Synthesis of zeolite Y encapsulated *N,N'*-bis(pyridinemethylene)-1,2-diaminoethane complexes (2PyEnY)

A general out line of the method used for the encapsulation of the metal Schiff base complexes is given in Chapter II. The corresponding metal exchanged zeolites (5gm) were refluxed with a solution of pyridine-2-carboxaldehyde (3.8 mL, 0.04M) in ethanol (15mL). After three hours the aldehyde chelate were filtered and purified by soxhlet extraction with methanol. The purified chelates were reacted with 1,2-diaminoethane (1.33 mL, 0.02M). The purification of the Schiff base complexes were carried out by soxhlet extraction with chloroform followed by methanol till the

washings were colourless. The complexes were re-exchanged with 0.01M NaCl solution and made free from chloride ions. All the complexes were stored in vacuum over anhydrous calcium chloride after drying at 120⁰C for 2 hours.

5.2.3. Analytical Methods

Details of the various analytical techniques and other characterization methods used are described in Chapter II.

5.3. RESULTS AND DISCUSSION

The synthesized complexes of Mn(II), Co(II), Ni(II) and Cu(II) with the Schiff base 2PyEn inside Y zeolite were characterized using techniques like chemical analysis, XRD, surface area, magnetic moment, electronic spectra, FTIR, EPR and TG analysis.

5.3.1. Chemical analysis

The analytical data of the zeolite encapsulated complexes are given in Table V.1. The Si/Al ratio was found to be in the range 2.3 to 2.4 as in the metal exchanged zeolites. So the possibility of dealumination could be disregarded.

Table V.1. Analytical data of the encapsulated 2PyEn complexes

Sample	% Metal	% Si	%Al	%Na	%C	%H	%N
Mn2PyEY	2.51	19.46	7.91	5.61	4.31	0.41	2.01.
Co2PyEnY	2.49	19.23	7.76	5.92	5.27	0.39	1.92
Ni2PyEnY	2.48	18.61	7.51	5.13	5.86	0.49	1.73
Cu2PyEnY	2.55	18.92	7.64	6.28	5.63	0.46	1.68

5.3.2. TG studies

The thermogravimetric studies of the complexes were carried out in inert atmosphere. The results are summarised in Table V.2. The TG curves are given in Fig. V.2 and V.3.

All the complexes are exhibiting a similar pattern of decomposition. The first stage corresponds to the loss of water. On completing this stage, the residue is collected and FTIR is taken. The spectra showed all the characteristics peaks of the encapsulated species. So the encapsulated species might not be decomposing at this stage. But, the weight loss at this stage is not fully due to the decomposition of the encapsulated complex.

Table V. 2 TG/DTG data

Sample	Weight loss-Stage I			Weight loss-Stage II		
	Temp. range(°C)	Peak temp. (°C)	% mass loss	Temp. range(°C)	Peak temp. (°C)	% mass loss
Mn ₂ PyEnY	70-190	-	14.0	340-570	400	7.5
Co ₂ PyEnY	75-210	100	10.0	300-550	450	15.0
Ni ₂ PyEnY	70-115	75	9.5	320-570	340	19.0
Cu ₂ PyEnY	50-216	-	6.1	350-560	345	17.5

5.3.3. X-ray diffraction studies

XRD patterns of all the complexes are given in Fig.V.4. The framework has been retained as such even after encapsulation as can be evidenced from the lack of change in the XRD patterns.

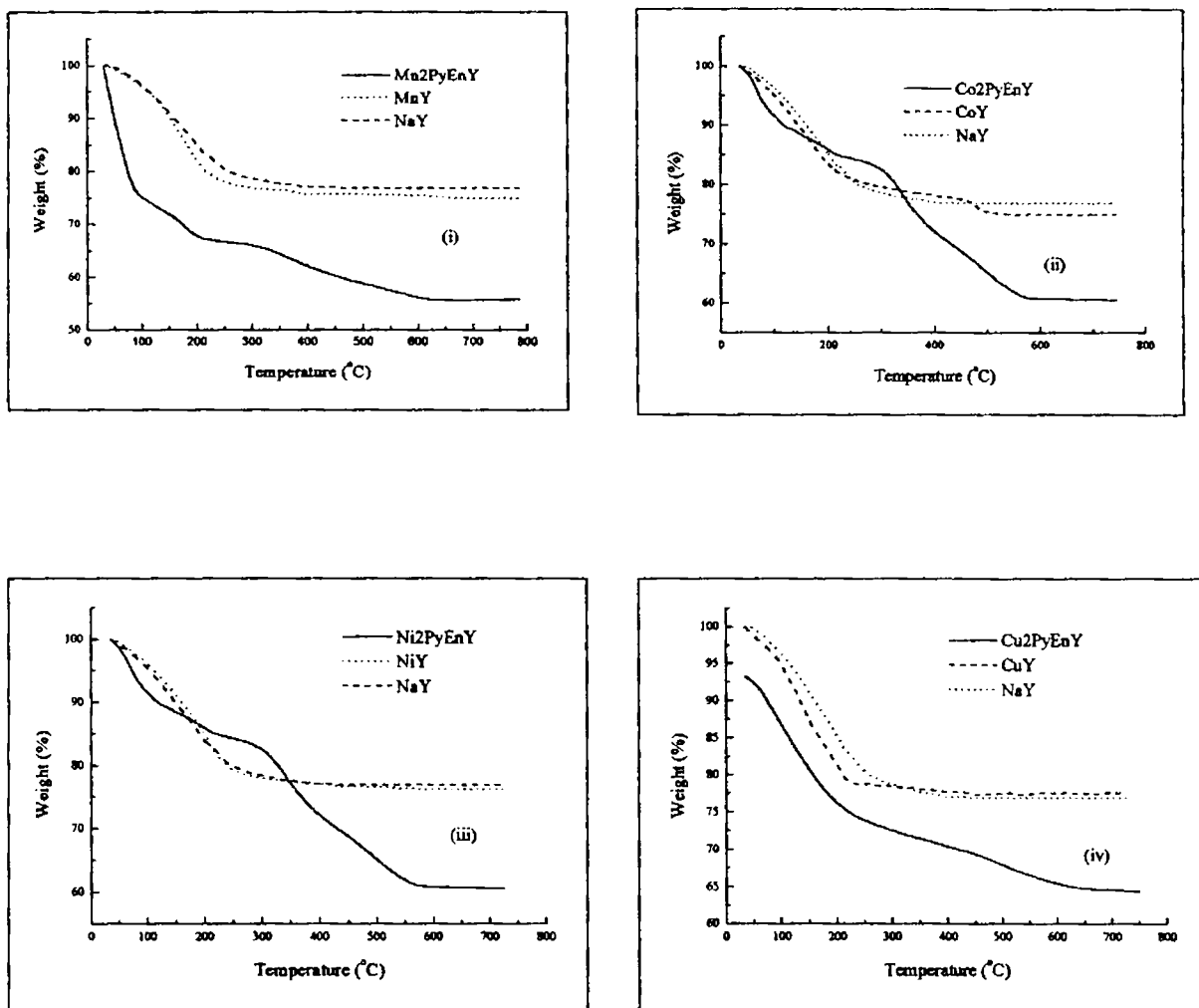


Fig. V.2. TG curves of zeolite complexes, metal exchanged zeolites and NaY

- (i) Mn_2PyEnY (ii) Co_2PyEnY
 (iii) Ni_2PyEnY (iv) Cu_2PyEnY

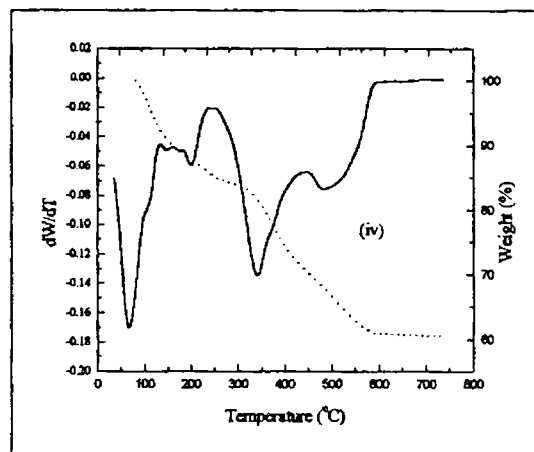
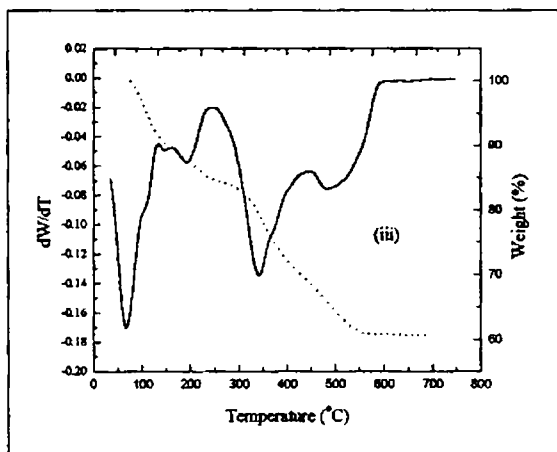
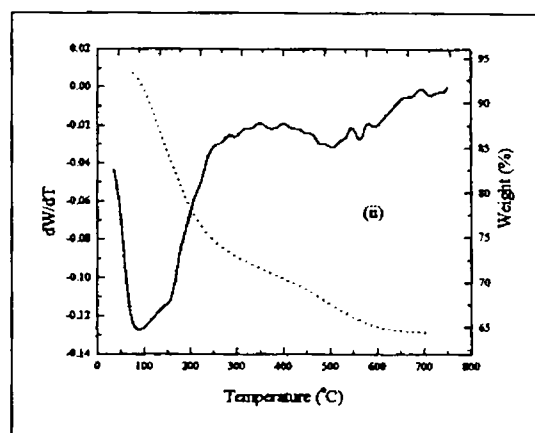
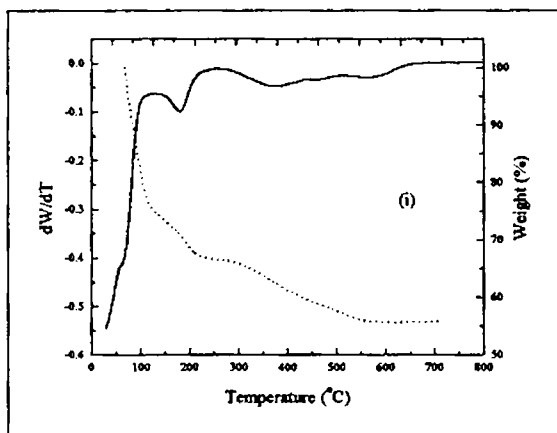


Fig. V.3. TG/DTG curves of encapsulated zeolite Y complexes

- | | | | |
|-------|-----------------------|------|-----------------------|
| (i) | Mn ₂ PyEnY | (ii) | Co ₂ PyEnY |
| (iii) | Ni ₂ PyEnY | (iv) | Cu ₂ PyEnY |

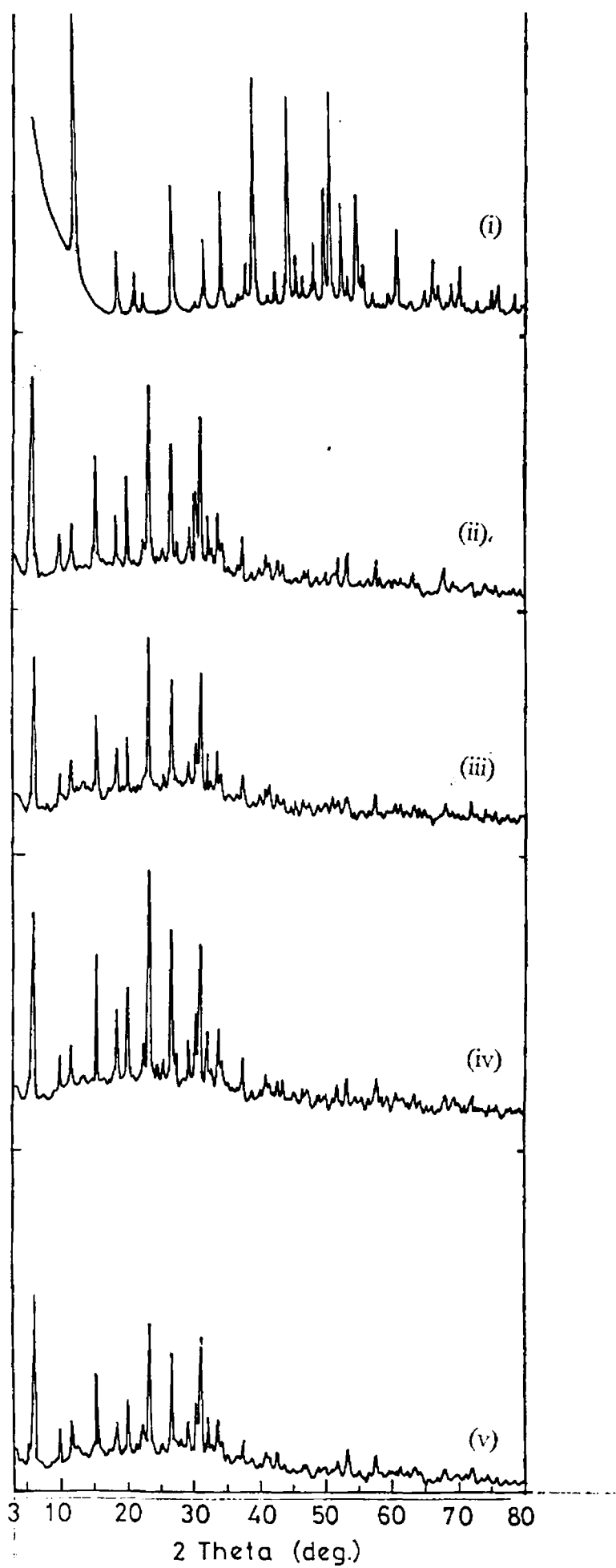


Fig. V.4 XRD Patterns of (i) NaY (ii) Mn₂Py EnY
(iii) Co₂Py EnY (iv) Ni₂Py EnY (v) Cu₂Py EnY

5.3.4. Scanning electron microscopy

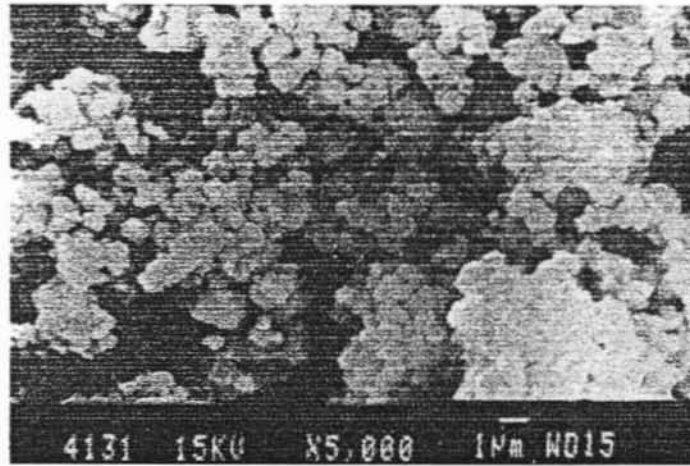
The scanning electron micrograph of the Mn₂PyEnY complexes before and after purification are given in Fig. V.5. It can be seen that the morphology of the parent zeolite Y is retained after encapsulation and purification. The surface is clean and the surface adsorbed species is removed as a result of soxhlet extraction. The average particle size is 1µm. So the morphology of the parent NaY has retained.

5.3.5. Surface area analysis

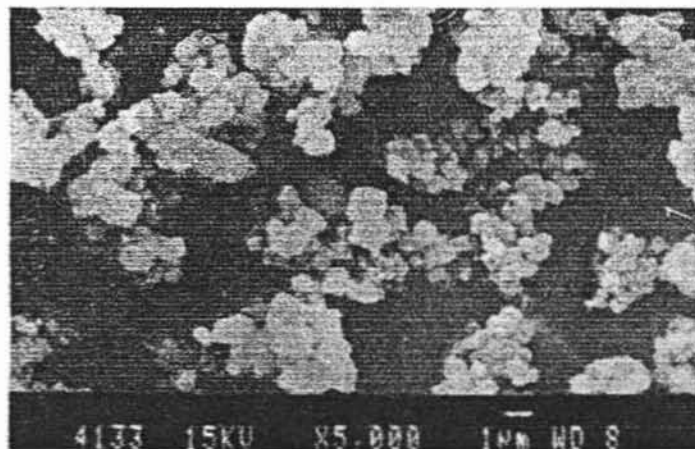
The surface area of the encapsulated complexes is supplied in Table V.3. The surface area of the complexes upon encapsulation has been reduced. In literature, the sharp decrease of the surface area has been noted earlier [9]. This is branded as a proof of encapsulation.

TABLE V.3 Surface area data of the encapsulated metal complexes

Sample	Surface area (m ² /g)		
	MY	MSOPY	%Loss
NaY	549	-	-
Mn ₂ PyEnY	539	324	41.5
Co ₂ PyEnY	532	363	25
Ni ₂ PyEnY	528	301	35.6
Cu ₂ PyEnY	528	386	36.55

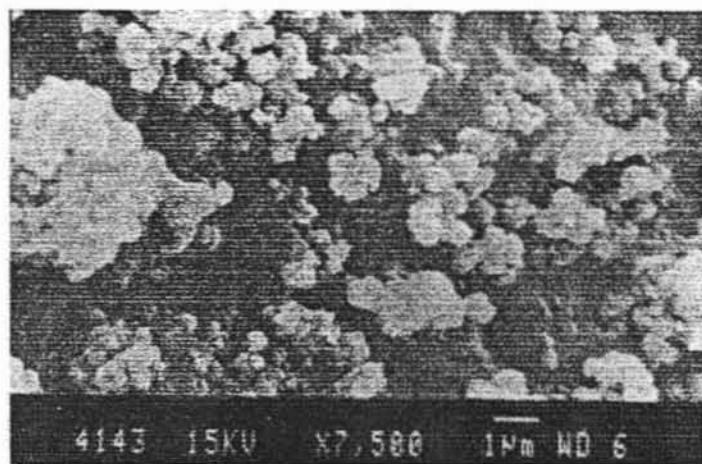


(i)

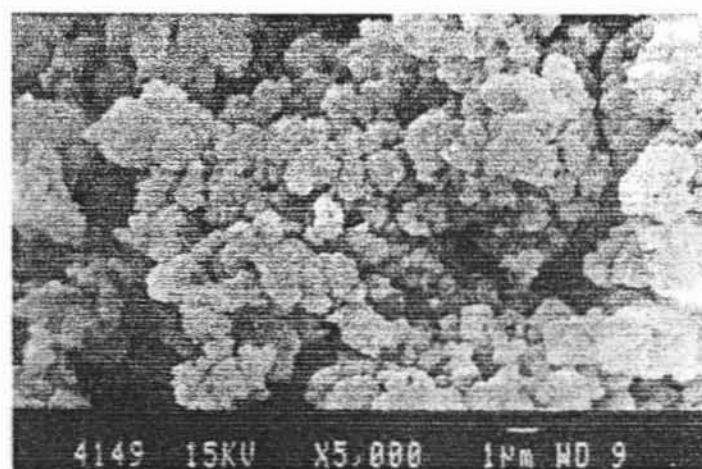


(ii)

Fig. V.5. SE Micropographs of (i) NaY (ii) MnY



(iii)



(iv)

Fig. V.5. SE Micropographs of Mn₂PyEnY

(iii) before and (iv) after Soxhlet extraction

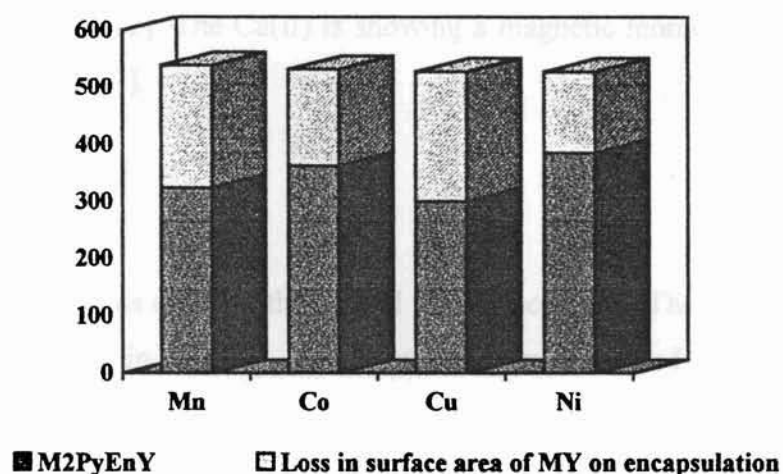


Fig V.6. Decrease of surface area of metal exchanged zeolites on encapsulation

5.3.6. Magnetic moment

Room temperature magnetic moment values of the 2PyEn complexes after encapsulation are given in Table V.4

Table V.4 Magnetic moment values of the 2PyEn complexes

Sample	Magnetic moment (BM)
Mn2PyEnY	6.0
Co2PyEnY	4.6
Ni2PyEnY	3.4
Cu2PyEnY	1.9

The magnetic moment values of the encapsulated Mn(II) complex is in agreement with a d^5 ion in the high spin state[10]. But there is no information about the stereochemistry of the complexes. For the Co(II) and Ni(II) complexes, the

obtained magnetic moment values may suggest a tetrahedral and a distorted tetrahedral structure respectively [11, 12]. The Cu(II) is showing a magnetic moment value of a tetragonal Cu(II) species [11].

5.3.7. Electronic spectra

The KM analysis was done on the optical reflectance data. The KM factor is plotted against wavelength in Fig.V.7. The electronic transitions and their tentative assignments are given in Table V.5.

In Mn2PyEnY, there is a broad d-d band around $16,670\text{cm}^{-1}$ which results from the five transition of the octahedral Mn(II) as described in chapter 4. Fig. V.7 represents the diffuse reflectance spectrum of the Mn2PyEnY, MnY and NaY. The complex formation is evident from the absorption spectra. From the earlier reported Mn(II) complex of 2PyEnY encapsulated in Y zeolite, the d-d band is said to be masked by the strong charge transfer band [12].

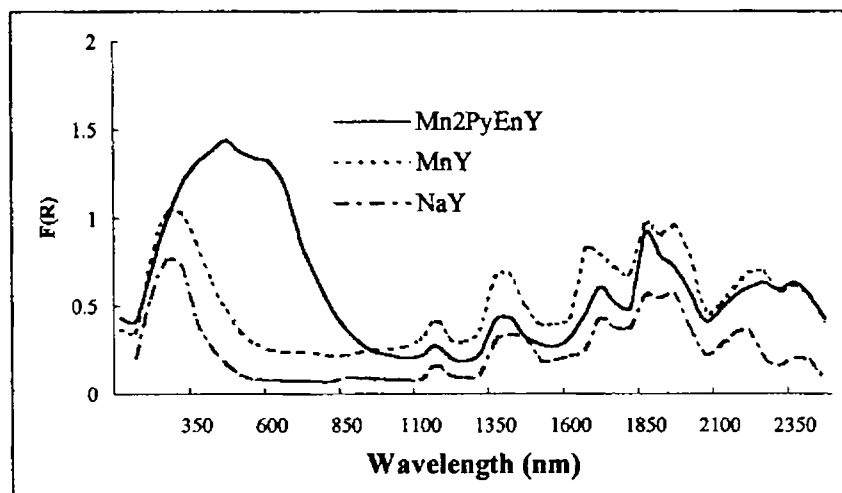


Fig. V. 7 Diffuse reflectance spectrum of Mn2PyEnY, MnY and NaY.

Fig. V.8. represents the diffuse reflectance spectrum of Co2PyEnY, CoY and NaY. The multiple absorption observed at $19,000\text{cm}^{-1}$, $15,870\text{cm}^{-1}$, and $13,800\text{cm}^{-1}$

due to the ${}^4T_1(P) \leftarrow {}^4A_2(F)$ transition of a tetrahedral Co(II). The corresponding Co(II) complex already reported has a four coordinate structure. It is also reported that the bands were masked by the strong charge transfer band. But here we could get the transitions resolved.

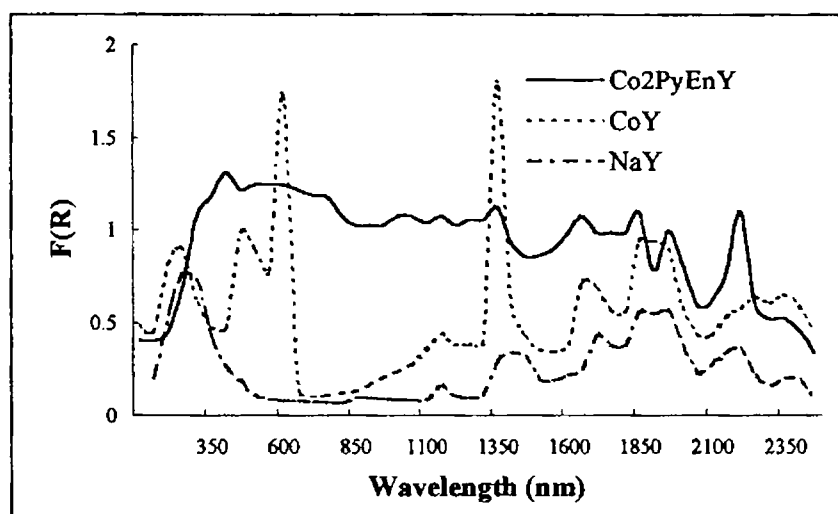


Fig. V.8. Diffuse reflectance spectrum of Co2PyEnY, CoY and NaY.

The absorption band at 7690cm^{-1} is the ${}^4T_1(F) \leftarrow {}^4A_2(F)$. The ${}^2T_2(F) \leftarrow {}^4A_2(F)$ transition is masked in the Co2PyEnY complex due to transitions from the framework. So the Co2PyEnY complex may be tetrahedral. The charge on the metal is neutralised by the oxide ions of the framework. There is already one report on the Co2PyEnY [14]. The complex is reported to be non planar.

Fig. V.9 represents the diffuse reflectance spectrum of Ni2PyEnY, NiY and NaY. The d-d band around $12,120\text{cm}^{-1}$ may be the ${}^3T_1(P) \leftarrow {}^3T_1(F)$ transition of a tetrahedral Ni(II). The band at $6,600\text{cm}^{-1}$ may be assigned as the ${}^3A_2(F) \leftarrow {}^3T_1(F)$ transition. The ${}^3T_2(F) \leftarrow {}^3T_1(F)$ transition is masked by the frame wrok. So a distorted tetrahedral structure may be assigned for Ni(II). The visible transitions are masked in the electronic spectrum of the Ni(II) complex encapsulated in zeolite Y.

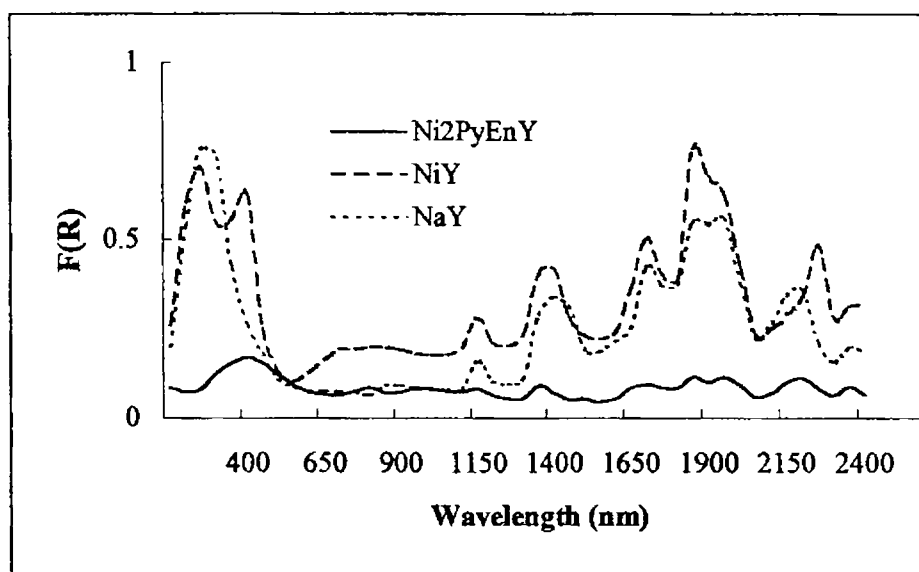


Fig. V.9. Diffuse reflectance spectrum of Ni₂PyEnY, NiY and NaY.

Fig V.10 represents the diffuse reflectance spectrum of Cu₂PyEnY, CuY and NaY. The d-d bands with multiple absorptions in the region 22,000-15,000 cm⁻¹ indicate a tetragonal geometry for Cu(II).

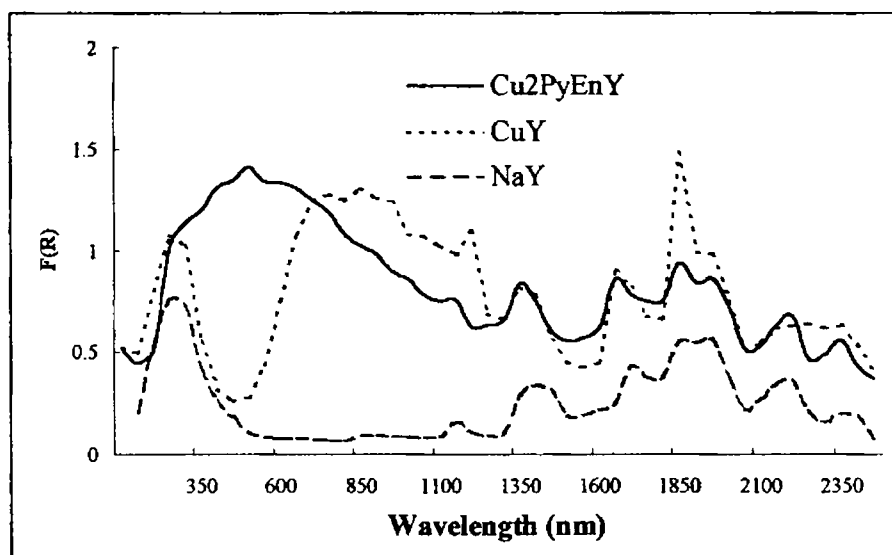


Fig. V.10. Diffuse reflectance spectrum of Cu₂PyEnY, CuY and NaY.

Table V.5. Electronic spectral data of the encapsulated complexes.

Sample	Abs. Max (cm ⁻¹)	Tentative assignments
Mn2PyEnY	25,000- 15,000 (broad band)	${}^4T_{1g}(G) \leftarrow {}^6A_{1g}$ ${}^4T_{2g}(G) \leftarrow {}^6A_{1g}$ $\left\{ \begin{array}{l} {}^4E_g(G) \leftarrow {}^6A_{1g} \\ {}^4A_{1g}(G) \leftarrow {}^6A_{1g} \end{array} \right.$ ${}^4T_{2g}(D) \leftarrow {}^6A_{1g}$ ${}^4E_g(D) \leftarrow {}^6A_{1g}$
Co2pyEnY	19,000 15,870 13,800 7,690	${}^4T_1(P) \leftarrow {}^4A_2(F)$ ${}^4T_1(F) \leftarrow {}^4A_2$
Ni2PyEnY	12,120 6,600	${}^3T_1(F) \rightarrow {}^3T_1(P)$ ${}^3T_1(F) \rightarrow {}^3A_2(F)$
Cu2PyEnY	22,000-15000	d-d transitions

5.3.8. Infrared Spectra

IR spectra of the ligand and the zeolite encapsulated metal complexes are given in Fig.V.11. The spectral bands of the ligand and the encapsulated metal complexes are given in Table V.6.

In the spectra of the free ligand the $\nu_{C=N}$ frequency occurs at 1630cm^{-1} . This band may be appearing in all the complexes after a shift to the higher frequency. In all the encapsulated ^{complexes} there appear a band around 1640cm^{-1} . This may be the azomethine stretching frequency shifted to a higher energy due to coordination of the ligand and encapsulation. Such a red shift has already been reported to some Salen complexes as a result of encapsulation and also for some other encapsulated complexes [10]. The aromatic ring vibrations, in the complexes are not masked by the framework vibrations. This also indicates the coordination of the ligand within the matrix.

5.3.9. EPR spectra

The EPR spectra of Cu₂PyEnY are given in Fig. V.12. The signals are very broad which may be due to the presence of one more type of Cu(II) center as an impurity. The excess metal present in the zeolite may be existing as a complex with different geometry. The g_{\parallel} and g_{\perp} values obtained are 2.265 and 2.0869. $g_{\parallel} > g_{\perp}$ in Cu₂PyEnY, which indicates axial symmetry for the copper complex. Co₂PyEnY exhibit a very broad EPR signal, which suggests cobalt(II) may be in the high spin state. No further information about the structure has been obtained from the EPR. The Mn₂PyEnY exhibits an EPR spectrum with six lines. The g value was found to be 1.94 and the A value to be 83 cm^{-1} . The forbidden transitions are also seen along with the signal.

Transmittance

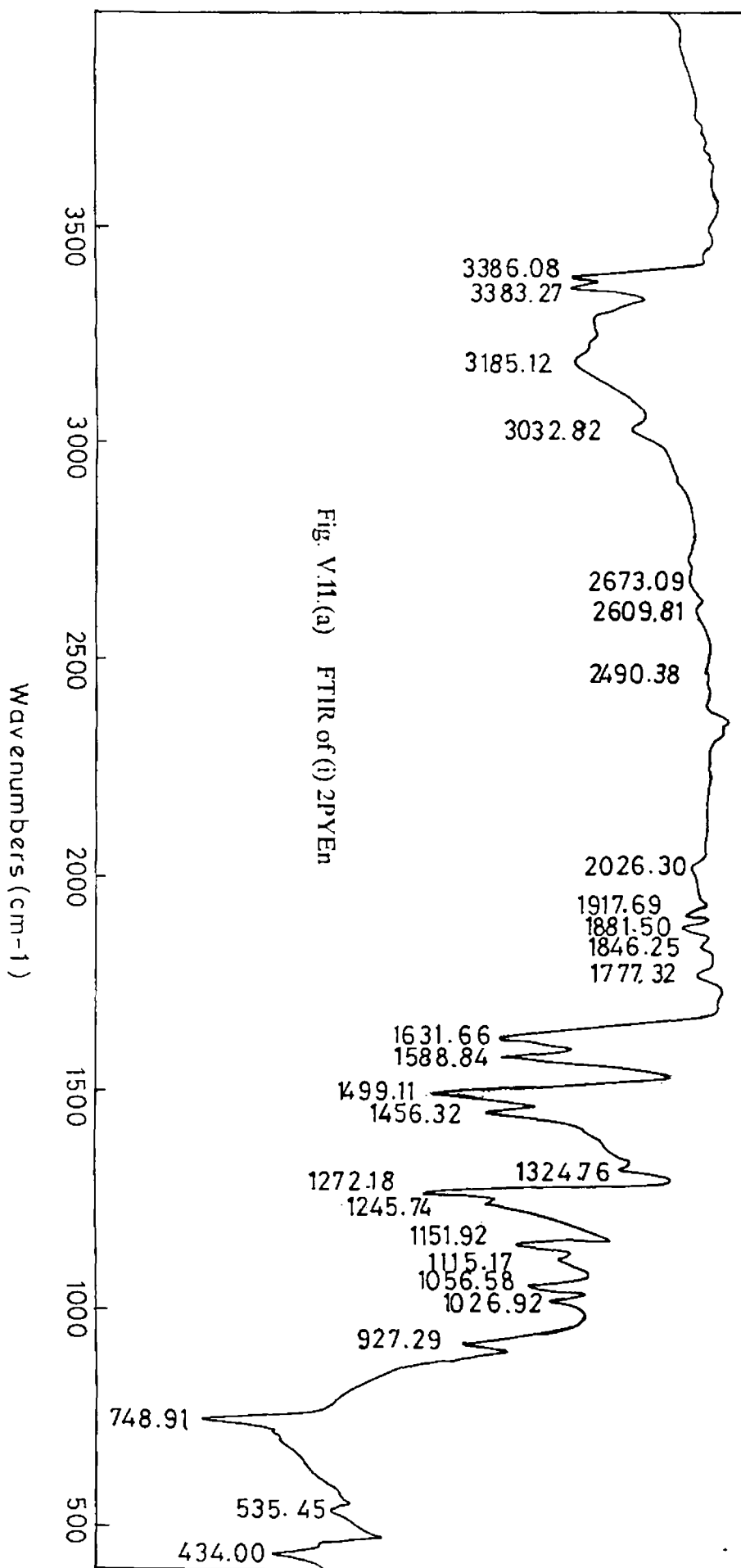


Fig. V.11.(a) FTIR of (i) 2PYEn

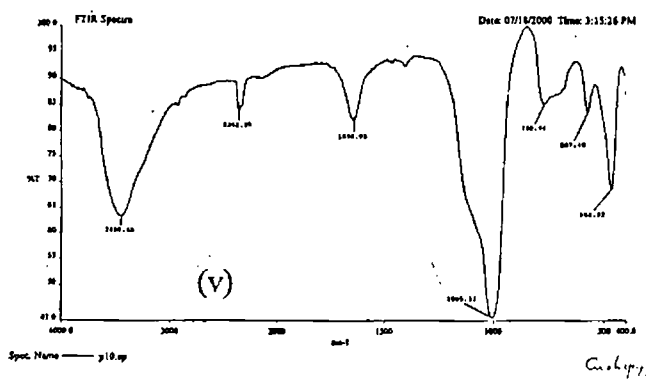
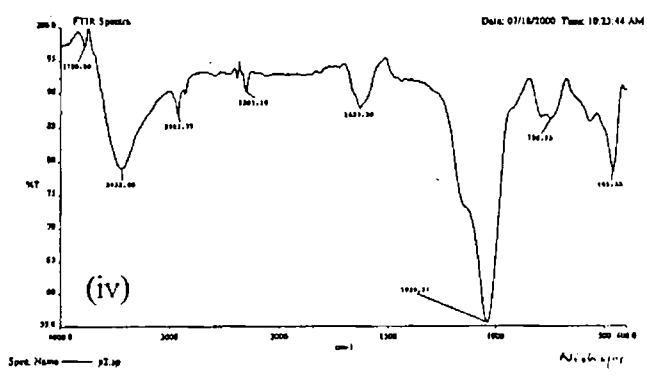
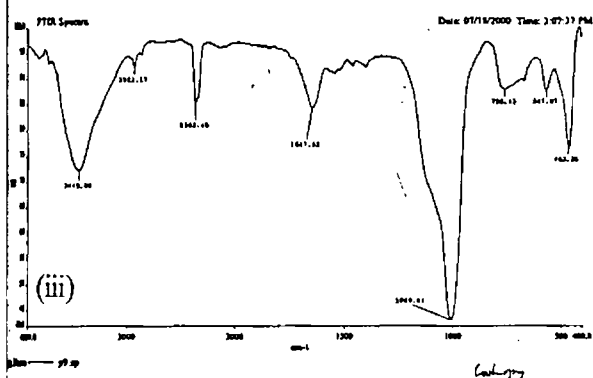
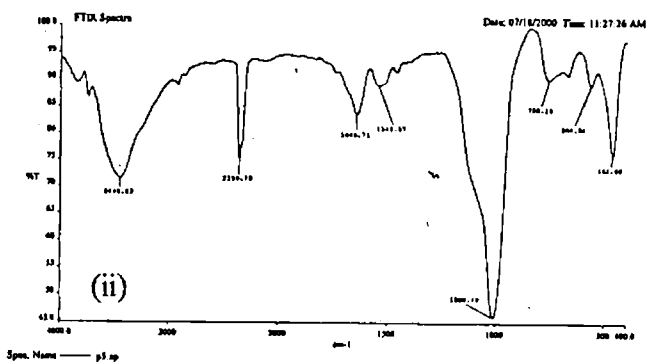
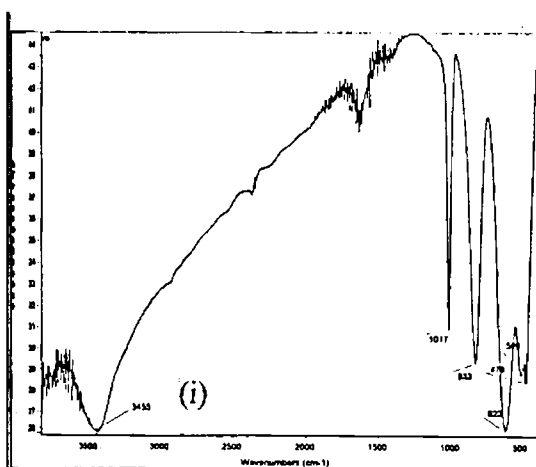


Fig. V.11. (b) FTIR of (i) NaY (ii) Mn₂PyEnY

iii) Co₂PyEnY

(iv) Ni₂PyEnY

(v) Cu₂PyEnY

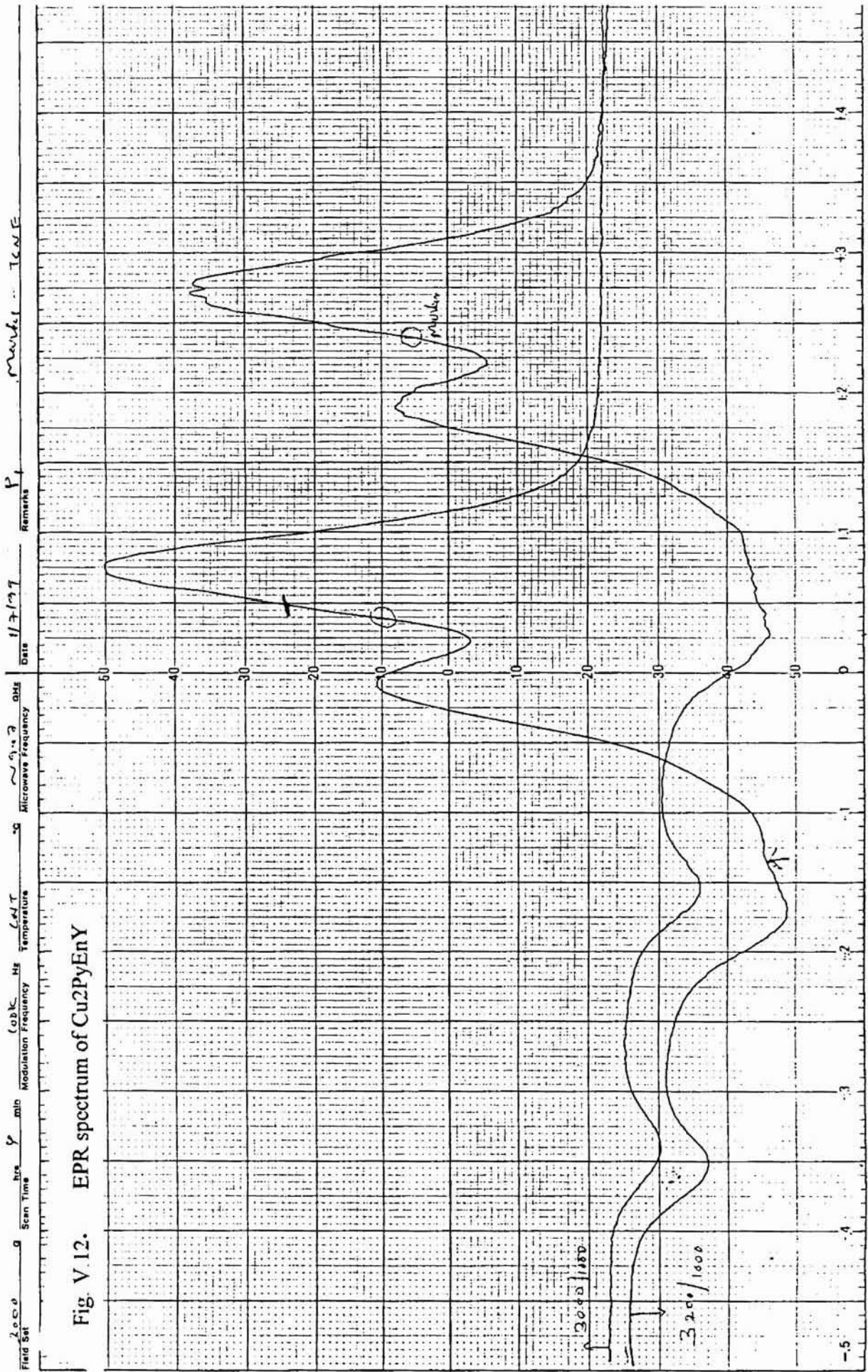
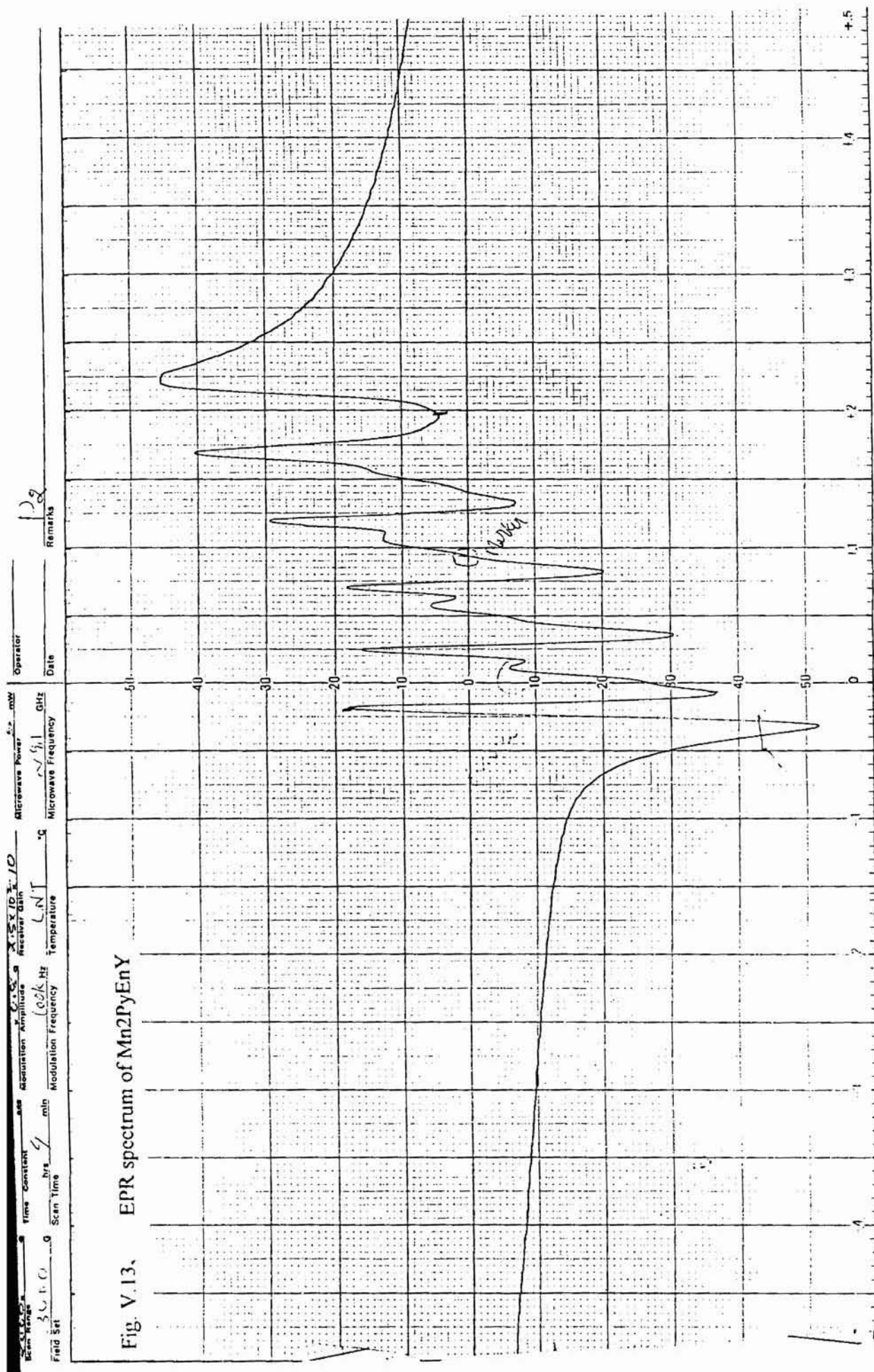


Fig. V.12. EPR spectrum of Cu₂PyEnY

SCALE RANGE



SCAN RANGE

REFERENCES

- [1] R.J. Taylor, R.S. Drago, J.E. George, *J. Am. Chem. Soc.*, **111** (1989) 6610.
- [2] K. Mizuno, S. Imamura, J.H. Lunsford, *Inorg. Chem.*, **23** (1984) 3510.
- [3] D.E. De Vos, E.J.P. Feijen, R.A. Schoonheydt, P.A. Jacobs, *J. Am. Chem. Soc.*, **116** (1994) 4746.
- [4] H. Masaaki, K. Kyoko, *Inorg. Chim. Acta.* **104** (1985) 47.
- [5] C.T. Spencer, L.T. Taylor, *Inorg. Chem.* **12** (1973) 644.
- [6] B. Kuncheria, G. Devi, P. Indrasenan, *Inorg. Chim. Acta.*, **155** (1989) 255.
- [7] F. Lions, K.V. Martin, *J. Am. Chem. Soc.* **79** (1957) 1572.
- [8] S. Imamura, J.H. Lunsford, *Langmuir* **1** (1985) 326.
- [9] S.P. Varkey, C.R. Jacob, *Ind. J. Chem.*, **37** (1998) 407.
- [10] F.A. Cotton, E. Bannister, *J. Chem. Soc.*, (1960) 1873.
- [11] N.N. Greenwood, A. Earnshaw, *Chemistry of the Elements*, 2nd Edn., Pergman Press, 1989.
- [12] D.E. De Vos, E.P.J. Feijen, R.A. Schoonheydt, P.A. Jacobs, *J. Am. Chem. Soc.*, **116** (1994) 4746.

CHAPTER VI

STUDIES ON THE ZEOLITE Y ENCAPSLUTED TRANSITION METAL COMPLEXES OF *N,N'*-Bis-(3-PYRIDINEMETHYLENE)-1,2-DIAMINOETHANE

6.1. INTRODUCTION

Transition metal Schiff base complexes catalyze a wide variety of reactions such as hydrolysis, decarboxylation, elimination, aldol condensation and redox reactions [1-3]. We have studied the catalytic properties of the zeolite Y encapsulated transition metal complexes of *N,N'*-bis-(3-pyridinemethylene)-1,2-diaminoethane, the results of which are presented in this chapter.

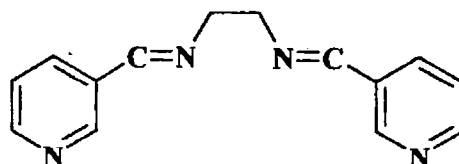


FIG VI. 1. Structure of the ligand

6.2. EXPERIMENTAL

6.2.1. Materials

The procedural details regarding the modifications to the zeolite support are given in chapter II.

6.2.2. Synthesis of zeolite encapsulated 3PyEn complexes.

A general outline of the preparation of the complexes is given in Chapter II. A mixture of metal exchanged zeolite (5g) and pyridine-3-carboxaldehyde (3.78 mL, 0.04 M) was refluxed in methanol (10 mL) for 3 hours, the chelate formed was condensed with 1,2-diaminoethane (1.34 mL, 0.02 M) for 2 h. It was then soxhlet extracted with ethanol till the washings are colourless. The re-exchange was carried out as reported earlier. The zeolite complexes were dried at 120°C for 2h. and preserved in vacuum over anhydrous calcium chloride.

6.2.3. Analytical Methods.

A detailed account of the various analytical methods employed and other characterisation techniques used are given in Chapter II.

6.3. RESULTS AND DISCUSSION

Zeolite encapsulated Mn(II), Co(II), Ni(II) and Cu(II) complexes of N,N'-bis(3-pyridinemethylene)-1,2-diaminoethane were prepared. The presence of the complexes and its structure were investigated using chemical analysis, XRD, surface area, magnetic moment, FTIR and EPR spectroscopy and TG analysis.

6.3.1. Chemical Analysis

The results of the chemical analysis of the zeolite encapsulated 3PyEn complexes were given in Table VI. 1. The data reveal that Si/Al ratio of metal exchanged zeolite remains unchanged in the zeolite complexes. This indicates that Y zeolite can withstand the conditions of encapsulation.

Table VI. 1. Analytical data of Encapsulated 3PyEn Complexes.

Sample	%Si	%Al	%Na	% Metal	%C	%H	%N
Mn3PyEnY	18.82	7.59	5.43	2.72	5.76	0.46	1.81
Co3PyEnY	17.96	7.25	6.19	2.55	5.68	0.51	1.89
Ni3PyEnY	18.57	7.49	6.36	2.04	5.76	0.39	1.99
Cu3PyEnY	17.84	7.2	5.39	2.48	5.60	0.40	1.87

6.3.2. TG DATA

TG/DTG data for the complexes is given in Table VI.2. All the complexes exhibit two stages of decomposition (Fig VI.2). The first stage is the water loss, in the second stage there is decomposition of the encapsulated species. The weight loss may not be strictly due to the decomposition of the encapsulated species. In the case of manganese complex, the second stage is not distinguishable.

Table VI.2 TG/DTG data

Sample	Weight loss-Stage I			Weight loss-Stage II		
	Temp. range(°C)	Peak temp. (°C)	% mass loss	Temp. range(°C)	Peak temp. (°C)	% mass loss
Mn3PyEnY	50-110		14.0	270-600	490	15.5
Co3PyEnY	50-110	90	15.5	410-600	400	7.0
Ni3PyEnY	50-110		14	470-610		2.0
Cu3PyEnY	90-220		12	400-620	600	2.0

6.3.3. X-ray Diffraction Studies

XRD patterns of Mn3PyEnY, Co3PyEnY and NaY are given in Fig. VI. 3. These patterns are very much identical to those of NaY. The framework structure remains intact during the synthesis of the complexes within the super cage.

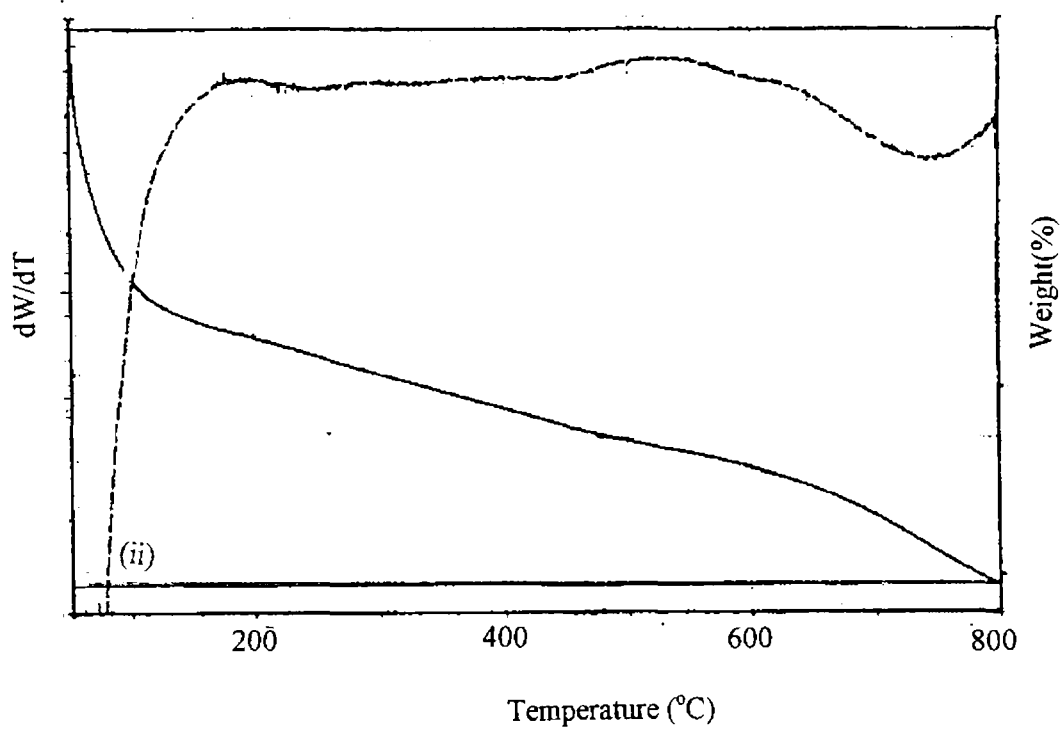
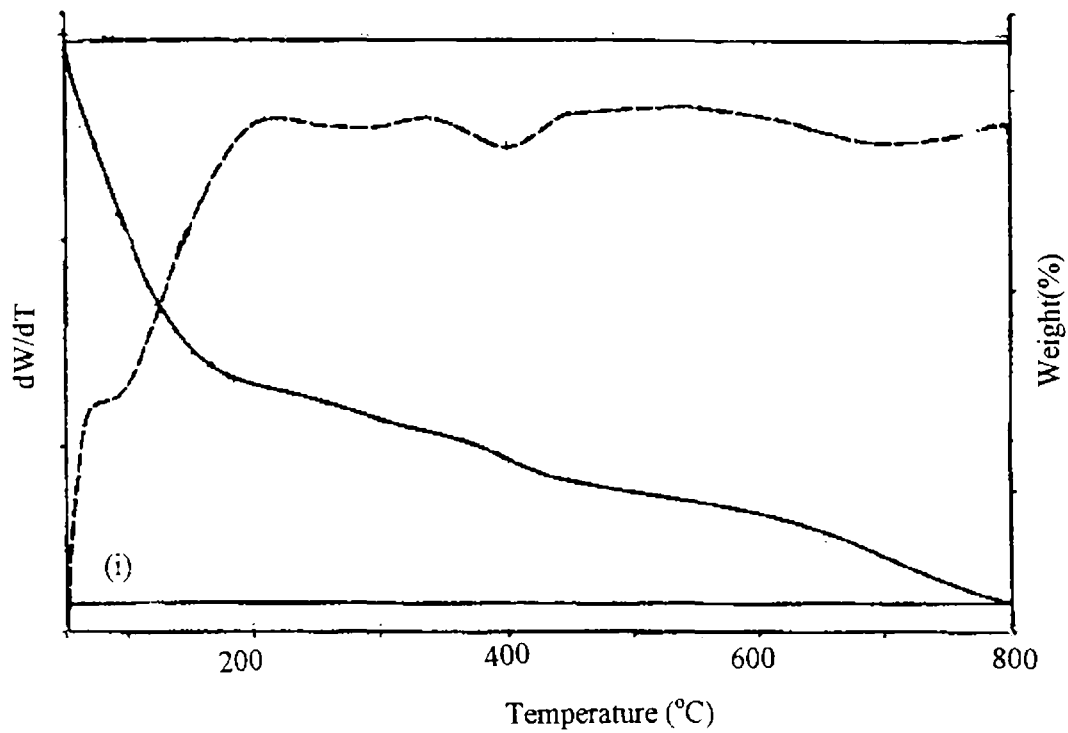


Fig.VI.2.A. TG / DTG Curves of (i) Mn₃PyEnY (ii) Co₃PyEnY

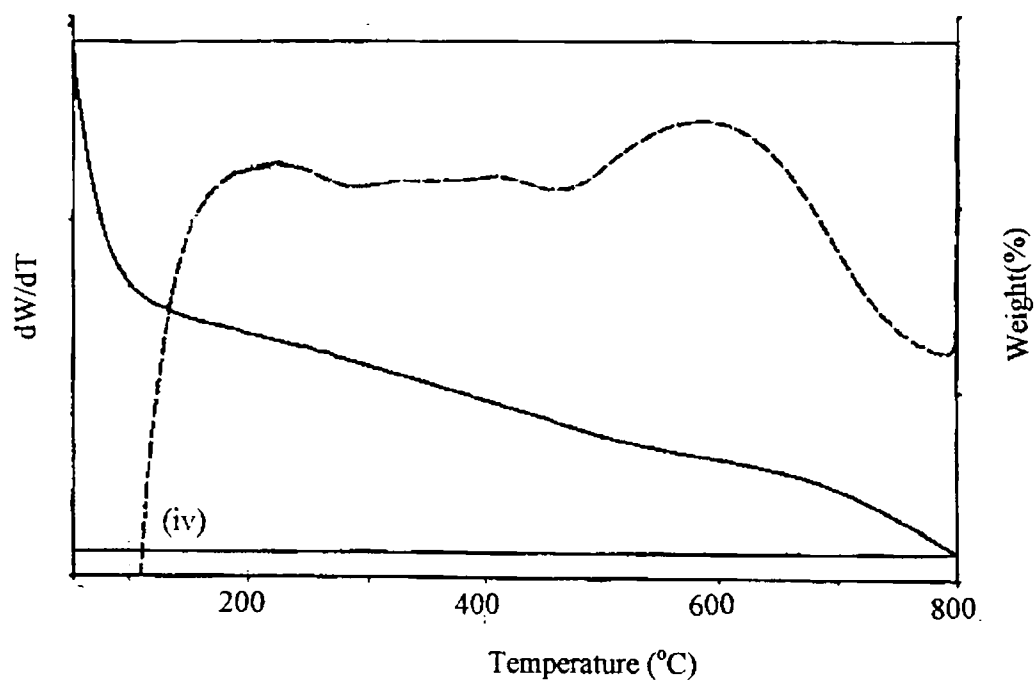
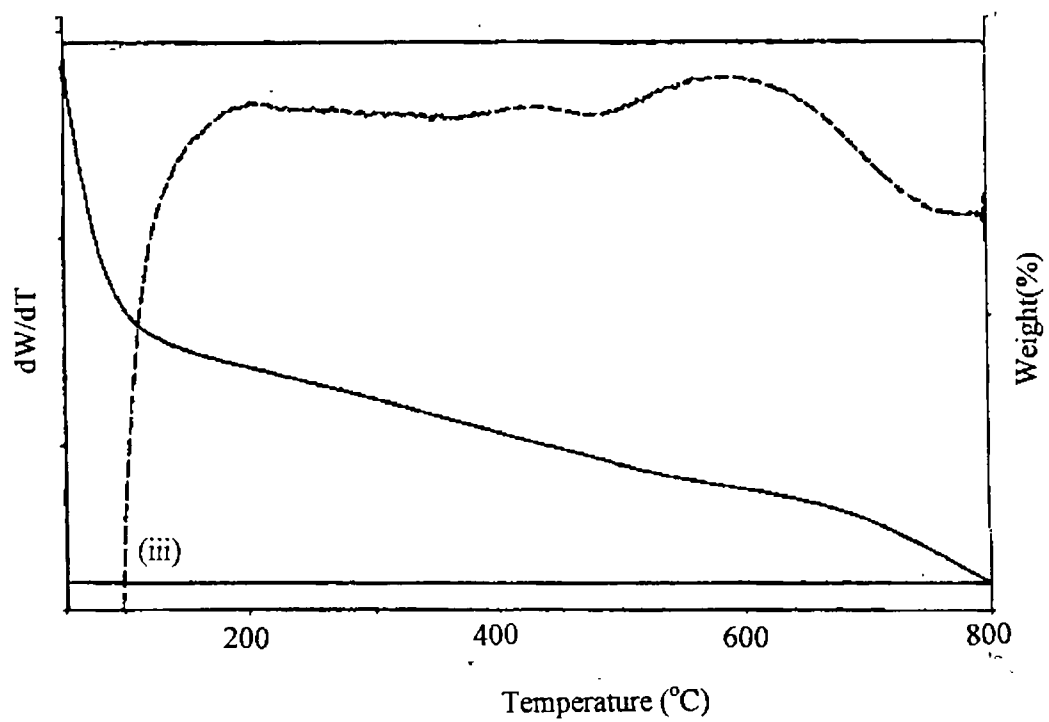


Fig. VI.2.B. TG/DTG Curves of (iii) Ni₃PyEn (iv) Cu₃PyEny

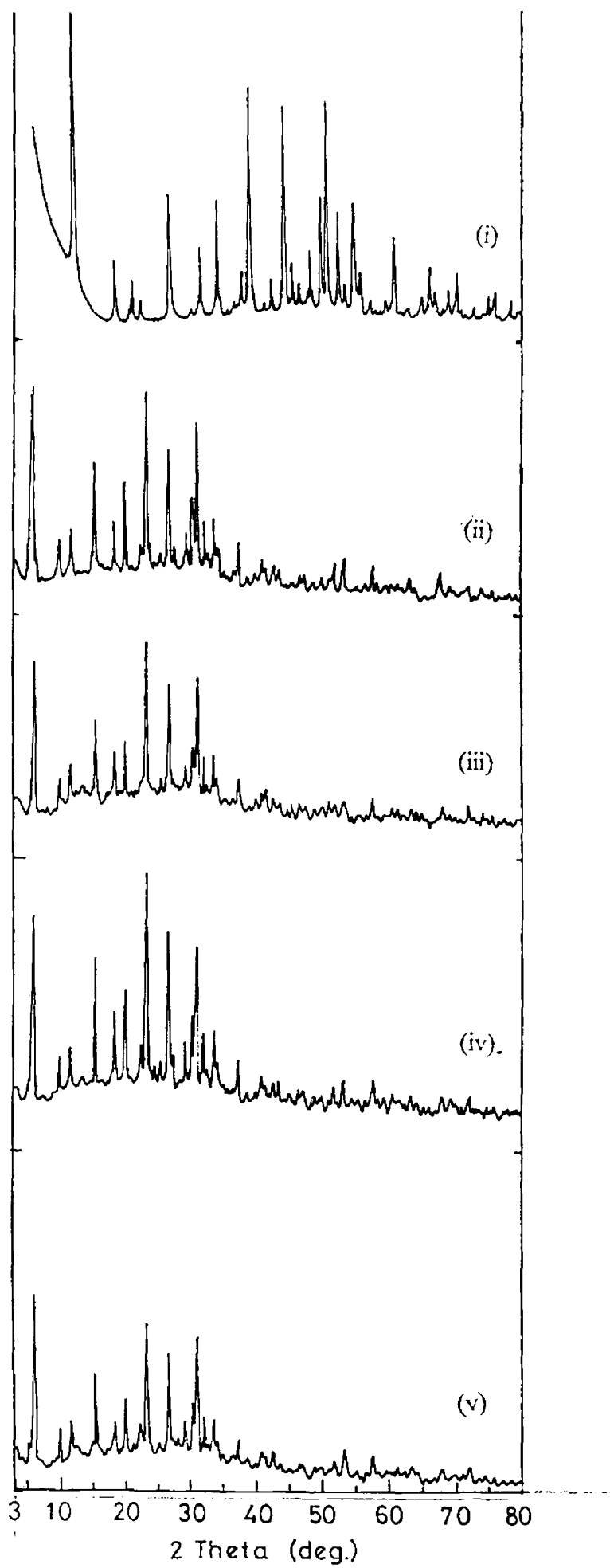


Fig. VI.3 XRD Patterns of (i) NaY (ii) $Mn_3P\gamma EnY$
(iii) $Co_3P\gamma EnY$ (iv) $Ni_3P\gamma EnY$ (v) $Cu_3P\gamma EnY$

6.3.4. SEM analysis

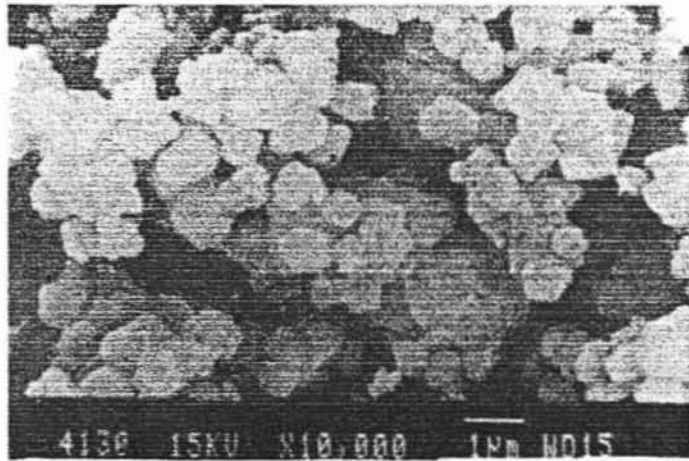
The SEM of the Mn3PyEnY complexes were taken before and after soxhlet extraction and are given in Fig.VI.4. From the micrographs, it can be seen that soxhlet extraction removed all the surface adsorbed complexes. The average particle size is 1 μ m in the complex.

6.3.5. Surface area analysis

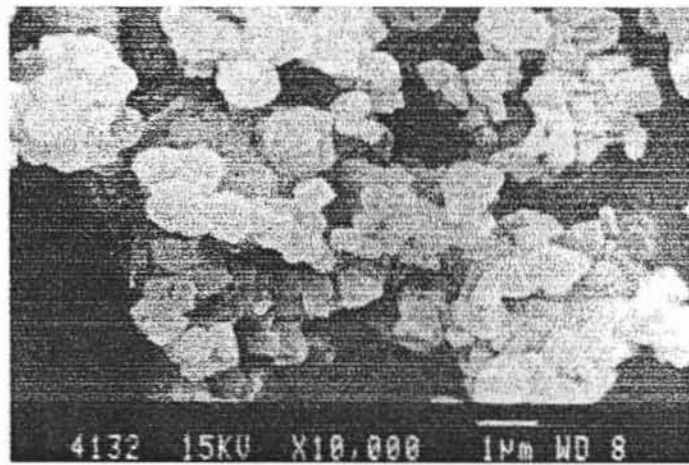
Surface area data is noted in Table VI. 3. Encapsulation of the complexes brings down the surface area of the metal exchanged zeolites. This is an ample proof for encapsulation. The decrease in surface area is shown in Fig VI. 5.

Table VI. 3 Surface area of encapsulated 3PyEn complexes.

Sample	Surface area (m ² /g)		
	MY	M3PyEnY	%Loss
NaY	549	-	-
Mn3PyEnY	539	264	51.02
Co3PyEnY	532	367	31.02
Ni3PyEnY	528	375	28.97
Cu3PyEnY	528	294	44.31

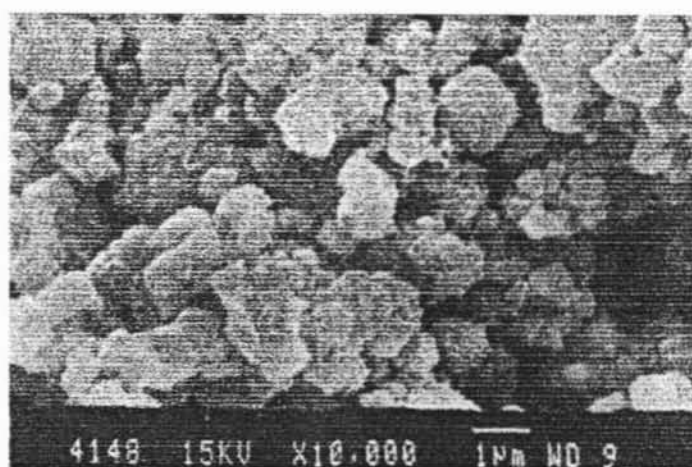


(i)

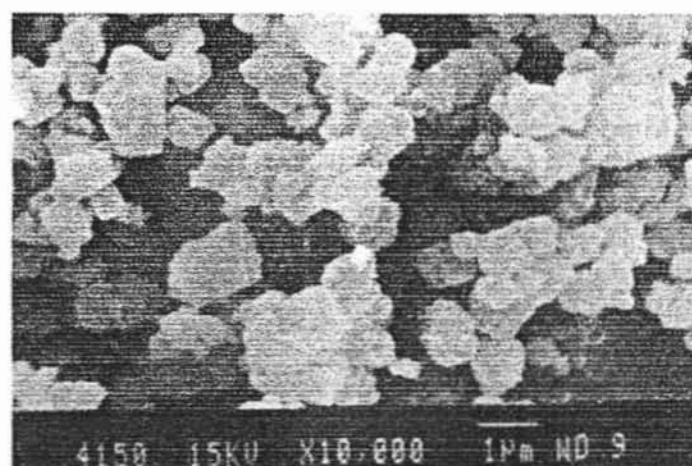


(ii)

Fig. VI.4. SE Micrographs of (i) NaY (ii) MnY



(iii)



(iv)

Fig. VI.4.B SE Micrographs of Mn₃PyEnY

(iii) before and (iv) after Soxhlet extraction

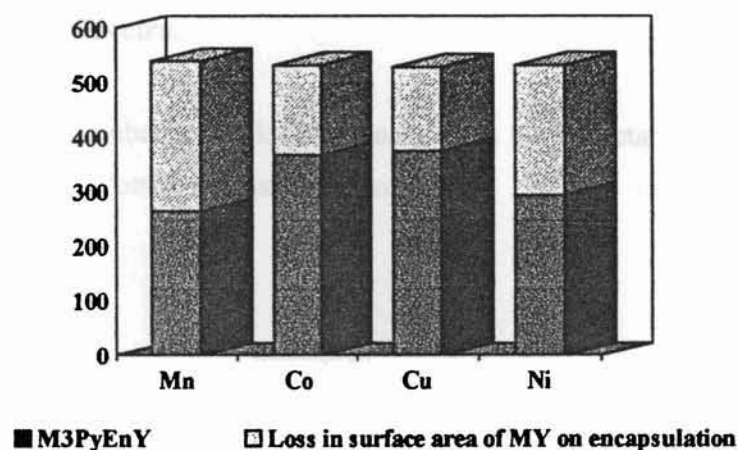


Fig.VI. 5. Loss of surface area of the encapsulated 3PyEn complexes

6.3.6. Magnetic Moment.

The room temperature magnetic moment values are given in Table VI. 4. The Mn3PyEn complex shows a magnetic moment value for a d^5 ion in the high spin state [4]. The Co3PyEnY complex exhibits a magnetic moment value expected for a tetrahedral Co(II) ion. The magnetic moment value of 3.6BM suggests a distorted tetrahedral geometry for the complex, Ni3PyEnY [4]. The magnetic moment value of Cu(II) is in agreement with that of an axially symmetrical d^9 ion.

Table VI. 4. Magnetic moment values of the encapsulated complexes

Sample	Magnetic moment (BM)
Mn3PyEnY	5.9
Co3PyEnY	4.8
Ni3PyEnY	3.6
Cu3PyEnY	1.9

6.3.7. Electronic Spectra.

After doing Kubelka-Munk (KM) analysis on the reflectance data, the $F(R)$ value obtained is plotted against wavelength.

The diffuse reflectance spectrum of Mn_3PyEnY along with that of MnY and NaY are given in Fig.VI.6. The complexation can be directly inferred by comparing the spectra.

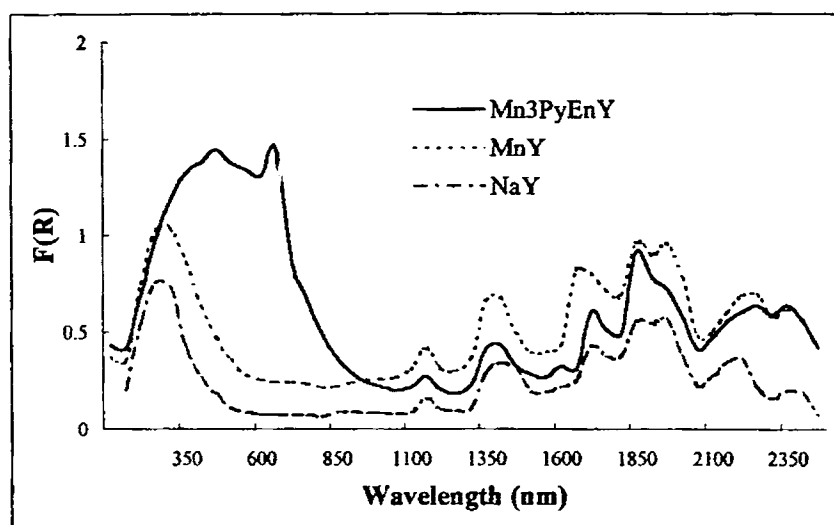


Fig.VI.6. Diffuse reflectance spectra of Mn_3PyEnY , MnY and NaY

In the diffuse reflectance spectra of the Mn_3PyEn complex, there is a broad band around $22,000\text{cm}^{-1}$ with a shoulder at $19,900\text{cm}^{-1}$. This is characteristic of $Mn(II)$ in the octahedral field [5]. This transition can be assigned as the two transitions ${}^4E_g(G) \leftarrow {}^6A_{1g}$ and ${}^4A_{1g}(G) \leftarrow {}^6A_{1g}$ transitions respectively. The other transitions may either be weak or masked in the case of encapsulated complexes

Fig.VI.7 represents the diffuse reflectance spectra of Co3PyEn, CoY and NaY.

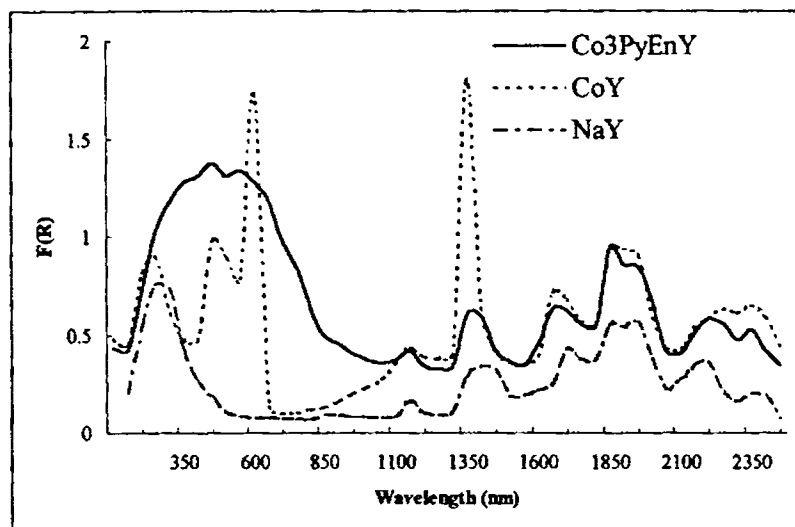


Fig.VI.7. Diffuse reflectance spectra of Co3PyEn, CoY and NaY

In this spectrum of the Co3PyEn there is multiple absorption in the visible region around $16,600\text{ cm}^{-1}$, which may be assigned to the ${}^4T_1(F) \leftarrow {}^4A_2$ transition characteristic of the Co(II) in a tetrahedral environment [6]. The ${}^4T_2 \leftarrow {}^4A_2$ transition may be masked by the absorption bands due to the zeolite framework.

The diffuse reflectance spectrum of the Ni3PyEn compared to that of the NiY and NaY is given in Fig.VI.8

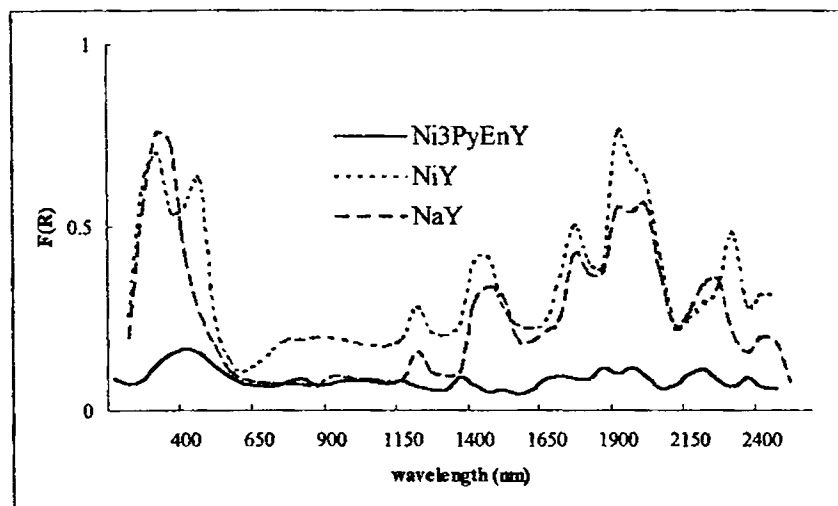


Fig.VL8. Diffuse reflectance spectra of Ni3PyEnY, NiY and NaY.

The absorption around $7,400\text{ cm}^{-1}$ may be the ${}^3A_2(F) \leftarrow {}^3T_1(F)$ transition of a distorted tetrahedral Ni(II). The ${}^3T_2(F) \leftarrow {}^3T_1(F)$ transition was masked in this spectrum. On the basis of this, a distorted tetrahedral structure may be assigned to the Ni3PyEnY complex [6].

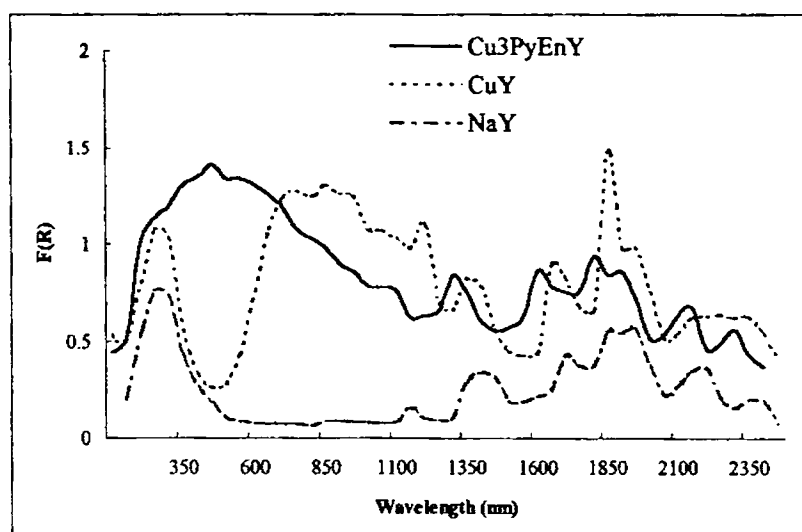


Fig.VL9 Diffuse reflectance spectra of Cu3PyEnY, CuY and NaY.

Fig.VI.11 represents the diffuse reflectance spectra of Cu₃PyEnY, CuY and NaY. The multiple d-d absorption around 15,000 cm⁻¹ may be the characteristic absorption of the tetragonal Cu(II). So a tetragonal geometry may be assigned to the Cu₃PyEnY complex [6].

6.3.8. FTIR Spectra

The IR spectral bands of the ligand and the encapsulated complexes are given in Table VI. 5. In Fig VI. 10, the IR spectra of the ligand and the zeolite encapsulated Co(II)₃PyEnY complex and the CoY are given.

The azomethine group vibration occurring at 1613 cm⁻¹ in the ligand has been shifted in all these complexes. This may be due to the coordination of the azomethine group to the metal ion. The peak around 770 cm⁻¹ in the ligand is seen in the complex with a shift. This may be a indication for the complexations.

6.3.9. EPR spectra

The Co₃PyEnY complex exhibits a very broad EPR signal. So it is evident that in the complex Co(II) is in the high spin state. The Cu₃PyEnY complex has given very broad signals. The broadening may be due to the presence of another Cu(II) site as impurity. The g_{||} value obtained is 2.26 and g_⊥ is 2.12. since g_{||} > g_⊥, the complex may be axially symmetrical. A_{||} value obtained is 96.5 x 10⁻³ cm⁻¹.

Table VI. 6. The IR spectral bands of the ligand and the encapsulated complexes

MY	3PyEnY	Mn3PyEnY	Co3PyEnY	Ni3PyEnY	Cu3PyEnY
450	418				
		464	459	462	464
615	615				569
	640	570	572	569	770
		671		670	
1050			751	757	
	712				
	777				
	821				
1600		1012		1029	1007
	992				
	1047				
	1160				
	1389				
	1420		1032		
	1472				
1572					
2300	1613				
	2912				
3250	3041	1640		1640	1639
	3812			1660	1660
3434		1660	1639	2361	
		2361			
3435		3455	2361		2361
			3434	3435	3454

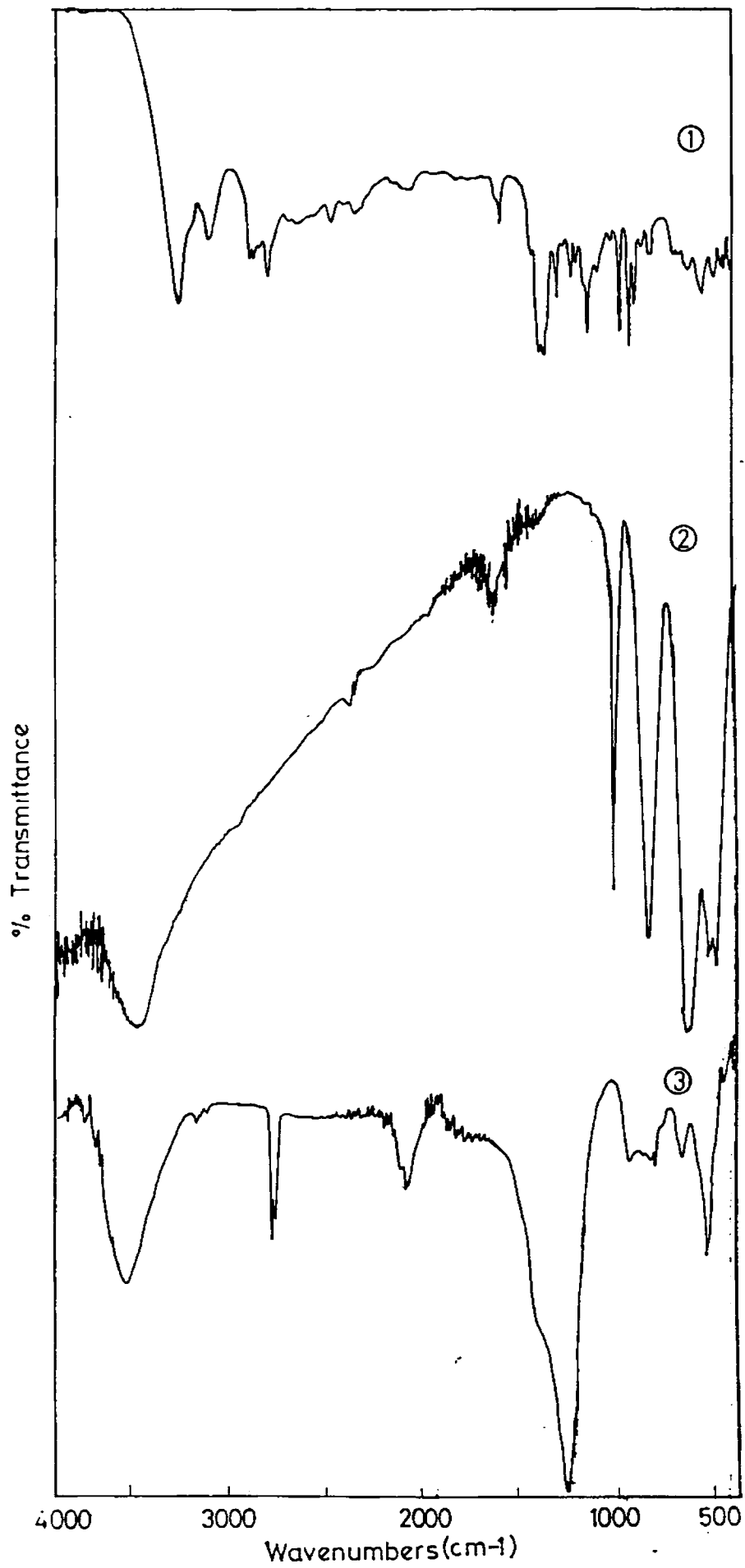


Fig. VI.10. FTIR of (i) NaY (ii) 3PYEn (iii) Co₃PYEnY

2000 x
 Scan Range
 3000
 Field Set
 0.05
 Time Constant
 4
 Scan Time
 100k
 Modulation Frequency
 100k
 Modulation Amplitude
 10x10² x 10
 Receiver Gain
 LNT
 Temperature
 5
 Microwave Power
 91
 GHz
 Microwave Frequency
 P
 Operator
 3/11
 Date
 Marker TCNE
 Remarks

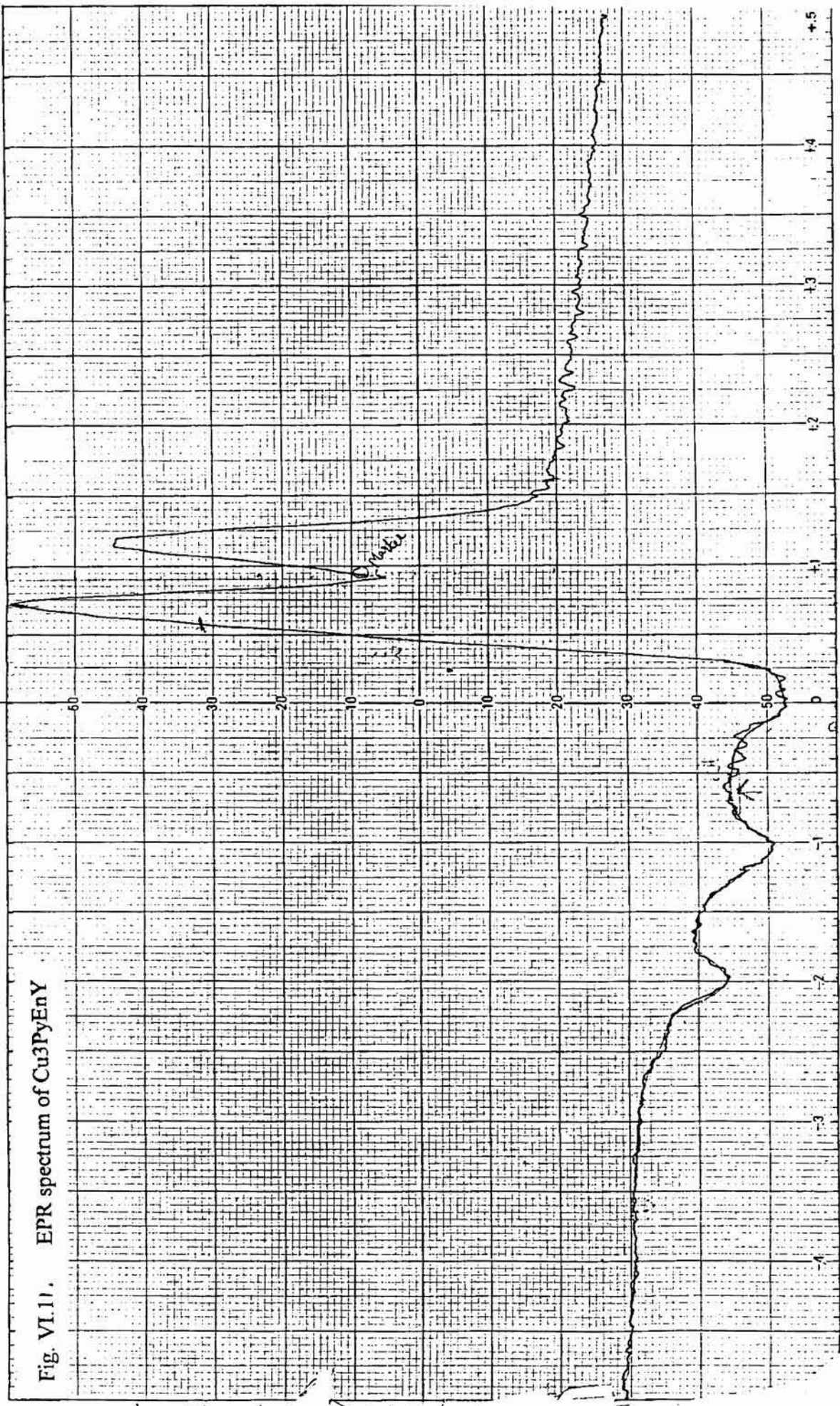


Fig. VI.11. EPR spectrum of Cu₃PyEnY

SCAN RANGE

REFERENCES

- [1] N. Kitajima, H. Fukui, Y. Mosso-oka, *J. Chem. Soc. Chem. Comm.* (1988) 485.
- [2] J.C. Bailer, *Catal. Rev. Ser. Eng.*, 10 (1974) 17.
- [3] M.M. Takui Khan, A.E. Martell, *Homogeneous catalysis by metal complexes* Academic Press, New York (1981).
- [4]. N.N. Greenwood, A. Earnshaw, *Chemistry of the elements*, Pergamon Press, New York
- [5] F.A. Cotton, G. Wilkinson, *Advanced Inorganic Chemistry*, 5th edition, John Wiley, New York (1988).
- [6] A.B.P. Lever, *Inorganic Electronic Spectroscopy*, 2nd edition, Elsevier, New York.

CHAPTER VII

CATALYTIC ACTIVITY STUDIES OF THE Y-ZEOLITE ENCAPSULATED SCHIFF BASE COMPLEXES

The synthesis of transition metal complexes inside the cage of a zeolite has received increasing attention in recent years, since the complex prepared in this way create favourable conditions for reversible addition of molecular oxygen and decrease considerably the rate of irreversible oxidation of central ion. These compounds may be used as catalysts combining the advantages of homogeneous and heterogeneous catalysis or as absorbents for the energy efficient separation of oxygen from air [1].

There are reports on the zeolite encapsulated cobalt complexes acting as reversible oxygen binders [2-5]. Tatsumi and coworkers synthesised zeolite encapsulated iron and manganese tetramethylporphyrin complexes and used them as oxidizing systems with H_2O_2 [6]. Several research groups are persuaded to explore the ability of the zeolites to act like the fascimiles of natural enzymes [7-10]. The zeolite frame work prevents encapsulated metal complexes from dimerising and the internal channels control the access of the molecules to the zeolite cage. In this way the frame work of the zeolite impose size and shape selectivity in the same way as the channels created by protein structure of the enzyme.

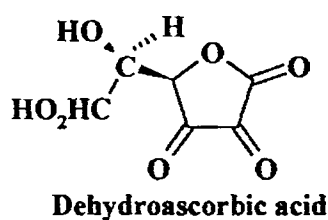
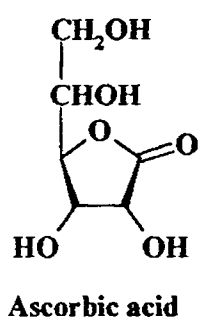
CATALYTIC ACTIVITY STUDIES OF THE ENCAPSULATED SCHIFF BASE COMPLEXES IN THE OXIDATION OF ASCORBIC ACID

Ascorbic acid has very interesting biological property. It is a lactone with 2,3-endiol group and is a very effective reducing agent with wide applications in analytical chemistry. The reactivity of the endiol group has been utilized in a number of organic syntheses. Biologically, ascorbic acid is the only water soluble vitamin for which no microbiological test is available [11].

Ascorbic acid is susceptible to oxidation in both acidic and basic media and is therefore used as an antioxidant in the food industry [12]. The products of the oxidation largely depend on pH. Its oxidation by various oxidizing agents in acidic solution produces dehydroascorbic acid, a lactone whose ring can be easily hydrolysed to give the free carboxylic group [13]. The fact that dehydroascorbic acid possesses vitamin C activity was recognised early in studies of ascorbic acid by several groups [14,15]. Since ascorbic acid is a good reducing agent that readily reacts with one-electron or two-electron oxidizing agents, it is needed to design reagents that do not over oxidize ascorbic acid and that give reaction products that are easily separated from dehydroascorbic acid.

There are a number of reports in literature about the oxidation of ascorbic acid catalysed by copper(II) and iron(III) [16-21]. Due to its biological significance most of the oxidation studies of ascorbic acid were carried out near the physiological pH range. Certain transition metal complexes of which ligands containing quinoxaline ring systems have been reported to be catalytically active in this oxidation using molecular oxygen [22].

Here the Y zeolite encapsulated Mn(II), Co(II), Ni(II) and Cu(II) Schiff base complexes of Saloph, OHOP, 2PyEn and 3PyEn were screened as catalysts for the oxidation of ascorbic acid to dehydroascorbic acid. Their catalytic activity is compared to the corresponding well known Salen complexes encapsulated in Y zeolite. The details of the study are presented in this chapter.



7.1.1. EXPERIMENTAL

7.1.1.1. Materials

The details regarding the preparation of the zeolite encapsulated complexes are given in Chapter II. The Y zeolite encapsulated Salen complexes of Mn(II), Co(II), Ni(II) and Cu(II) were prepared using the well established ship in a bottle method [23].

7.1.1.2. Preparation of stock solution

A solution of L-ascorbic acid ($1.0 \times 10^{-3} \text{ mol l}^{-1}$) has been prepared in triply distilled water afresh before each catalytic reaction.

7.1.1.3. Reaction mixtures

To the stock solution L-ascorbic acid (1.25 mL) was added distilled water(10 mL). The catalyst (~0.005g) was then added to this solution. The catalyst to substrate ratio was kept at 1:10.

7.1.1.4. Apparatus

A Shimadzu UV-Vis 160A spectrophotometer with 1cm quartz cells is used for absorbance measurements.

7.1.1.5. Catalytic Experiments

All the reactions were carried out at a temperature of $28.0\pm 0.1^{\circ}\text{C}$. The reaction was initiated by transferring the calculated amount of the ascorbic acid into the reaction bottle containing the required amount of the catalyst. After 30 minutes it was filtered and made upto 25 mL. The absorbance of ascorbic acid was noted at 265 nm where it has maximum absorbance and all other substances present in the reaction mixture have negligible absorbance. The concentration of ascorbic acid was obtained from the absorbance data using a molar absorption coefficient of 7500 at 265 nm. The oxidation efficiency of the various catalysts is given in Table VII.1 and also given as a bar chart in Fig. VII.1.

Recyclability and Stability of the catalysts: The reaction mixture was colourless after the experiment. Each mixture was tested for the presence of metal ions and the result showed that there was no leaching out of the metal complexes during the reaction. On completion of the reaction all the catalysts were recovered

by filtration, washed with acetone and dried. They were again used for another catalytic run and was found to be active for the oxidation of ascorbic acid. The FTIR of the used catalysts showed the presence of the complex inside the matrix after the reaction. The UV-Vis spectra of the catalysts were taken as the nujol mull and confirmed that the complexes were safe within the super cage. So these catalysts are stable and recyclable in the present reaction conditions.

7.1.2. RESULTS AND DISCUSSION

In the context of catalysis the aim was to simply produce stable zeolite encapsulated oxidation catalysts. Almost all the Mn(II), Co(II), Ni(II) and Cu(II) complexes studied are active in the oxidation of ascorbic acid to dehydro ascorbic acid. The percentage conversion in respect of the various complexes are represented as bar charts. It may be noted that metal exchanged zeolites have almost negligible activity in this oxidation reactions. This suggests that the chelate ligands tune the electronic environment of these metal ions so that better activity is observed in these cases. Drawing conclusions from order of activities of the complexes may be too speculative due to the lack of detailed kinetic studies of the oxidation. Also the complexes used in the present work may lead to intermediate complexes of different geometries. The reaction path way also may be different depending upon the metal ion involved. For example a molecular oxygen bonded M(III) intermediate may be possible in the case of Mn(II), Co(II) and Ni(II) complexes. But in the case of Cu(II) catalysed oxidation the role of molecular oxygen was to oxidise the reduced Cu(I) substrate intermediate only. There need not be essentially O₂-Cu(I)- substrate intermediate. More over various redox couples involved in the above reaction also affect the rate of the oxidation. The lack of knowledge about the structure of the exact intermediate, diffusion rates of the substrate and molecular oxygen and the active species taking part in the reaction further complicates the situation. However in the present study the complexes used may be treated as catalyst precursors rather than active catalysts.

All the Mn(II) complexes catalyze the oxidation of ascorbic acid. The O⁻ part of the ligands and the axially coordinated water molecules or O⁻ ions of the framework are considered to be labile and these labile ligands can be substituted easily by donor sites of ascorbic acid. MnSOPY is found to be least active in this case. This might be due to the rigid nature of the ligand and the complex. The active metal site may not be easily available for the formation of O₂-Mn(III) substrate intermediate. MnOHOPY has higher activity. Mn₂PyEnY and Mn₃PyEnY also show good activity in this case. The axially coordinated weak framework oxide ions in the Mn₂PyEnY and Mn₃PyEnY (which may be needed for charge neutralisation of the complexes) may be considered less basic than the OH groups in SOPY, OHOPY ligands. This may lead to increased activity for the Mn₂PyEnY and Mn₃PyEnY.

All the Co(II) complexes are highly active in the oxidation of ascorbic acid. Complexes with square planar geometry are expected to be highly active in this case. The reaction may be progressing through one electron transfer steps between the metal center and molecular oxygen. A vacant coordination site is favourable for such an electron transfer process. All the Co(II) complexes are found to be active. A little higher activity is shown by the complex CoSOPY.

It is interesting to note that all the Ni(II) complexes are also catalyzing the oxidation of ascorbic acid. Normally Ni(II) ion is considered least active in this kind of reactions. The redox couple involved must be a Ni(II)/Ni(III) cycle. The Ni(III) ion is usually very unstable, but may be stabilized by the electric field present within the cage. Such an electric field may reduce the oxidation potential of the Ni(II) ion and thus render it favourable for oxidation by oxygen in the super cage of zeolite Y. The resultant Ni(III) species can be considered as a highly active oxidation catalyst.

The Cu(II) chelate catalysed oxidation of ascorbic acid has been well studied [24]. The oxidation reaction progress through an intermediate with a lesser coordination number where some of bonds of chelate is ruptured to facilitate the reaction. In such a case it is easy for the formation of the Cu(II)-substrate intermediate. The formation of such an intermediate is favorable in the case of Cu₂PyEnY complexes in which the charge neutralization are through frame work oxide ions. This may be the reason for the increased activity in the case of Cu₂PyEnY and Cu₃PyEnY complexes. All the other complexes have comparable activity. These weakly basic oxide ions may be more labile and result in the easy formation of the Cu(II)-substrate intermediate.

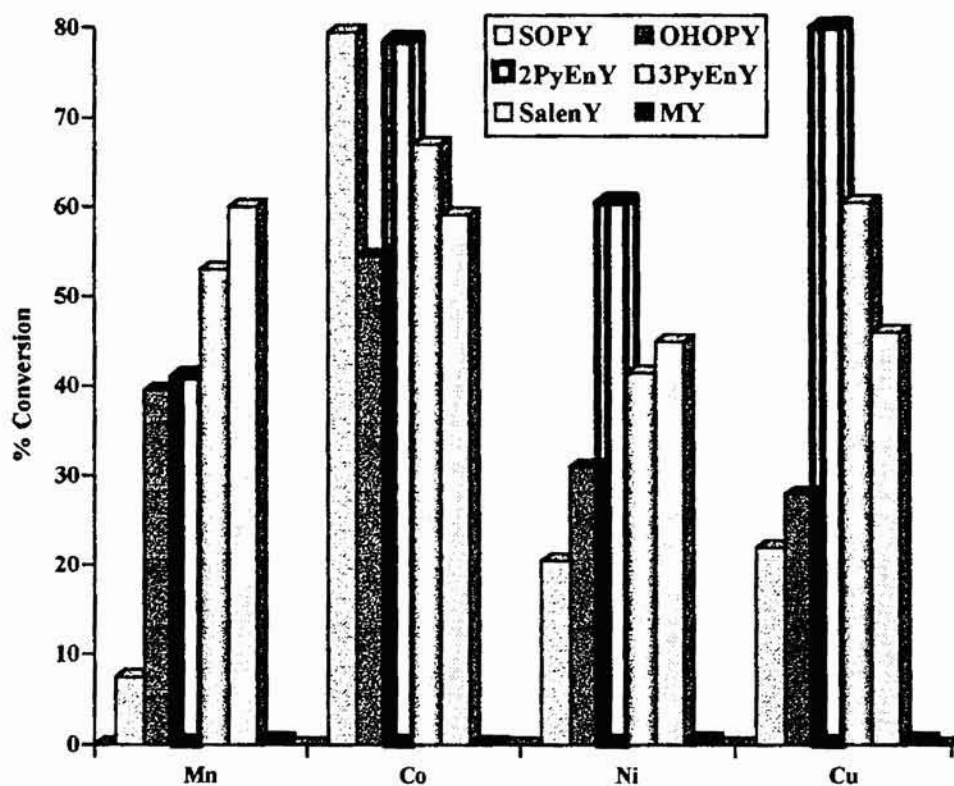


Fig VII.1 Percentage conversion of ascorbic acid over zeolite encapsulated complexes

7.2. CATALYTIC ACTIVITY STUDIES OF THE ENCAPSULATED SCHIFF BASE COMPLEXES IN THE OXIDATION OF 3,5-DI-TERT-BUTYLCATECHOL

Catalysts to effect the liquid-phase oxidation of catechol and its derivatives is a developing area of interest. A variety of metal complexes such as Cu(II) [25, 26], Ru(II) [27] and V(V) [28] could be used in the oxidative cleavage of catechol. It has been reported that the main product was 3,5-di-tert-butyl-o-benzoquinone when the oxidation of 3,5-di-tert-butylcatechol was carried out in slightly alkaline aqueous methanol [29]. Tyson and Martell and coworkers have reported the kinetic studies of the autoxidation of 3,5-di-tert-butylcatechol in 50% methanol by various techniques like manometry, EPR and spectrophotometry [30].

In nature, transition metals are components of numerous enzymes to facilitate transformation to a tremendous array of organic molecules. The coordination environment of an enzyme is responsible for its specific properties to effect catalysis. Interest in synthetic metal complexes is derived due to their existence in biological systems and their capability to act as catalysts for numerous chemical reactions as well [28-30]. In an ideal synthetic complex, geometric and electronic features of the ligand should serve a similar role. Models for biological systems should mimic as many of the structural, spectroscopic and reactivity properties of a metallo-enzyme as possible. In dioxygen transport and in electron-transfer systems, copper containing proteins function as mono and di oxygenases [34-35]. There are many reports on the use of Co(II) Schiff base complexes as synthetic oxygen carriers. An extensive work has been carried out by Calvin and his group on such system [36]. To resolve the possibility of such a study, we have carried out the oxidation of 3,5-di-tert-butylcatechol using the prepared Co(II) and Cu(II) Schiff base complexes encapsulated in zeolite Y. The catalytic activity of these complexes was compared with that of the corresponding Salen complexes encapsulated in Y zeolite.

7.2.1. EXPERIMENTAL

7.2.1.1. Materials

Details about the synthesis of the Y zeolite encapsulated Co(II) and Cu(II) Schiff base complexes are given in Chapter II.

7.2.1.2. Reaction Mixtures

DMSO was selected as the solvent to avoid vaporisation during the course of the reaction. The oxidation of DTBC was monitored in the same solvent system making use of some Y zeolite encapsulated metal complexes earlier [37]. It was made 0.1 M with respect to triethylamine. The DTBC solution (0.01 g in 10 mL solvent) was prepared afresh before each experiment to avoid auto oxidation. Catalyst to substrate ratio selected for the present study is 1:100.

7.2.1.2. Catalytic Experiments:

All the kinetic runs were carried at a temperature of $28 \pm 1^\circ\text{C}$ using atmospheric oxygen as the oxidant. The reaction is initiated by adding the DTBC solution to 0.005 g of the catalyst. The progress of the reaction was monitored by measuring the change in absorbance of the product at 400 nm. The blank was the solvent containing the same amount of catalyst. The concentration of DTBC undergoing oxidation could be obtained from the absorbance data using a molar extinction coefficient value of 2818 for DTBQ at 400 nm.

The rate of conversion is obtained by fitting the concentration versus time data into a polynomial and taking the slope of the curve at $t=0$ [38]. All the kinetic results were found to be reproducible within an error of 2.5%.

7.2.2. RESULTS AND DISCUSSION:

As greater activity was observed for Co(II) and Cu(II) complexes in the oxidation of ascorbic acid, it was thought worthwhile to study the oxidation of DTBC using these complex catalysts. The oxidation of DTBC in DMF alone was found to be very slow. So the triethylamine was added to the reaction mixture to have a measurable rate. In the presence of the amine, DTBC may be partially dissociated and interact with the atmospheric oxygen in presence of the catalyst. The results of these studies are given in Table VII.1

Oxidation activity of metal exchanged zeolite was very much lower than the encapsulated complexes. It has been reported that in the case of simple Co(II) chelates, the complexes in which cobalt(II) ion is chelated by four oxygen atoms have been found to be the most active. The chelates in which the cobalt(II) ion is surrounded by N_2O_2 donor set have intermediate activity for the oxidation of DTBC. The reaction mechanism assumed here includes associative oxygen species absorbed on metal ion. The greater dioxygen affinity of Co may be the reason for its better activity.

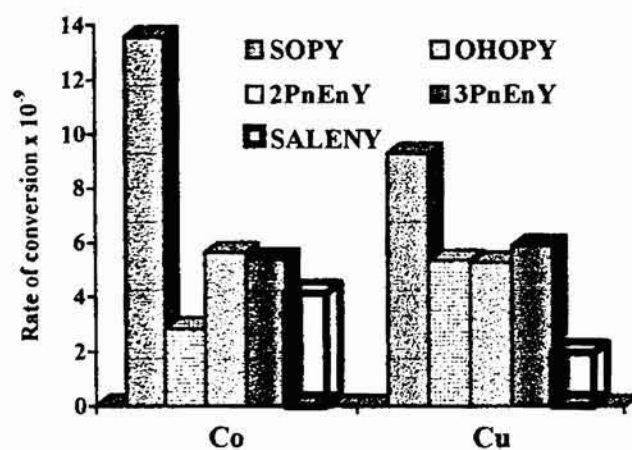


Fig. VII. 2 Rate of conversion of DTBC on zeolite Y encapsulated complexes

Table VIII.2. Rate of oxidation of DTBC to DTBQ.

Sample	Rate of Conversion (mol dm ⁻³ s ⁻¹)
CoSOPY	1.3556x10 ⁻⁸
CoOHOPY	2.851 x 10 ⁻⁹
Co2PnEnY	5.045 x 10 ⁻⁹
Co3PnEnY	5.388 x 10 ⁻⁹
CoSALENY	4.146 x 10 ⁻⁹
CuSOPY	9.286 x 10 ⁻⁹
CuOHOPY	5.335 x 10 ⁻⁹
Cu2PyEnY	5.276 x 10 ⁻⁹
Cu3PyEnY	5.879 x 10 ⁻⁹
CuSALENY	1.958 x 10 ⁻⁹

REFERENCES:

- [1]. D.W. Berck, *Zeolite Molecular Sieves*, Wiley, New York, 1974.
- [2] K. Mizuno, S. Imamura, J.H. Lunsford, *Inorg. Chem.* **23** (1984) 3510.
- [3] N. Herron, *Inorg.Chem.* **25** (1986) 4714.
- [4] R.J. Taylor, R.S. Drago, J.P.Hage, *J.Am.Chem.Soc.* **111** (1989) 6610.
- [5] R.J. Taylor, R.S. Drago, J.P. Hage, *Inorg. Chem.* **31** (1992) 253.
- [6] M. Nakamura, T. Tatsumi, H. Tominaga *Bull.Chem.Soc.Jpn.* **63** (1990) 3334.
- [7] A.E. Shilov, *J.Mol. Catal.* **47** (1988) 351.
- [8] M.G.B.D. Drew, N.J. Juston, P.C.H. Mitchell, S.A. Wass, *Polyhedron* **8** (1989)1817.
- [9] C.A. Tolman, N.Herron, *Oxygen complexes and oxygen activation by metals*, Eds.A.E.Martell and D.T.Sawyer, Plenum Press, London, 1988.
- [10] B.V. Romanovski, *Immobilisation of Transition metal Complexes on supports*, in Proc. 8th Int. Congr. On Catalysis, Weinheim, Verlag Chemie, IV (1984) 657.
- [11] P.A. Seib, B.M. Tolbert, *Ascorbic acid: Chemistry, Metabolism and Uses*, American Chemical society, Washington DC, 1982.
- [12] L.R.C. Barclay, K.A.Dakin, H.A. Zahalka, *Can.J.Chem.* **70** (1992) 2148.
- [13] W. Friedrich, *Vitamins*, Walter de Gruyter, Berlin, 1988.
- [14] F.W.Fox, L.F.Levy, *Biochem.J.* **30** (1936) 211.
- [15] E.Todhunter, T. Mc Millan, D.Ehmke, *J.Nutr.* **42** (1950) 297.
- [16] M.M.T. Khan, A.E. Martell, *J.Am.Chem.Soc.* **89** (1967) 4176.
- [17] P. Martinz, D. Uribe, *Ann.Quim.* **76** (1987) 201.
- [18] L. Ferrari, A.Alonso, *Ann.Quim.* **79** (1983).
- [19] B.Bansch, P.Martinez, J. Zuhragam, D. Uribe, R. Van Eldik, *Z. Phys Chem.* **170** (1991) 59.
- [20] P. martinez, J.Zuhraga, D.Uribe, R. Van Eldik, *Inorg.Chim.Acta*, **136** (1987) 11.
- [21] M.L. Jose, L.D. Pedio, G. Begona, I. Saturnino, *J.Chem.Soc. Faraday Trans.*

89 (1993) 3571.

[22] K.K.M. Yusuff, Jose Mathew, *Ind. J. Chem.*, **36A** (1997) 303

[23] N. Herron, *Inor. Chem.*, **25** (1986) 4714.

[24] M.M. Taqui Khan, A.E. Martell, *J. Am. Chem. Soc.*, **89** (1967) 4176

[25] J. Tsuji, H. Takayanagi, *Chem. Lett.* (1980) 65.

[26] T.R. Demmin, M.D. Swendorff, M.M. Rogic, *J. Am. Chem. Soc.* **103** (1981) 5795.

[27] N. Matsumoto, K. Kuroda, *J. Am. Chem. Soc.* **104** (1982) 1433.

[28] Y. Tatsumo, M. Tatsumo, S. Otsuka, *J. Chem. Soc., Chem. Comm.* (1982) 1100.

[29] R.R. Grinstead, *Biochemistry* **3** (1964) 1308.

[30] C.A. Tyson, A.E. Martell, *J. Phys. Chem.* **74** (1970) 2601.

[31] P.A. Vigato, S. Tamburini, D.E. Fenton, *Coord. Chem. Rev.* **106** (1990) 223.

[32] J.A. Ibers, R.H. Holm, *Science* **209** (1980) 223.

[33] A.E. Martell, D.T. Sawyer, *Oxygen Complexes and Oxygen Activation by Transition Metals*, Plenum, New York, 1987.

[34] J. Reedijk, *Bioinorganic Catalysis*, Marcel Dekker, New York, 1993.

[35] K.D. Karlin, Z. Tyeklar (Eds.), *Bioinorganic Chemistry of Copper*, Chapman and Hall, New York, 1993.

[36] A.E. Martell, M. Calvin, *Chemistry of the Metal Chelate Compounds*, Prentice-Hall, Englewood Cliffs, N.J., 1952, 336-357.

[37] Sudha G. Valavi, Ph.D. Thesis, Cochin University of Science and Technology, Kochi, Kerala, India.

[38] N. Sridevi, Ph.D. Thesis, Andhra University, Visakapatnam, Andhrapradesh, India.

CHAPTER VIII

STUDIES ON γ ZEOLITE ENCAPSULATED CHIRAL TRANSITION METAL COMPLEXES

8.1. INTRODUCTION

There is a continuing interest in search of new catalysts for the synthesis of the building blocks for pharmaceutical and agrochemicals. In this regard there is an essential need for the designing of stable catalysts that can give high yields of the desired product. Many pharmaceuticals, agrochemicals and food additives are chiral and are often available as racemic mixtures. These enantiomers may show different biological activities. So the synthesis of pure enantiomers has gained new impetus, especially in the field of drugs. Epoxides constitute versatile synthetic intermediates because of the easiness in their transformation to a large variety of useful functional groups by means of regioselective ring opening reactions. Catalytic enantioselective epoxidation of unfunctionalised olefins using chiral transition metal complexes is an interesting strategy for the syntheses of a variety of enantiomerically enriched chiral compounds [1]. To date, such asymmetric synthesis have been mostly carried out in the liquid phase using homogeneous catalysis. This may lead to difficulty in product recovery and catalyst separation. Although the reaction is typically carried out by peracid oxidation in laboratory-scale with remarkable selectivities, the pursuit of highly efficient and selective catalytic methods that are simple and safe to operate on a large scale remains as an area of current interest. Transition metal complexes such as chiral metalloporphyrins [2] and chiral Mn(III)-Schiff base[3] complexes are used as catalysts for this purpose. Chiral Mn(III) Salen system (Fig VIII.1) is particularly interesting because they are amenable to structural tuning [4]. Their catalytic activity can be preserved with a large number of terminal oxidants [5]

There is intrinsic research going on in the identification of heterogeneous asymmetric catalysts since such catalysts readily overcome the problems typically encountered with homogeneous systems. Besides the easy recovery and reuse of the insoluble catalysts, greater stability may be expected when compared to their homogeneous counter parts. Furthermore these catalysts may not be deactivated through dimerisation of the complexes. In the presence of an external oxygen source the simple complex usually undergo dimerisation to form the inactive μ -oxo species [6].

We have successfully encapsulated some chiral SALEN type catalysts into the super cages of large pore zeolite Y. Studies on these complexes are presented in this chapter. The chapter has two sections. In the section A, the details regarding the characterisation of the encapsulated complexes are presented and the results of the catalytic activity studies in the asymmetric epoxidation of styrene are presented in Section B

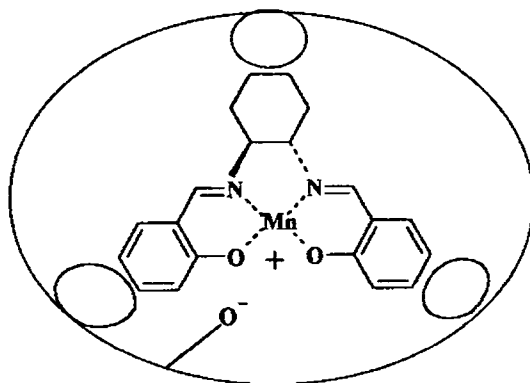


Fig VIII.1 Schematic diagram of Mn(III) complex

8.2.A. EXPERIMENTAL

8.2.A.1. Materials

Details regarding the modification of the Y zeolite support to the metal exchanged zeolite has been given in Chapter II. These modified zeolites are used for further preparation of the encapsulated asymmetric catalysts.

8.2.A.2 Synthesis of zeolite encapsulated asymmetric catalysts (MSALHENY)

A mixture of the corresponding metal exchanged zeolites (5 g) is complexed with salicylaldehyde (3.27 mL, 0.04 mol) in dichloromethane solvent (10 mL). The salicylaldehyde complexes formed were Soxhlet extracted with methanol. The purified salicylaldehyde complexes were condensed with the chiral amine *trans*-(*R,R'*)-1,2-diaminocyclohexane (1.54 mL, 0.02 mol) in dichloromethane for 12 h. The complexes formed were Soxhlet extracted with dichloromethane to colourless washings. Any trace of uncomplexed metal that may be present on the surface of the Y zeolite is removed by back exchanging with 0.01M NaCl solution for 2 h. The complexes were made chloride free by washing with hot water and dried. They were stored over anhydrous CaCl₂.

8.2.A.3 . Analytical Methods

A series of Y zeolite encapsulated asymmetric complexes of the Salen type ligand, *N,N'*-bis (salicylidene) *trans*(*R,R'*) 1,2- diaminocyclohexane (SALHEN) were successfully encapsulated to have the zeolite based asymmetric catalysts. They were characterized by chemical analysis, XRD, surface area, electronic, FTIR and EPR spectroscopy and TG studies.

8.3.A. RESULTS AND DISCUSSION

8.3.A.1. Chemical analysis

The results of the chemical analysis of the asymmetric catalysts encapsulated in zeolite Y (M Salen) are given in Table VIII.3.A.1. The Si/Al ratio is the same, around 2.4 in all these complexes. So there was no dealumination as a result of the encapsulation. The CHN data gives the molar ratio of 1:1 for the metal to ligand in the encapsulated complexes.

Table VIII.3.A.1. Analytical data of the encapsulated complexes

Sample	% Si	% Al	% Na	% Metal	%C	%H	%N
Mn(SALHEN)Y	19.2	5.84	5.54	1.96	4.28	1.73	0.72
Co(SALHEN)Y	18.60	5.67	6.37	2.01	9.85	2.06	0.36
Ni(SALHEN)Y	18.41	5.61	5.59	1.25	1.93	1.23	0.32
Cu(SALHEN)Y	17.90	5.44	5.61	1.73	4.61	1.55	1.22

8.3.A.2. X-ray diffraction pattern

The XRD patterns of all the asymmetric complexes are given in Fig.VIII. 2. They are showing similarity to the XRD of the metal exchanged zeolites. Hence crystallinity of the zeolite has been retained even after the encapsulation.

8.3.A.3. SEM analysis

The SEM of the Mn(II) complexes was taken (Fig.VIII.3.). It can be seen that the surface adsorbed species were removed as a result of the soxhlet extraction. In

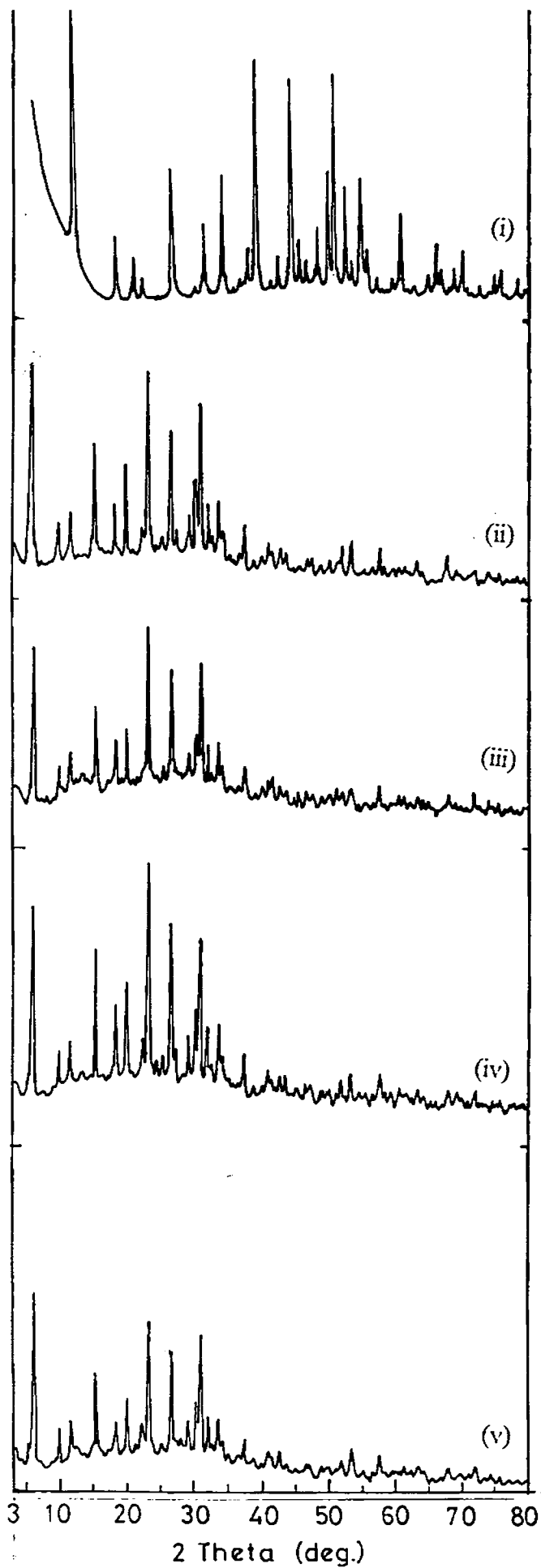
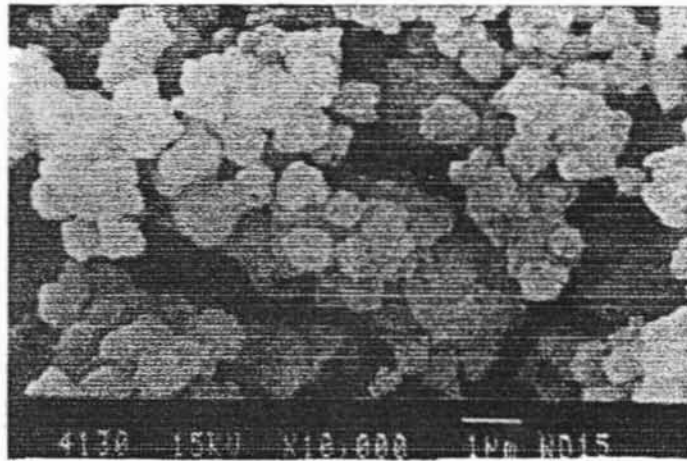
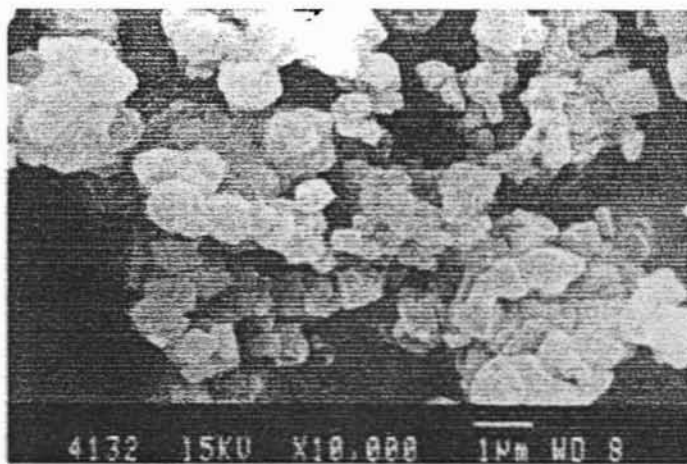


Fig. VIII.2. XRD Patterns of
(i) NaY
(ii) Mn(SALHEN)Y
(iii) Co(SALHEN)Y
(iv) Ni(SALHEN)Y
(v) Cu(SALHEN)Y

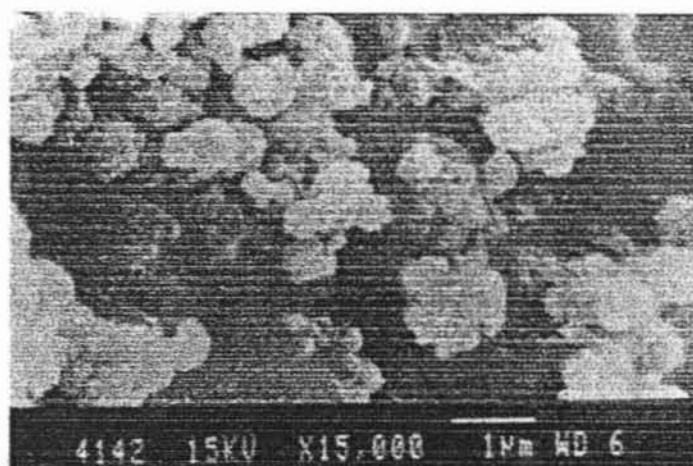


(i)

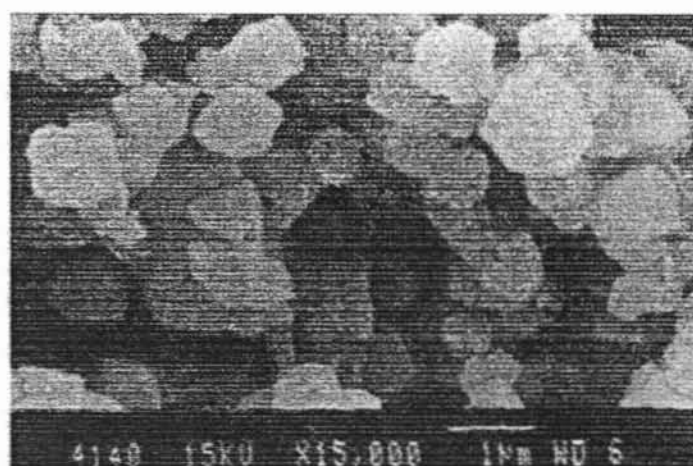


(ii)

Fig. VIII.3. SE Micrographs of (i) NaY (ii) MnY



(iii)



(iv)

Fig. VIII.3 SE micrographs of Mn(SALHEN)Y
(iii) before and (iv) after Soxhlet extraction

the encapsulated complexes, the morphology of the catalyst has been retained as that of the parent NaY.

8.3.A.4. Surface area analysis

The surface area data are given in Table VIII.A.2. The lowering of surface area is an indication of the internal confinement of the complexes. The % loss of surface area on encapsulation is given as a bar chart in Fig.VIII.4.

Table VIII.A.2. Surface area of the asymmetric catalysts

Sample	Surface area (m ² /g)		
	MY	MSALHENY	%Loss
NaY	549	-	-
Mn(SALHEN)Y	539	265	50.80
Co(SALHEN)Y	532	218	59.02
Ni(SALHEN)Y	528	254	48.10
Cu(SALHEN)Y	528	317	60.03

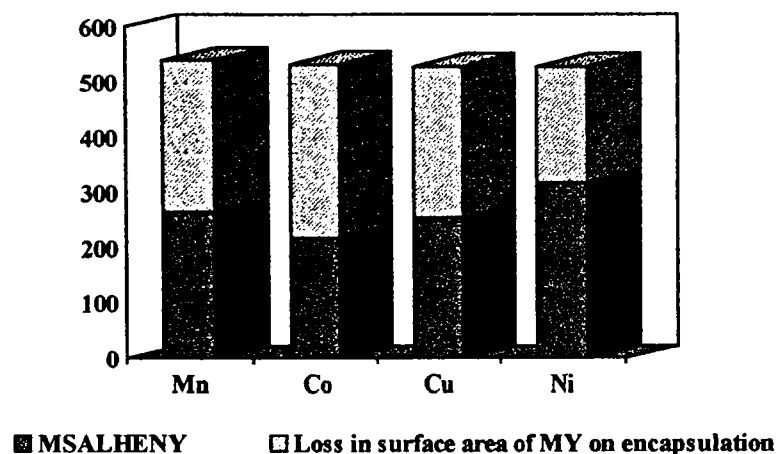


Fig. VIII. 4. Loss of surface area of the encapsulated SALHEN complex

8.3.A.5. Magnetic moment

The magnetic moment values of zeolite complexes were measured using the Gouy method at room temperature. The values are given in the Table VIII.3.A.3. The Mn(II) complex has a magnetic moment of 6.0BM, which only indicates the presence of 5 unpaired electrons. No conclusive evidence regarding the structure could be drawn from magnetic moment alone. The Co(II) complex shows magnetic moment value of 2.3BM, which is indicative of a square planar low spin structure with only one unpaired electron. The zeolite encapsulated Ni(II) complex is diamagnetic. The copper complex has a moment of 1.75BM close to the spin only value of 1.73BM indicating a square planar geometry.

Table VIII.3.A.3. Magnetic moment of zeolite complexes.

Sample	Magnetic moment (BM)
MnSALHEN	6.0
CoSALHEN	2.3
NiSALHEN	Diamagnetic
CuSALHEN	1.75

8.3.A.6. Electronic spectroscopy

The Kubelka-Munk (KM) analysis was carried out on the reflectance data of the encapsulated complexes. The electronic spectral data of the Mn(SALHEN) is given in Fig.VIII.5.

This spectrum is very similar in appearance to the electronic spectrum of Mn(II) in octahedral coordination. The weak band in the spectrum around $25,000\text{cm}^{-1}$ with shoulder can be assigned to the ${}^4E_g(G) \leftarrow {}^6A_{1g}$ and ${}^4A_{1g}(G) \leftarrow {}^6A_{1g}$ transitions [10]. The small absorptions around $14,290\text{ cm}^{-1}$ and $13,790\text{ cm}^{-1}$ are possibly the ${}^4T_{1g} \leftarrow {}^6A_{1g}$

and ${}^4T_{2g} \leftarrow {}^6A_{1g}$ transitions. From this data, an octahedral geometry may be assigned to the Mn(SALHEN)Y complex.

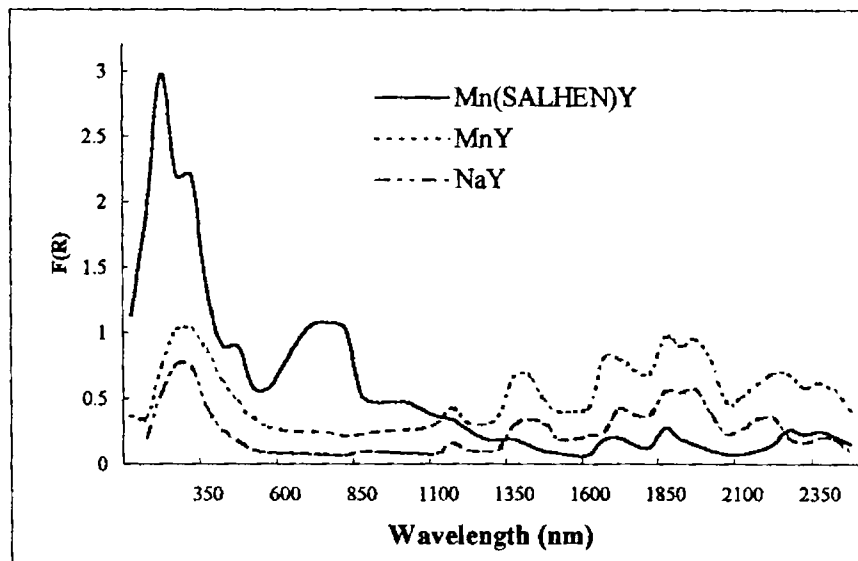


Fig.VIII.5. Diffuse reflectance spectrum of Mn(SALHEN)Y, MnY and NaY

The diffuse reflectance spectra of the Co(SALHEN)Y are given in Fig.VIII.6. the spectra of the complex are similar to the four coordinate square planar (low spin) cobalt(II) complexes. In the case of square planar systems, the symmetry is so low that d_{xz} and d_{yz} are not degenerate and may complicate the analysis of the spectra. The low spin square planar Co(II) complexes exhibit several transitions in the region $3900-7000\text{ cm}^{-1}$. However because of the presence of the bands due to zeolite structure in this region, conclusive evidence for the structure has to be arrived from the EPR spectra. The complex also exhibits multiplet of three bands in the region $8000-11000\text{ cm}^{-1}$ and three transitions in the visible region. All these facts point towards a low spin square planar structure for the cobalt(II) complex. [10,11].

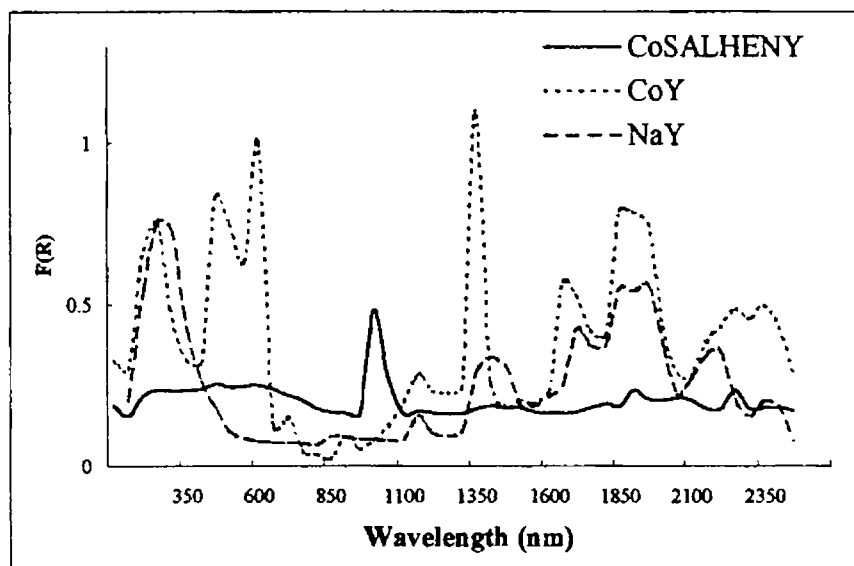


Fig.VIII.6. The diffuse reflectance spectrum of Co(SALHEN)Y, CoY and NaY

The diffuse reflectance spectrum of the Ni(SALHEN)Y is given in Fig.VIII.7. The multiple bands in the visible region of the spectrum is characteristic of a square planar structure. The broad band around $20,000\text{ cm}^{-1}$ in the spectrum may be taken as characteristic of Ni(II) in a square planar geometry. [10-12]. The transition in the near IR region may be masked by the bands due to the absorption of the zeolite framework.

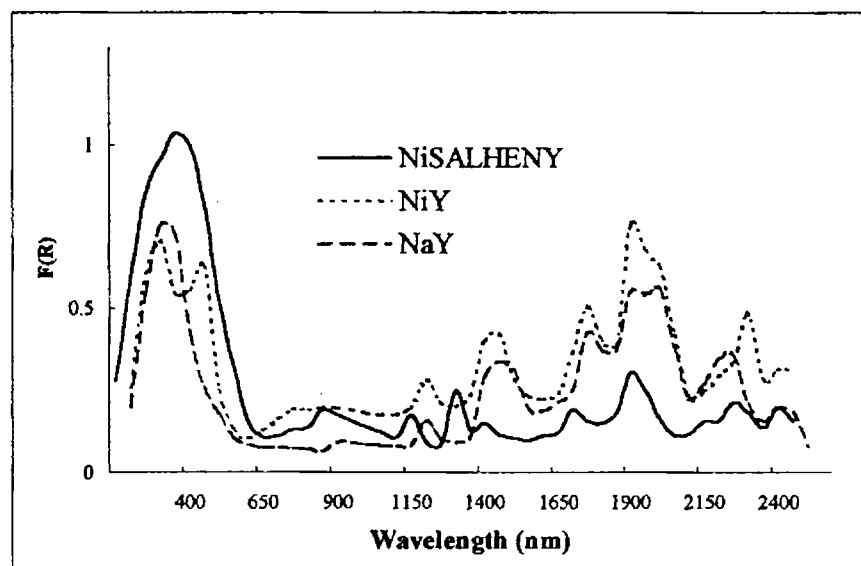


Fig.VIII.7. Diffuse reflectance spectrum of Ni(SALHEN)Y, NiY and NaY.

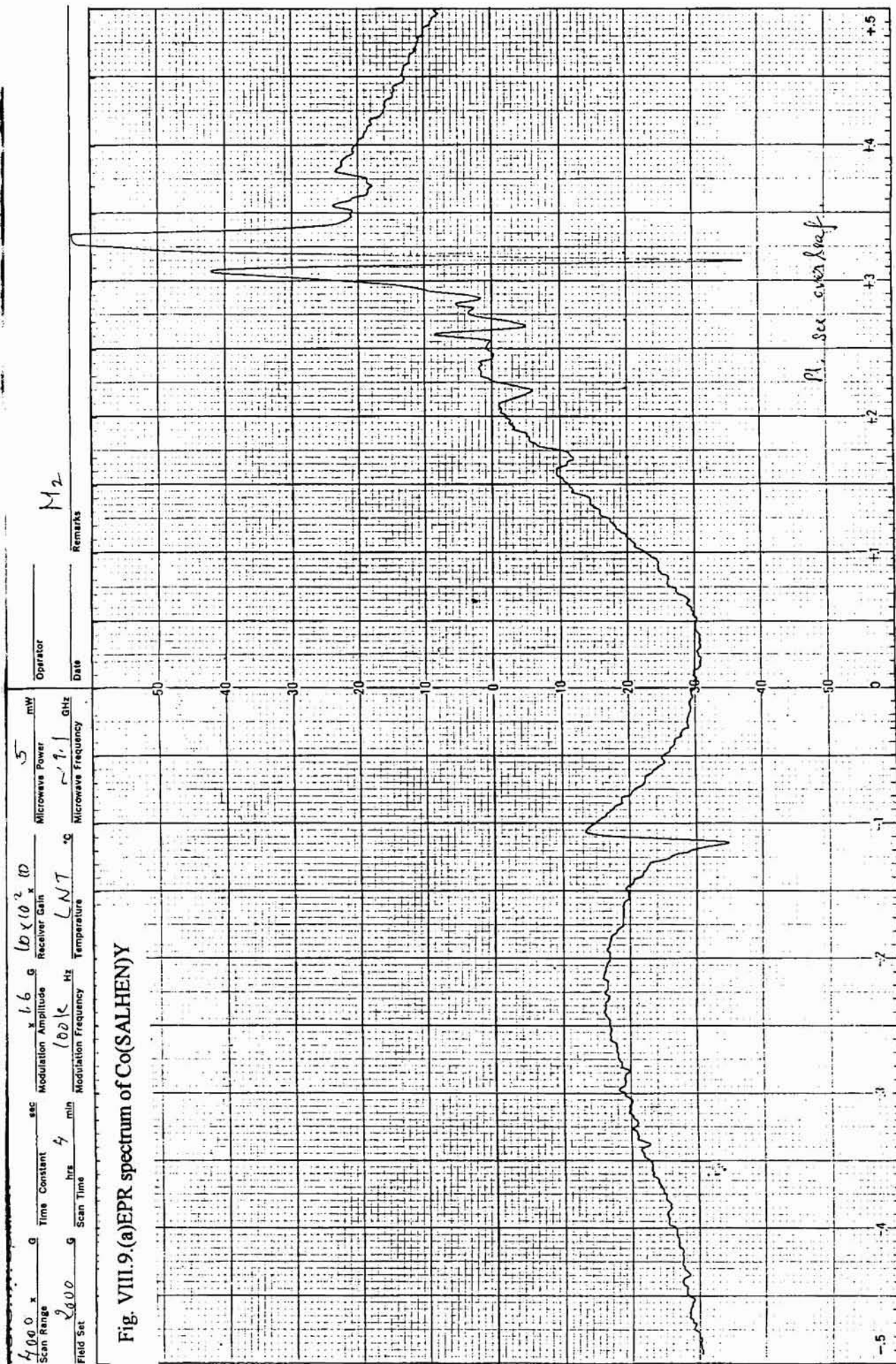


Fig. VIII.9.(a) EPR spectrum of Co(SALHEN)Y

SCAN RANGE

RSIC, IIT, BOMBAY

Scan Range $4000 \times$ g Time Constant 5 sec Modulation Amplitude 5×10^{-2} g Receiver Gain $3.2 \times 10^2 \times 10$ Microwave Power 5 mW
Field Set 3000 g Scan Time 4 hrs min Modulation Frequency 100 K Hz Temperature LNT Microwave Frequency 9.1 GHz Date 16/04/01 Operator M2 (u.s.)
Remarks

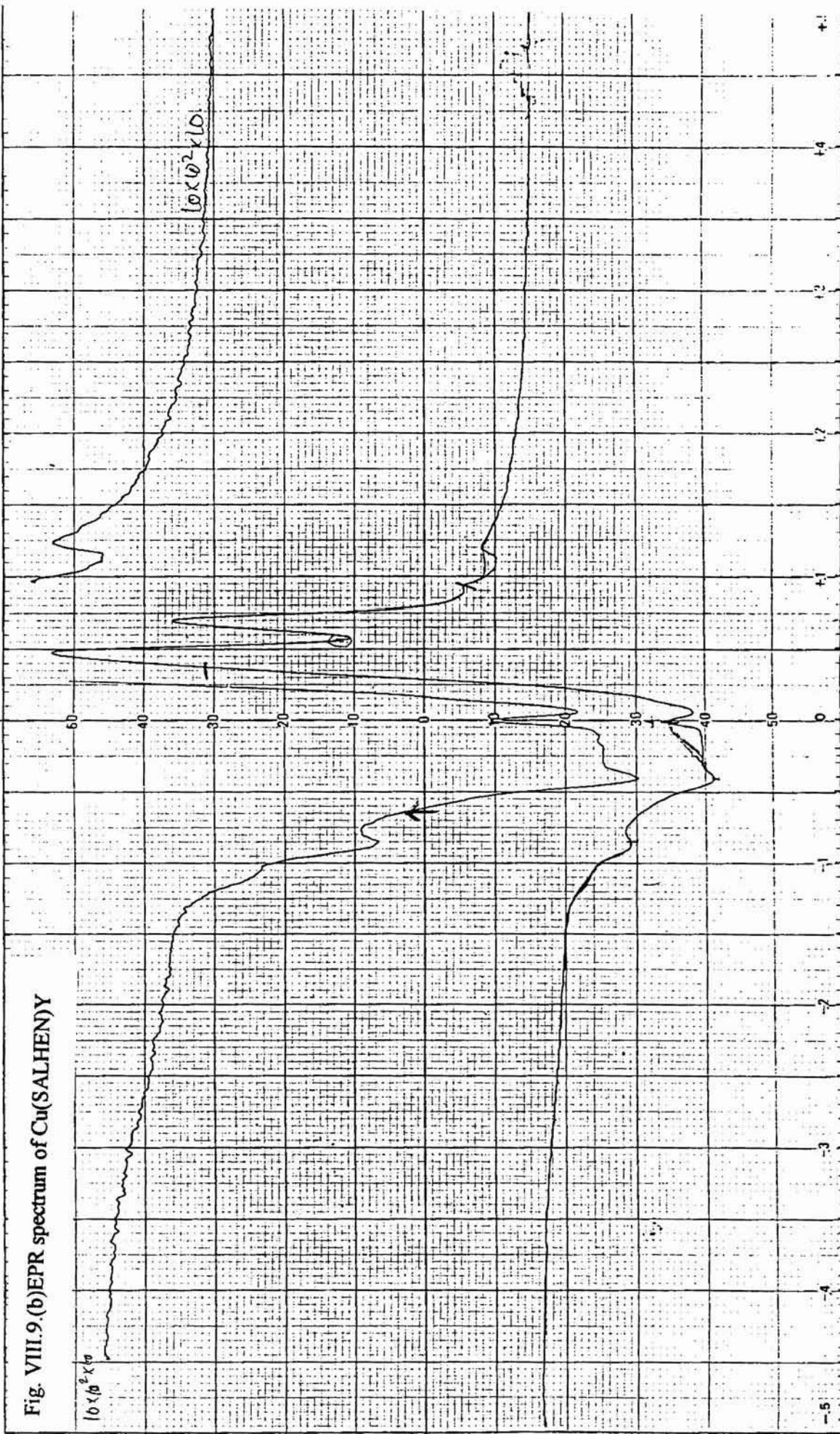


Fig. VIII.9.(b) EPR spectrum of Cu(SALHENY)

The diffuse reflectance spectrum of the Cu(SALHEN)Y is given in Fig.VIII.8. The absorption band of the Cu(SALHEN)Y is showing multiple absorptions. Due to overlapping of the bands it is very difficult to assign positions. This type of multiple absorption of the visible band is reported for Cu(II) complexes with a lower symmetry. A square planar structure may be assigned for the Cu(II) complex also[10,11].

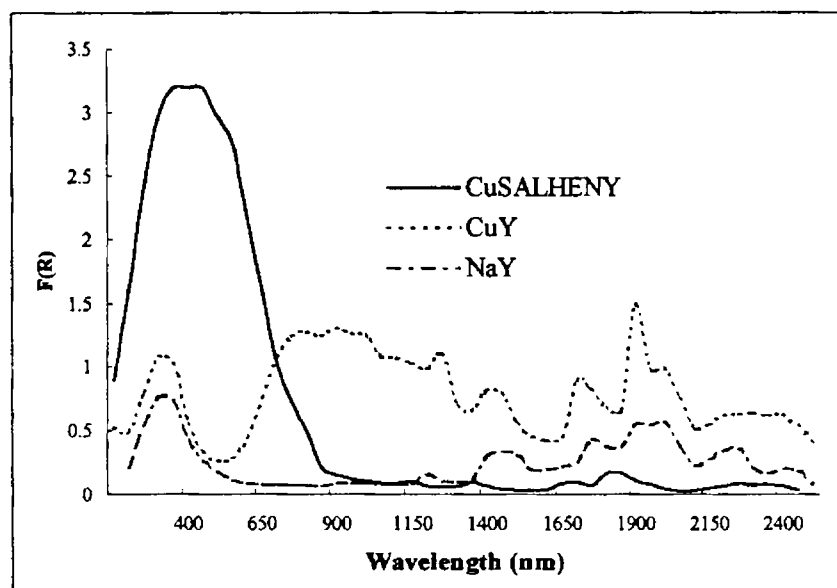


Fig.VIII.8. Diffuse reflectance spectrum of Cu(SALHEN)Y, CuY and NaY.

8.3.A.7 EPR Spectroscopy

ESR analysis of two complexes was carried out. Resolvable spectra could be obtained only in the case of Co(II) and Cu(II) and shown in Fig VIII.9. The Co(II) complex shows strong signals with hyperfine splittings at $g \sim 2$ indicating the low spin nature of the complex, which is confirmative of its square planar geometry. The Ni(II) complex is EPR silent. Ni(II) ion does not have any unpaired electron in a square planar environment. The EPR of the Cu(SALHEN) has spectral features similar to that of the Cu(II) Schiff base complex in a square planar environment.

SECTION-B

8.B.1. Asymmetric Catalytic Activity Studies

Asymmetric epoxidation of styrene was carried out using the encapsulated catalysts. Our attempts to prepare the Jacobsen epoxidation catalyst, which is Mn(III) complex with Salen ligand inside the cage was not successful. Even oxidation of the zeolite encapsulated complex with bromine in acetic acid did not yield the Mn(III) complex. Therefore the asymmetric epoxidation was tried with the prepared catalysts, in the lower oxidation state. The next hurdle was the selection of a suitable oxidising agent. Jacobsen has described a number of different oxidation systems that are effective for carrying out the epoxidation [13]. A variety of oxidizing agents like commercial bleach, H₂O₂, *tert*-butyl hydroperoxide, 3-chloroperoxy benzoic acid etc. was tried as the oxidants for this reaction. The results of our catalytic activity studies are presented in this section.

8.B.2. EXPERIMENTAL

8.B.2.1. Materials

The preparation of the asymmetric catalysts was carried out according to the procedure given in the previous section of this chapter. The purification of commercial grade styrene was done as mentioned in chapter II. The detailed procedures for the reaction with different oxidants are given as follows.

8.B.3. Asymmetric epoxidation of styrene

Among the various oxidants tried, only those that could bring about epoxidation have been presented.

8.B.3.1. Sodiumhypochlorite

During the early stages, when the asymmetric systems are about to develop towards the asymmetric epoxidation, Jacobsen used commercial bleach as the oxidising agent. This method is considered as a path to green chemistry. Jacobsen's procedure was employed with slight modifications for the epoxidation of styrene. A brief description of the procedure is as follows.

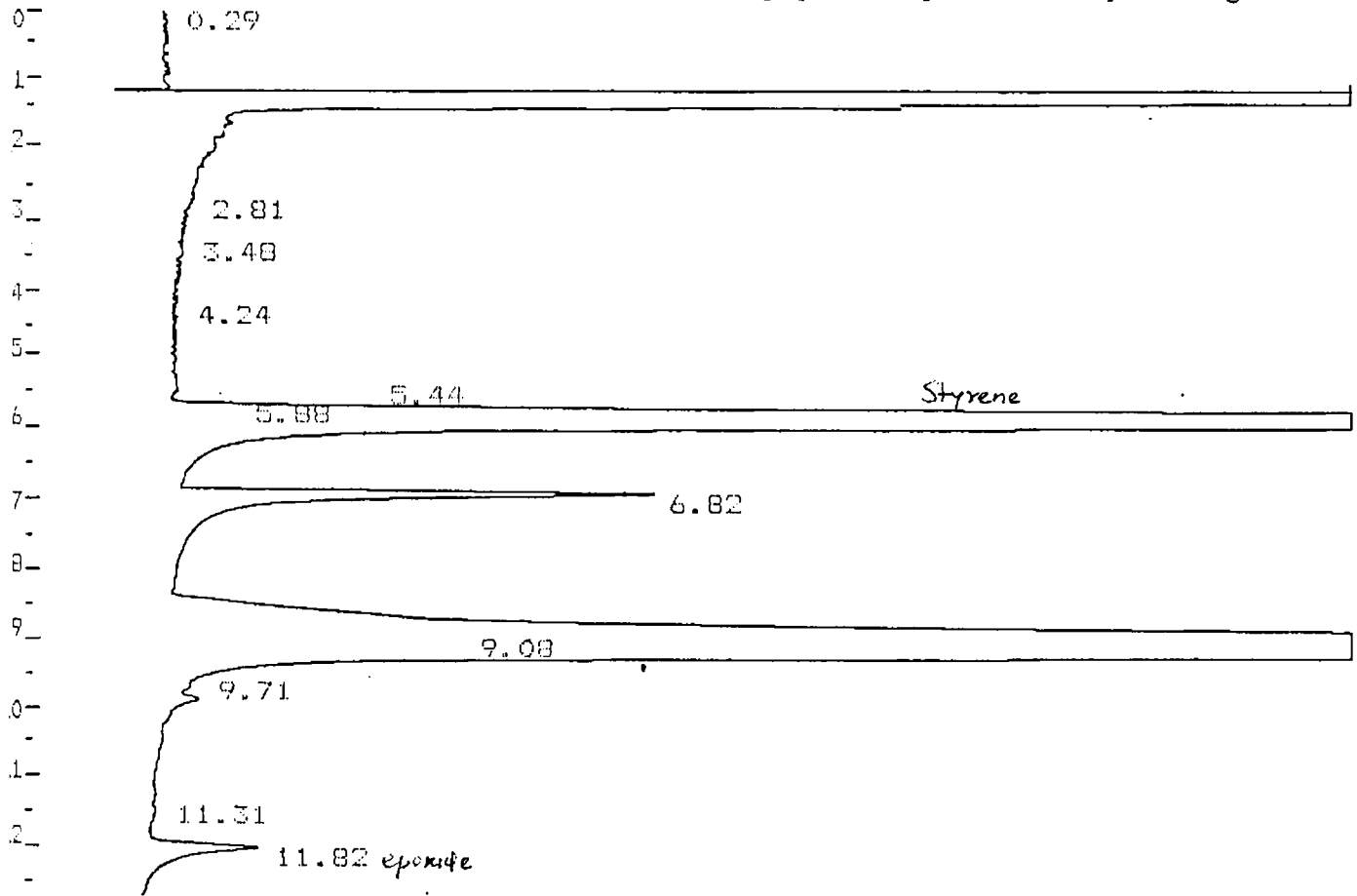
A solution of Na_2HPO_4 (0.05M, 5 mL) was added to commercial bleach (12.5 mL, 5.5 %). The pH was adjusted to 11.3. The solution was then added to a suspension of styrene (0.5 g) and the catalyst (10 mol %) in of CH_2Cl_2 (5 mL) taken in a 50 mL conical flask. The progress of the reaction was monitored by TLC. When the reaction was complete (around 2 h.), the organic phase was washed twice with 10 % NaCl solution, and dried. The solvent was removed at atmospheric pressure. The percentage conversion was obtained from the G.C.data by comparing it with that of the pure styrene oxide. The optical activity of the product was determined polarimetrically. Both the yield and enantiomeric excess were found to be very low for the Co(II), Ni(II) and Cu(II) complexes. But for the Mn(II) complexes the yield of epoxide was 60%. But there were so many other oxidation products such as benzaldehyde, benzylalcohol etc. The GC chart of this is given in Fig.VIII.B.1. The optical activity of the product was not to the extent of a measurable level.

8.B.3.2. *tert*-Butylhydroperoxide

The reaction was carried out in a 100 mL R. B equipped with a reflux condenser. Styrene was added to a suspension of the catalyst (10 mol %) and TBHP (0.1 g) in acetonitrile (5 mL). The solution was refluxed for 12 h. at 343 K. The reaction mixture after cooling to room temperature was analysed for the products using GC. Significant conversion was observed only in the case of manganese(II) complex. Here, only the Mn(II) SALHENY gave a reasonable yield for the epoxide. The GC chart is given in Fig.VIII.B.2. The chart indicates the presence of some other

HTRRJ 5 ARREJ 6 PKWD 4 ATTN " CHTSPD % ZERO SLPSTV BSSTV SKMSTV

Fig. VIII.B.1 The chromatograph of the epoxidation of styrene using NaOCl



HTREJ	ARREJ	PKWD	ATTN	CHTSPD	ZERO	SLPSTV	BSSTV	SKMSTV
5	1	4	0	1.0	10	32	16	8

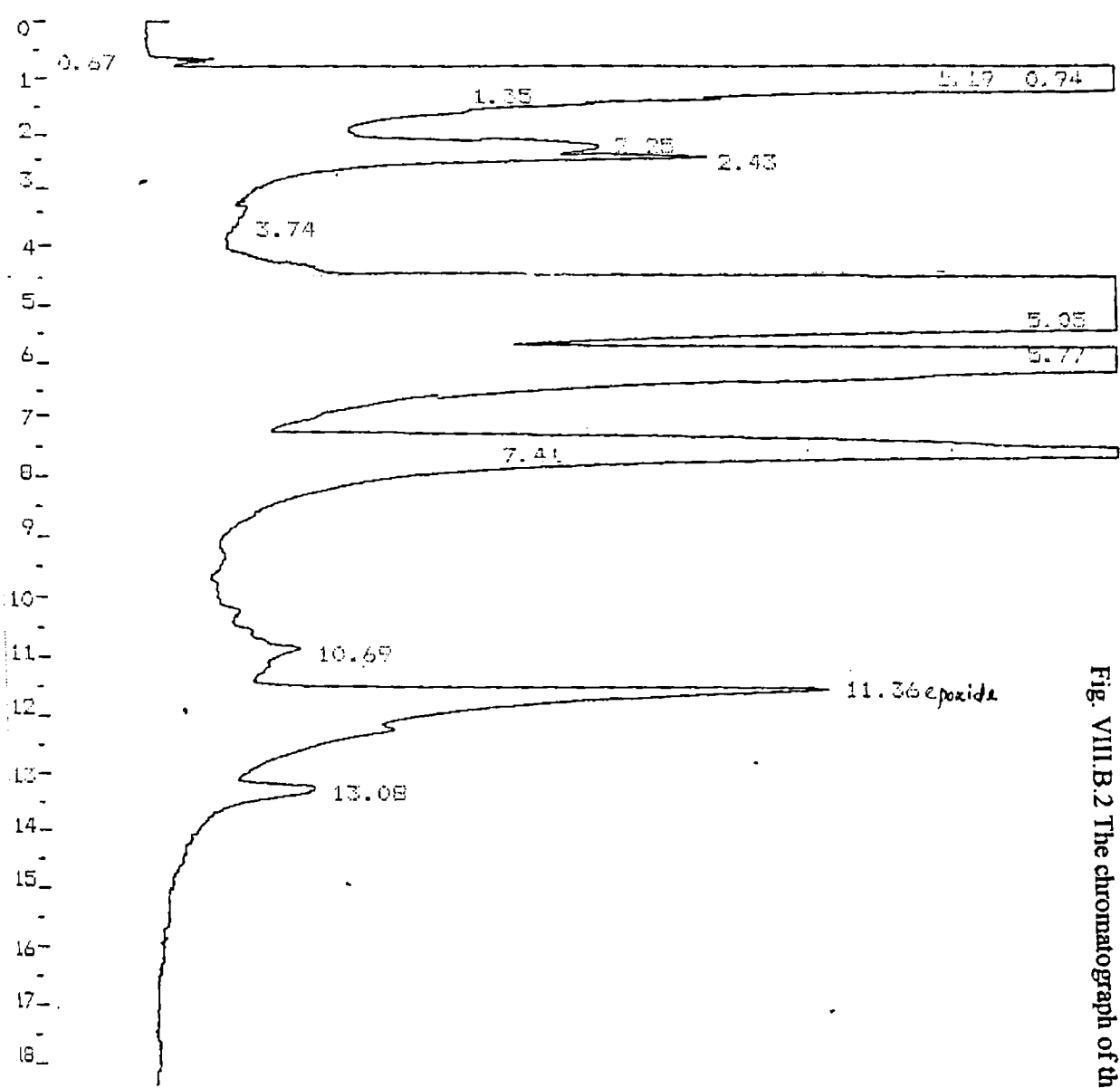


Fig. VIII B. 2 The chromatograph of the epoxidation of styrene using TBHP.

oxidation products also. The optical activity of the products was also very disappointing.

8.B.3.3. 3-Chloroperoxybenzoic acid

Styrene was added to a stirred mixture of 3-chloroperoxybenzoic acid (15 g, 87 mmol) in dichloromethane (150 mL) held at 0°C and the chiral catalyst. The solution was stirred for 2h at room temperature. After the filtration of the catalyst, the organic phase was washed with 10 % NaHCO₃ solution and dried over anhydrous Na₂SO₄. The progress of the reaction was monitored by TLC using 5 % ethylacetate in hexane. The solvent was removed at atmospheric pressure and epoxide was separated by column chromatography using hexane as the eluent. The yield was determined by GC. Evaluation of enantiomeric excess was done by chiral GC analysis using chiraldex GTA column. The results are summarised in Table VIII.B.1. The chiral GC chart for the epoxide mixture obtained with Ni(SALHEN)Y is given in Fig.VIII.B.3. The product the reaction mixture was found to be laevo rotatory. The Chiral GC analysis of the epoxide mixture was carried out for the Cu(SALHEN)Y and is given in Fig.VIII.B.4. The absolute configuration of this was determined and was found to be R.

8.B.4. Recyclability and stability of the catalyst

All the catalysts were completely recovered by filtration after the epoxidation reaction. The aqueous layer was checked for the presence of any metal ion. As the metal ions are absent, any possibility of leaching out of the catalyst during the reaction is ruled out. The XRD of the recovered catalyst showed that the framework and crystallinity of the zeolite framework is retained during the reaction. The activity of the catalyst is also not reduced to any significant level.

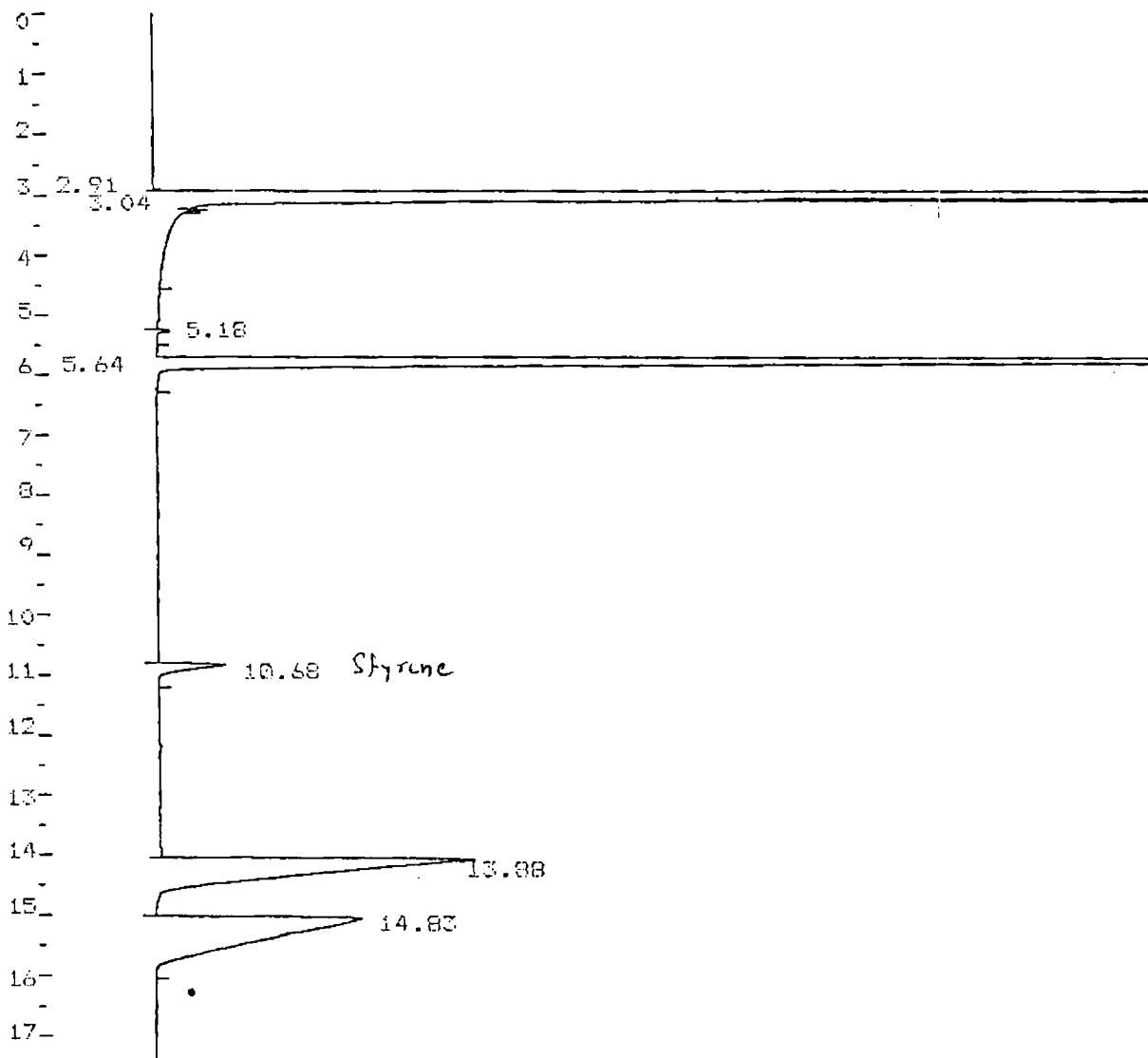


Fig. VIII.B.3 The chiral GC data of the asymmetric epoxidation of styrene using (i)Cu(SALHEN)Y

HTREJ 5 ARREJ 6 FKWD 4 ATTN 1 CHTSPD 1.0 ZERO 10 SLPSTV 32 BSSTV 16 SKMSTV 8

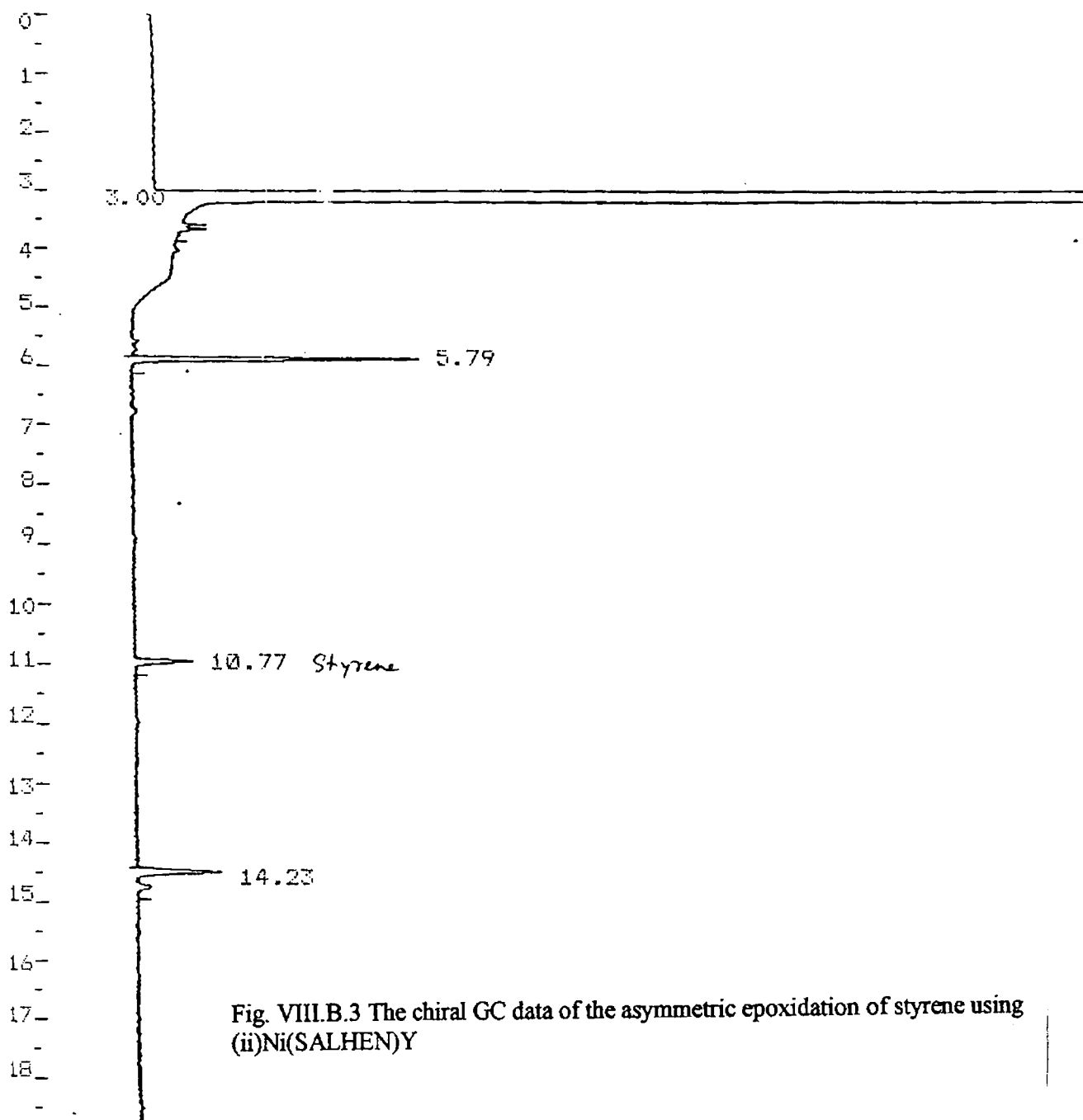


Fig. VIII.B.3 The chiral GC data of the asymmetric epoxidation of styrene using (ii)Ni(SALHEN)Y

8.B.5. RESULTS AND DISCUSSION

The catalytic activity for the asymmetric epoxidation reaction was found to be in best with NiSALHENY. The enantiomeric purity in this case was found to be above 99%. There is no such report till date for such high enantiomeric excess in a heterogeneous catalytic system where the asymmetric catalyst is supported. The Cu(II) chiral complex also showed a comparable activity with some enantiomeric excess. The square planar cobalt(II) complexes are well known for their oxygen carrying capacity. But surprisingly this complex is not a good catalyst in the epoxidation of styrene by all the reagents. The zeolite Y encapsulated nickel(II) complex was found to be an excellent catalyst with very high yield of the epoxide and almost 98 % enantiomeric excess. Recently Chatterjee *et al.*, reported epoxidation of alkenes using SALEN type Ni(II) complexes in homogeneous condition [9]. Usually Ni(II) complexes are not considered to be epoxidation catalysts. Therefore it may be assumed that Ni(III) species will be formed in the course of the reaction and probably the zeolite frame work structure would be able to stabilise this oxidation state. The lower activity for Mn(II) complex may be due to the difficulty in oxidising the Mn(II) complexes to Mn(III) complex during the oxidation reaction. Copper (II) complex also gave moderate enantiomeric excess (15%).

Square planar Ni(II) complexes of macrocyclic ligands and Salen are reported to act as catalysts for epoxidation of alkenes with PhIO or NaOCl as terminal oxidants [14-21]. The mechanism involving Ni(III) species has been proposed [14,19]. Although there are still some controversies over the involvement of high valent metal-oxo intermediates [20,21]. It has been reported that the formation of Ni(II)-O-Ni(III) species reduces the yield of epoxide [19]. In the present encapsulated complexes the formation of such species will be avoided. Regarding the mechanism, the first step may be either direct oxygen transfer from 3-chloroperoxybenzoic acid oxidant to Ni(II) complex. The oxidized nickel species may react with alkene to produce epoxide via a second intermediate with the bound substrate in either radical or carbocation form. Ni(II)/Ni(III) oxidation potential may have a role in the catalytic activity. The oxidation potential can be varied by change

of different type of ligands. Lower oxidation potential is expected to increase the yield of epoxide. Further the ligand should exert less steric hindrance around metal ion for easy axial approach of oxidant. Probably these factors may be responsible for the increased activity of the nickel(II) complex.

The planar metal oxo complexes such as Mn(V)=O , Fe(V)=O has been proposed as an active species for olefin epoxidation reaction [22]. Further from the crystal field activation energy calculation, Ni(II) complex is more inert than the other complex. This inert nature might be responsible for the reaction of chiral activity of the Ni(SALHEN)Y .

REFERENCES:

- [1].V. Schuring, F. Betschinger, *Chem. Rev.* **92** (1992) 873.
- [2].J.P. Collman, X. Zhang, V.J. Lee, E.S. Ufferman, J.I. Brauman, *Science* (1993) 261.
- [3].E.N. Jacobsen, W. Zhang, M.L. Guler, *J. Am. Chem. Soc.* **113** (1991) 6865.
- [4].E.N. Jacobson in *Catalytic asymmetric Synthesis*, I. Ojima (Ed.) VCH, Weinheim,1993, p 159.
- [5].M. Palucki, P. J. Pospisil, W. Zhang, E. N. Jacobsen, *J. Am. Chem. Soc.* **116** (1994) 9333.
- [6].K. Srinivasan, P. Michaud, J. K. Kochi, *J. Am. Chem. Soc.* **108** (1986) 2309.
- [7] Murugavel, H. W. Roesky, *Angew. Chem., Int. Ed. Engl.* **36** (1997) 477.
- [8] C. J. Liu, W. Y. Yu, S. G. Li , C. M. Che, *J. Org. Chem.* **63** (1998) 7364.
- [9] D. Chatterjee, S Mukherjee, A. Mitra, *J. Mol.Catal. A:* **154** (2000) 5(English)
- [10] N.N. Greenwood, A. Earnshaw, *The Chemistry of The Elements*, Pergamon Press, New York, 1989.
- [11] F.A. Cotton, G. Wilkinson, *Advanced Inorganic Chemistry*, 5th Edn., John Wiley and Sons., New York, 1988.
- [12] A.B.P. Lever, *Inorganic Electronic Spectroscopy*, 2nd Edn., Elsevier, New York, 1984.
- [13] E.N. Jacobsen, *Catalytic Asymmetric Synthesis*, I. Ojima Ed., VCH, New York, 1993.
- [14] J. F. Kinncary, J. S. Albert, C. J. Burrnows, *J. Am. Chem. Soc.*, **110**, (1988), 6124.
- [15] K. A. Jorgensen, *Chem. Rev.*, **89**(1989), 3.
- [16] M. Yamuda, S. Ochi, H. Suzuki, A. Hisazumi, S. Kuroda, I. Shiman, K. Araki, *J. Mol catal.*, **87**(1994) 195.
- [17] J. F. Kinncary, T. R. Wagler, C. J. Burrnows, *Tet. Lett.*, **29**(1988), 877.
- [18] T. R. Wagler, Y. Fang, C. J. Burrnows, *J. Org. Chem.*, **54**(1989) 1584.
- [19] J. D. Koola, J. K. Kochi, *Inorg. Chem.*, **26**(1987)908.
- [20] W. Nam, J. S. Valentine, *J. Am. Chem. Soc.*, **142** (1990), 4977.
- [21] Y Yang, F. Diederich, J. S. Valentine, *J. Am. Chem. Soc.*, **142**(1990), 7826.
- [22] K.A. Jorgenson *J. Am. Chem. Soc.*, **109** (1987), 697

SUMMARY AND CONCLUSIONS

The theme of the present investigation is mainly concentrated on the synthesis, characterization and catalytic activity studies of some zeolite encapsulated transition metal complexes. Synthesis of a series of Y zeolite encapsulated chiral transition metal complexes, their characterisation and efficiency as catalysts in inducing chirality in the epoxidation of a prochiral olefin was investigated. The characterization studies were mainly based on the XRD studies to check the crystallinity, surface area determinations to know the extent of encapsulation, and magnetic and spectral studies to confirm the complexation. The catalytic efficiency with respect to oxidation activity, recyclability and stability of the catalytic system were examined. Chapter I is an introductory chapter that presents a general discussion on zeolite encapsulated metal complex systems and the catalytic studies reported based on such systems. This chapter also provides a brief account of various methodologies for the synthesis of zeolite complexes. The scope of the present investigation is also presented in this chapter.

Chapter II gives the general procedures for the synthesis of the Y zeolite encapsulated complexes, the details of reagents and materials used, and the characterization techniques employed. The techniques used in the present study include chemical analysis, CHN analysis, TG, GC, ICP, XRD, SEM, BET surface area and magnetic moment measurements, diffuse reflectance, FTIR and EPR spectrometry.

Studies on the synthesis and characterization of Y zeolite encapsulated Mn(II), Co(II), Ni(II) and Cu(II) complexes of some Schiff base ligands are presented in chapters III, IV, V, and VI. Chapter III deals with the results of our studies on the complexes of the ligand, N,N'-bis(salicylidine)-1,2-

phenylenediamine (SOPY). The zeolite NaY used for supporting the complexes was found to possess a unit cell of formula $\text{Na}_{56}[(\text{AlO}_2)_{56}(\text{SiO}_2)_{36}]\cdot x\text{H}_2\text{O}$. The unit cell formulae of metal exchanged zeolites were also derived from the analytical data. The Si/Al ratio of metal exchanged zeolites is found to be approximately in the range 2.3 – 2.4 and it is almost near to that of the parent zeolite indicating that there is no collapse of the zeolite framework. It was prevented in the present study by the use of dilute metal salt solutions. Surface area, XRD and FTIR data of metal exchanged zeolites also reveal the retention of zeolite framework.

The empirical formulae of the zeolite encapsulated SOPY complexes could be obtained from the analytical data. SE micrographs of the encapsulated complexes, before and after soxhlet extraction, indicate that surface adsorbed complexes are absent. XRD patterns and Si/Al ratio indicate the retention of zeolite framework on encapsulation. The lower surface area of encapsulated complexes as compared to those of the corresponding metal exchanged zeolites suggest encapsulation of the complexes within the zeolite pores.

The geometry of the Mn(II) complex is assigned to be octahedral from the spectral and magnetic studies. The complex also gives EPR spectrum characteristic of $I = 5/2$ systems. From the spectral and magnetic studies, the Co(II) and Ni(II) complexes are assigned a tetrahedral and distorted tetrahedral geometries respectively. The zeolite Y encapsulated Co(II)SOPY complex is also found to be EPR active and its EPR indicates Co(II) ion in the high spin state. The electronic spectrum and the magnetic moment value suggests a tetragonal geometry for CuSOPY. EPR spectrum indicates an axial symmetry for CuSOPY. It also reveals the ionic nature of the metal ligand bonding in this complex.

The formation of the complexes in the zeolite pores was also confirmed from the IR data. The $\nu_{(\text{C}=\text{N})}$ bond of the Saloph ligand, which is found to undergo a blue shift in all the complexes. Such a blue shift of the band is also reported earlier for zeolite encapsulated complexes. The TG patterns of the encapsulated complexes indicate two stages of decomposition. The approximate stability of the

complexes could be ascertained in most of the cases. However, due to the small concentration of the complex in the zeolite no quantitative inferences could be drawn from the TG data.

Chapter IV presents our studies on the zeolite encapsulated transition metal complexes of the *N,N'*-bis(2-hydroxymethylbenzylidene)-1,2-phenylenediamine (OHOPY). Surface area and XRD studies provide strong evidence for the encapsulation of the complex without the loss of crystallinity. Based on magnetic moment, electronic and EPR spectral data, the encapsulated Mn(II), Co(II), Ni(II) and Cu(II) complexes are expected to have an octahedral, tetrahedral, distorted tetrahedral and tetragonal geometries respectively. IR spectra confirm the formation of complexes in the zeolite cages and indicate the coordination of the ligand. TG patterns of the all complexes are similar and show two stages of decomposition.

Chapter V describes our studies on the zeolite Y encapsulated transition metal complexes of the ligand *N,N'*-bis-(2-pyridinemethylene)-1,2-diaminoethane (M2PyEnY). The diffuse reflectance spectra and the magnetic susceptibilities suggests an octahedral geometry for the Mn(II) complex, a tetrahedral and distorted tetrahedral symmetry for Co(II) and Ni(II) complexes and a tetragonal geometry for the Cu(II) complex. The EPR spectrum shows axial symmetry for the encapsulated Cu(II) complexes. TG data indicates the formation of complexes in zeolites.

Chapter VI deals with the studies on the encapsulated complexes of *N,N'*-bis(3-pyridinemethylene)-1,2-diaminoethane. The Mn(II) complex is octahedral. A tetrahedral structure is assigned for Co(II) and Ni(II) complexes. The Cu(II) complex has a tetragonal symmetry around the metal ion. The structural features are concordant with the EPR spectral data obtained. T.G. analysis data of these complexes is also provided in this chapter.

Chapter VII describes our studies on the catalytic activity of the Y zeolite encapsulated Schiff base complexes. All the Mn(II) complexes catalyse the oxidation of ascorbic acid among which Mn(SOPY) is found to be the least active complex and MnOHOPY has highest activity. Mn₂PyEnY and Mn₃PyEnY also show good activity. All the Co(II) complexes are highly active in the oxidation of ascorbic acid. The Ni(III) complexes are found to be considerably active in the oxidation of ascorbic acid. The involvement of a Ni(III) species as an intermediate may be the reason for this interesting observation. All the Cu(II) complexes are also active in the oxidation of ascorbic acid. The activity of Cu₂PyEnY and Cu₃PyEnY complexes are substantially higher, which may be due to the formation of a Cu(I)-substrate intermediate. All the complexes are found to be good catalyst precursors rather than good catalysts.

Chapter VIII deals with our studies on the zeolite Y encapsulated chiral transition metal complexes. Their structures arrived from the electronic spectral and magnetic moment studies are octahedral for Mn(II) and square planar for Co(II), Ni(II) and Cu(II) complexes. The complexation of the ligand is confirmed from the IR Spectra. The XRD and surface area measurements reveal the formation of the complex within the zeolite framework keeping its crystallinity. The catalytic efficiency and effectiveness in inducing chirality of the complexes were examined in the epoxidation of styrene, which is a terminal prochiral olefin. Catalysis using many oxidizing agents was investigated. We could get substantial yield of the epoxide with 3-chloroperoxybenzoic acid as the oxidant. A number of unwanted side-products were formed with all other oxidants. The enantiomeric excesses were calculated for the products obtained with 3-chloroperoxybenzoic acid. The Ni(II) complex was found to be highly enantioselective (ee = more than 98 %). The enantiomeric excess (ee) was found to be moderate for the Cu(II) complex. The Mn(II) and Co(II) complexes were giving only negligible enantiomeric excesses.

The general conclusions drawn from these studies are as follows

1. Transition metal complexes were successfully encaged within the Y zeolite framework by carefully synthesizing the metal exchanged zeolites and zeolite complexes at optimized conditions.
2. The use of zeolite encapsulated complexes as catalysts provide information regarding the advantages of heterogenisation of the homogeneous catalytic systems by the encapsulation. The encapsulated complexes prepared exhibited higher stability, better catalytic activity and recyclability in certain reactions by retarding the deactivation processes.
3. Zeolite encapsulated complexes were found to be active in the oxidation of ascorbic acid to dehydroascorbic acid. The Cu(II) complexes were the most active catalysts. Interestingly, the Ni(II) complex was also found to be highly active. This may be due to the formation of a Ni(III) species as intermediate, which is stabilized by the electronic field present within the cage.
4. The geometry of the encapsulated complexes plays a vital role in regulating the functioning of the catalyst by providing vacant reaction sites. Encapsulated complexes interact with the framework of the zeolite, thus distorting the geometry resulting in modified catalytic activity. Hence, the activity and poison resistance of these catalysts can be optimised by varying the stereochemistry with bulkier ligands.
5. The successful encapsulation of chiral SALEN type metal complexes within Y zeolite has been achieved and the enantio-selectivity of the catalysts in the epoxidation of styrene was observed. The Ni(II) complex was found to give very high enantiomeric excess.